
THE ROLE OF ACTIVE DANCERS IN TENSION
CONTROL OF WEBS

By

LOKUKALUGE PRASAD PERERA

Bachelor of Science

Oklahoma State University

Stillwater, Oklahoma

1999

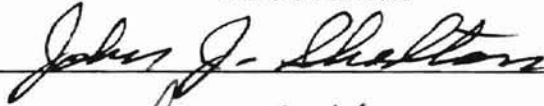
Submitted to the Faculty of the
Graduate College of the
Oklahoma State University
in partial fulfillment of
the requirements for
the Degree of
MASTER OF SCIENCE
August, 2001

THE ROLE OF ACTIVE DANCERS IN TENSION
CONTROL OF WEBS

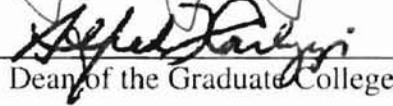
Thesis Approved:



Thesis Adviser






Dean of the Graduate College

ACKNOWLEDGMENTS

I wish to express my sincerest appreciation to my major advisor, Dr. Prabhakar R. Pagilla for his intelligent supervision, constructive guidance, inspiration, and friendship.

I would like to extend my warmest thanks to my masters committee members: Dr. John J. Shelton and Dr. Gary E. Young for their support and suggestions in completion of this research. Their guidance and understanding made the development of this thesis a positive learning experience.

I would also like to thank my colleagues at Oklahoma State University Ramamurthy V. Dwivedula, Fu Yuet, Yongliang Zhu and Gimkhuan Ng. I am grateful for the technical support provided by Jerry Dale and James Davis.

TABLE OF CONTENTS

Chapter	Page
1 INTRODUCTION	1
1.1 Background	1
1.2 Previous Studies	2
1.3 Thesis Contributions	5
1.4 Thesis Outline	5
2 MODELING AND ANALYSIS OF AN ACTIVE DANCER SYSTEM	6
2.1 Modeling	7
2.1.1 Input/Output Model	8
2.1.2 State Space Model	9
2.2 Analysis of the Input/Output Model	11
2.2.1 Time domain simulations	14
2.2.2 Interpretation of the effect of span lengths on tension control	15
3 EXPERIMENTAL WEB PLATFORM	21
3.1 Hardware	21
3.1.1 Active Dancer System	24
3.1.2 Web Guide System	26
3.1.3 Sensor Calibration	28
3.1.4 Computer System	29
3.2 Software Structure	32
3.2.1 Real-time Software	34

Chapter	Page
4 CONTROL DESIGN AND EXPERIMENTAL RESULTS	37
4.1 Controller Design	38
4.1.1 State-space Model for Active Dancer System	38
4.1.2 PID Controller	39
4.1.3 IMC Controller	39
4.1.4 LQR Controller	41
4.2 Experimental Results	43
5 CONCLUSIONS AND FUTURE RESEARCH	59
5.1 Conclusions	59
5.2 Future Research	60
BIBLIOGRAPHY	62
A DYNAMICS OF BASIC ELEMENTS OF WEB HANDLING SYSTEMS	65
A.1 Assumptions for Mathematical Models	65
A.2 Unwind Roller	66
A.3 Rewind Roller	66
A.4 Free Roller (Rotational dynamics)	67
A.5 Driven Roller (Rotational Dynamics)	68
A.6 Dancer Roller (Translation Dynamics)	69
A.7 General Free Span	69
A.8 Downstream Span of the Dancer	71
A.9 Upstream Span of the Dancer	73
A.10 Web Span next to the Unwind Roller	74
A.11 Linearized Dynamics	75
A.12 Transfer Functions	75

Chapter	Page
B INPUT/OUTPUT MODEL FOR ACTIVE AND PASSIVE DANCER SYSTEMS	77
B.1 Active Dancer System	77
B.1.1 System Equations	77
B.1.2 Simplified Dancer Subsystem Model and Analysis	78
B.2 Active Dancer System	81
B.3 Passive Dancer System	81
 C MATLAB PROGRAM FOR LQR CONTROLLER AND LUENBERGER OB- SERVER	 84
 D AUTOCAD DRAWINGS AND PHOTOGRAPHS OF EXPERIMENTAL PLAT- FORM	 86

LIST OF TABLES

Table		Page
2.1	Web and roller parameters for root-locus	11
2.2	Open-loop zeros and poles for $L_1 = 36$ in and $L_2 = 9$ in	12
2.3	Open-loop poles and zeros for $L_1 = 9$ in and $L_2 = 9$ in	13
2.4	Open-loop poles and zeros for $L_1 = 9$ in and $L_2 = 36$ in	13

LIST OF FIGURES

Figure	Page
2.1 Active dancer system	7
2.2 Root locus plot for $L_1 > L_2$	16
2.3 Root locus plot for $L_1 = L_2$	16
2.4 Root locus plot for $L_1 < L_2/2$	17
2.5 Web tension for $L_1 > L_2$ with proportional control	18
2.6 Web tension for $L_1 = L_2$ with proportional control	19
2.7 Web tension for $L_1 < L_2/2$ with proportional control	20
3.1 Sketch of the experimental web platform	22
3.2 Functional block of the experimental web platform	23
3.3 Schematic of active dancer tension control system	24
3.4 Block diagram of the tension control system	25
3.5 Fife analog lateral control system	27
3.6 Schematic of analog lateral control system	27
3.7 Schematic of lateral computer control system with velocity inner-loop	28
3.8 Lateral computer control system with tachometer velocity feedback	29
3.9 Schematic diagram for processing web velocity output	30
3.10 Calibration of web velocity sensor	31
3.11 Calibration of loadcell	31
3.12 Calibration of active dancer velocity input	32
3.13 A/D and D/A channel configuration	33
3.14 Software structure	34

Figure	Page
4.1 Active dancer system	38
4.2 Active dancer tension control system	40
4.3 Experimental web platform with uneven roll surface	46
4.4 Summary of tension disturbance reduction with PID and IMC controllers; out-of-round passive dancer roller	47
4.5 Tension with active dancer PID control; $v_r = 300$ FPM, $t_r = 18$ lb	48
4.6 Tension with active dancer IMC control; $v_r = 300$ FPM, $t_r = 18$ lb	49
4.7 Tension with active dancer PID control; $v_r = 350$ FPM, $t_r = 25$ lb	50
4.8 Tension with active dancer IMC control; $v_r = 350$ FPM, $t_r = 25$ lb	51
4.9 Tension with active dancer PID control; $v_r = 400$ FPM, $t_r = 26$ lb	52
4.10 Tension with active dancer IMC control; $v_r = 400$ FPM, $t_r = 26$ lb	53
4.11 Summary of tension disturbance reduction with PID, IMC, LQR controllers; out-of-round idle roller	54
4.12 Tension with out-of-round idle roller; $v_r = 200$ FPM, $t_r = 36$ lb	55
4.13 Tension with out-of-round idle roller; $v_r = 250$ FPM, $t_r = 10$ lb	56
4.14 Tension with out-of-round idle roller; $v_r = 300$ FPM, $t_r = 15$ lb	57
4.15 Tension with out-of-round idle roller; $v_r = 350$ FPM, $t_r = 20$ lb	58
A.1 Unwind roller	66
A.2 Rewind Roller	67
A.3 General free span with driven roller	67
A.4 Active dancer system	68
A.5 Control volume of a web span	69
B.1 Active dancer system	77

NOMENCLATURE

A	Cross-sectional area of web
B_f	Bearing friction
b	Damping coefficient
\bar{b}	Ratio of damping coefficient vs roller mass (b/M)
E	Young' s Modulus of elasticity
F_a	Dancer input force
h	Web thickness
J	Polar moment of inertia of roller
k	Spring constant
\bar{k}	Ratio of spring constant vs roller mass (k/M)
L	Length of web span
M	Mass of a roller
R	Radius of a roller
t	Web tension
$[t]_v$	Tension due to web velocity
$[t]_d$	Tension due to dancer motion
T	Change in tension from reference
u	Input to a roller
U	Change in input from reference
v	Roller velocity
V	Change of roller velocity from reference
w	Web width

ω	Roller angular velocity
Ω	Change of roller angular velocity from reference
x	Linear displacement of dancer
X	Change of linear displacement of dancer roller from reference
α	Web span constant $((EA - t_r)/v_r)$
θ	Angle of wrap of web over a roller
ρ	Web density
η	Web handling system constant (β/α)
τ	Time constant of a web span (L_n/v_r)
τ_t	Time
β	Inertia constant of a roller (J_n/R_n^2)
$\bar{\beta}$	Ratio of inertia constant vs mass (β/M)
γ	Friction constant of a roller (B_{fn}/R_n^2)
ϵ	Web strain

Subscripts :

n	Pertaining to n-th element
r	Pertaining to reference values
$n0$	Pertaining to intial values

CHAPTER 1

INTRODUCTION

1.1 Background

A web is any material in continuous flexible strip form which is very long compared to its width and very wide compared to its thickness. Examples of web include all forms of paper, fabric, plastic wrap, adhesive tape, photographic film, and strip metals. Handling of a web during processing directly affects the quality of the finished web. Lateral control, also called web guiding, involves controlling the web fluctuations in the directions perpendicular to the travel of the web. Control of web guides to maintain the lateral position of the web on the roller prior to coating, printing, winding and other processes is essential in the web processing industry. Longitudinal control involves controlling the tension or velocity parallel to the direction of web travel.

With the need for increased performance and productivity in the web processing industry, accurate modeling and effective controller design for web handling systems is essential for increasing the web processing speed and the quality of the processed web. Accurate tension control has always been a key element of web handling systems. An important objective of the tension control system is to maintain tension within the desired limits under a wide range of dynamic conditions such as speed changes, variations in roll sizes, and web property. Tension variations affect printing quality and tend to cause web breakage and wrinkles.

A dancer mechanism is used as a feedback element in a number of tension control systems. The tension control system is driven by the variations in the position of the dancer mechanism as opposed to the variations in actual tension from the desired tension. The

requirement to maintain the desired tension within a narrow range from the unwind zone to the first printing unit places a demand on better design of the dancer mechanism. Periodic tension disturbances arising from uneven wound rolls and misalignment of the idle rolls have to be attenuated by the dancer mechanism in order to minimize their propagation into the process section.

Currently, passive dancers are widely used as dancer mechanisms. Passive dancers have known to act as good tension feedback elements for low speed web lines; they have limitations in dealing with a wide range of dynamic conditions experienced in high speed web lines. It is expected that by introducing an active element into a dancer mechanism gives a control engineer more flexibility in attenuating periodic tension disturbances and also to maintain lower tension fluctuations. The focus of this project is on modeling, control design and experimental investigation of active dancer mechanisms for tension disturbance attenuation.

1.2 Previous Studies

Early development of mathematical models for longitudinal dynamics of a web can be found in [1, 2, 3, 4, 5]. In [1], extensive theoretical and experimental analysis on belt drive fundamentals was reported; it studied effects such as centrifugal force, angle of contact, fixed versus floating shaft on tension in the belt. Although the mass of the belt is considerable when compared to the web during transport, similarities exist between belt drive systems and web handling systems. Early work describing the longitudinal dynamics of a web can be found in the book by Campbell [2]. Campbell developed a mathematical model for longitudinal dynamics of a web span between two pairs of pinch rolls, which are driven by two motors; the model is based on Hooke's law, i.e., the variation in web tension in the span is proportional to the positional change of the pinch rolls. Campbell's model does not predict tension transfer and does not consider tension in the entering span. A modified model that considers tension in the entering span was developed in [4].

In [5], the moving web was considered as a moving continuum and the general methods of continuum mechanics such as the conservation of mass, conservation of momentum, and conservation of energy were used in the development of a mathematical model. This comprehensive study by Brandenburg [5] included the steady state and transient behavior of tensile force, stress, strain and register error as functions of variables such as wrap angle, position and speed of the driven rollers, density, cross-sectional area, modulus of elasticity and temperature. Tension variations in pliable material due to friction between the web and guide rollers has been considered in [6].

In [19], equations describing tension dynamics are derived based on the fundamentals of the web behavior and the dynamics of drives used for web transport. A simple example system was considered to compare torque control versus velocity control of a roll for the regulation of tension in a web. Tension control using optimal output feedback technique in a multi-span web transport system was reported in [11]. A decentralized observer was developed to estimate the forces due to web tension on the driven rollers. The decentralized observer leads to improved speed response of the driven rollers in multi-span web transport systems.

Study on steady state and transient behavior of a moving web was reported in [17]. Non-ideal effects such as temperature and moisture change on web tension were studied. Based on the models developed, methods for distributed control of tension in multi-span web transport systems were studied. Analysis of a multi-span web system with a passive dancer for minimizing disturbances due to eccentric unwind roll was also reported.

A study on dynamic behavior of dancers in web transport systems was reported in [20]. Computer simulation studies were conducted on an example system to investigate disturbance rejection for three cases: (1) without a dancer; (2) with a classical dancer with passive elements; and (3) with an inertia compensated dancer. Simulation results show attenuation of tension disturbances in the case of both a classical dancer and an inertia compensated dancer. Control of tension during start-up/shut-down in a multi-span web transport system

was considered in [16]. Since start-up or shut-down conditions involve large variations in roller velocities, nonlinear models were considered in the simulation study. Simulation results of a PID tension controller were reported. It is shown in the simulation study that a controller designed for one start-up condition when used at a substantially different operating condition could result in web breakage.

An overview of lateral and longitudinal dynamic behavior and control of moving webs was presented in [21]. A review of the problems in tension control of webs was reported in [12]. A comprehensive study on tension regulation of a web is reported in [24]. Discussions on tension control versus strain control and torque control versus velocity control were given. An extensive analysis and discussion is reported on modeling and design of a tension control station with both inertia compensated dancers and classical passive dancers. Practical recommendations for modular design of tension control stations were given.

An active dancer system for reducing the variation of tension in wire and sheet materials was proposed in [10]. This is one of the early comprehensive work on active dancers that was reported in literature. Construction of an active dancer system with a D.C. motor was discussed. A mathematical model for an active dancer system within a web transport system is derived. An output feedback controller was designed for the active dancer system for tension regulation. Experimental results were reported based on an apparatus with an active dancer system. The main drawback of the apparatus is that the results can be obtained for a stationary web. The construction and testing of an active dancer system that is capable of rejecting periodic cyclic process induced tension disturbances was reported in [13]. This report considers early web tension dynamic models for active dancer control design. It is assumed that the web velocity upstream of the dancer is constant in the model, which may not be true in general. The control system is designed using nonlinear functional block diagrams.

1.3 Thesis Contributions

The main goal of this project is to investigate the effectiveness of active dancer mechanisms in tension control of webs. Modeling, analysis, control design and experimentation were considered to achieve the main goal. A generic active dancer system, which can be included in a web process line, has been considered for the development of the mathematical model. An input/output model and a state space model have been developed based on the dynamics of the basic web handling elements. The input is the active dancer translational velocity and the output is the tension in the downstream span of the dancer roller. The model is investigated and conditions under which effective tension disturbance attenuation is possible using the active dancer are developed.

An active dancer system is developed for conducting experiments. Experiments were conducted with a PID controller, Internal model based controller (IMC), and a linear quadratic optimal controller. Experimental results are discussed and compared. Experimental results validate the claim that an active dancer system is more effective than a traditional passive dancer system, which has been known to reject low frequency disturbances.

1.4 Thesis Outline

The rest of the report is organized as follows. Chapter 2 develops an input/output and a state space model of an active dancer system. Investigation of the models is conducted and suggestions on the choice of dancer system physical parameters is reported in chapter 2. Details of the experimental web platform that is developed for conducting active dancer experiments are given in chapter 3. Chapter 4 contains control designs for the active dancer system and experimental results. Discussion of the experimental results and comparison of different controllers is also given. Chapter 5 contains some conclusions and future research.

CHAPTER 2

MODELING AND ANALYSIS OF AN ACTIVE DANCER SYSTEM

In this chapter modeling and analysis of an active dancer system is presented. The approach taken in the design of the active dancer system is generic in the sense that it can be included as a subsystem anywhere in the web process line where precise tension regulation is required. Two types of models for the active dancer system are developed in this chapter: input/output model and state space model. An input/output model is derived in the Laplace domain with the output as the span tension that needs to be regulated and input as the dancer translational velocity. Analysis of the input/output model to variations in the physical parameters such as length of spans and modulus of elasticity, etc., is conducted using the root-locus approach. A compact state space model is also derived based on a unique transformation of the physical variables.

Complete derivations of the dynamics of the basic elements of web handling systems, input/output model of the active dancer system are presented in appendices A and B. The models in the appendices A and B are derived based on the previous work on modeling presented in [2, 5, 6, 19, 17, 16].

The outline of this chapter is as follows. Section 2.1 deals with the modeling of the active dancer system and subsections 2.1.1 and 2.1.2 present input/output and state-space models. Section 2.2 focuses on root-locus analysis of the active dancer system. Simulation results of the state space model are discussed in Section 2.3. Summary of this chapter with discussions is given in Section 2.4.

2.1 Modeling

A typical active dancer system shown in Fig. 2.1, is considered for deriving the input/output and state space models. This system contains web spans adjacent to the dancer roller in upstream and downstream directions and three rollers including the dancer roller. It is assumed that T_0 and T_3 are tension disturbance from upstream and downstream directions of the active dancer roller that are to be rejected/attenuated. The linearized dynamics of the

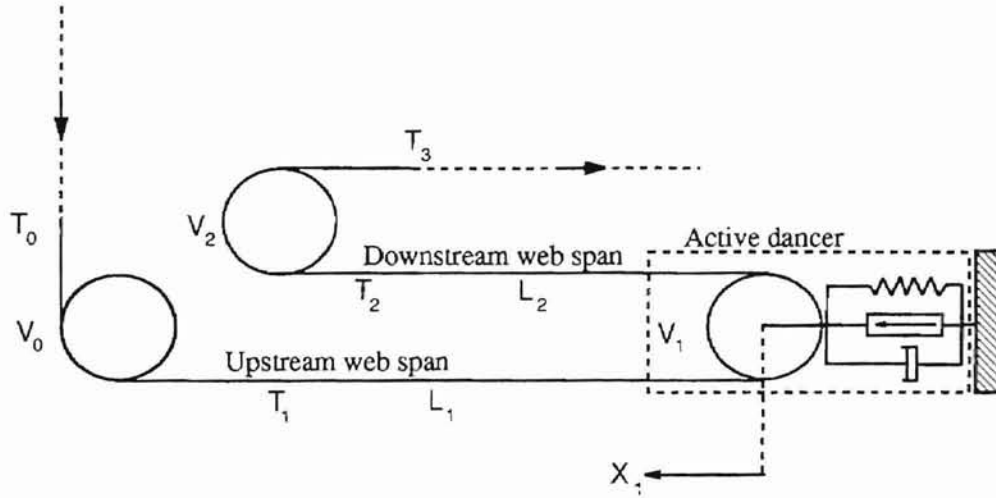


Figure 2.1: Active dancer system

active dancer system shown in Fig. 2.1 is given by the following equations.

$$\beta \dot{V}_0 = -\gamma V_0 + (T_1 - T_0) \quad (2.1)$$

$$\tau_1 \dot{T}_1 = -T_1 + T_0 + \alpha(V_1 - V_0) + \frac{\alpha}{\tau_1} X_1 + \alpha U \quad (2.2)$$

$$\beta \dot{V}_1 = -\gamma V_1 + (T_2 - T_1) \quad (2.3)$$

$$\tau_2 \dot{T}_2 = -T_2 + T_1 + \alpha(V_2 - V_1) + \alpha \left(\frac{1}{\tau_2} - \frac{1}{\tau_1} \right) X_1 + \alpha U \quad (2.4)$$

$$\beta \dot{V}_2 = -\gamma V_2 + (T_3 - T_2) \quad (2.5)$$

$$\dot{X}_1 = U \quad (2.6)$$

where $\beta = J/R^2$, $\gamma = B_f/R^2$, $\alpha = EA/v_r$, $\tau_1 = L_1/v_r$, and $\tau_2 = L_2/v_r$.

2.1.1 Input/Output Model

In this section, input/output model for the active dancer system is presented. Velocity of the dancer roller (\dot{X}_1) is considered as the control input and measured tension (T_2) at the roller immediately downstream of the dancer roller is considered as measured output. The tension disturbance is variation in tension of the web span upstream of the active dancer. The complete derivation of the input/output model is given in appendix B.

The input/output model is obtained by taking Laplace transform of the linearized dynamics and simplifying the resulting equations. Equations (2.2) and (2.4) in Laplace domain are

$$T_1(s) = \frac{1}{\tau_1 s + 1} T_0(s) + \frac{\alpha}{\tau_1 s + 1} [V_1(s) - V_0(s)] + \frac{\alpha (\tau_1 s + 1)}{\tau_1 (\tau_1 s + 1) s} U(s) \quad (2.7)$$

$$T_2(s) = \frac{1}{\tau_2 s + 1} T_1(s) + \frac{\alpha}{\tau_2 s + 1} [V_2(s) - V_1(s)] + \frac{\alpha (\tau_1 \tau_2 s + \tau_1 - \tau_2)}{\tau_1 \tau_2 (\tau_2 s + 1) s} U(s) \quad (2.8)$$

where the input $U(s)$ is the dancer velocity, i.e., $U(s) = sX_1(s)$. The dynamics of each roller is given by

$$V_0(s) = \frac{1}{\beta s + \gamma} [T_1(s) - T_0(s)] \quad (2.9)$$

$$V_1(s) = \frac{1}{\beta s + \gamma} [T_2(s) - T_1(s)] \quad (2.10)$$

$$V_2(s) = \frac{1}{\beta s + \gamma} [T_3(s) - T_2(s)] \quad (2.11)$$

Notice that the variable definition is same in both time domain and frequency domain; explicit dependence of the variables on the Laplace variable “s” will be shown in the frequency domain throughout the report. Combining equations (2.7) through (2.11) and simplifying (see appendix B) gives the following input-output dynamic model for the active

dancer:

$$T_2(s) = \frac{D_{ad}(s)}{C_{ad}(s)}U(s) + \frac{A_{ad}(s)}{C_{ad}(s)}T_0(s) + \frac{B_{ad}(s)}{C_{ad}(s)}T_3(s) \quad (2.12)$$

$$A_{ad}(s) = (\eta s + 1)^2 \quad (2.13)$$

$$B_{ad}(s) = (\eta s(\tau_1 s + 1) + 2) \quad (2.14)$$

$$C_{ad}(s) = ((\eta s(\tau_1 s + 1) + 2)(\eta s(\tau_2 s + 1) + 2) - (\eta s + 1)) \quad (2.15)$$

$$D_{ad}(s) = \beta \left((\eta s + 1) \left(s + \frac{1}{\tau_1} \right) + (\eta s(\tau_1 s + 1) + 2) \left(s + \frac{1}{\tau_2} - \frac{1}{\tau_1} \right) \right) \quad (2.16)$$

where $\eta = Jv_r/EAR^2$.

The above input/output model has been obtained by assuming that the roller bearing friction is negligible. A full expression with non-zero bearing friction can be found in appendix B. Also, notice that the model is obtained under the assumption that the moment of inertia and radius of all the rollers in the dancer system are same, i.e., $J_i = J$ and $R_i = R$ for $i = 1, 2, 3$.

Expansion of the numerator, $D_{ad}(s)$, and the denominator, $C_{ad}(s)$, of the plant transfer function gives

$$C_{ad} = \eta^2 \tau_1 \tau_2 s^4 + \eta^2 (\tau_1 + \tau_2) s^3 + \eta (\eta + 2\tau_1 + 2\tau_2) s^2 + 3\eta s + 3 \quad (2.17)$$

$$D_{ad} = \beta \eta \tau_1 s^3 + \beta \eta \left(1 + \frac{\tau_1}{\tau_2} \right) s^2 + \beta \left(3 + \frac{\eta}{\tau_2} \right) s + \beta \left(\frac{2}{\tau_2} - \frac{1}{\tau_1} \right) \quad (2.18)$$

Notice that if $\tau_2 > 2\tau_1$, i.e., $L_2 > 2L_1$, then the constant term of the numerator polynomial, $D_{ad}(s)$, is negative, which results in a right-half-plane zero.

2.1.2 State Space Model

In this section, state space model for the active dancer system is presented. The dynamic model of the active dancer system shown in Fig. 2.1 is given by equations (2.1) through

(2.6). Notice that both the translational displacement and velocity of the active dancer appear in the upstream and downstream tension dynamics. Since the translational velocity of the dancer (U) is the input, appearance of dancer displacement would require definition of another state variable resulting in the state equation $\dot{X}_1 = U$. To circumvent this problem, consider the following change of coordinates of the system,

$$\begin{aligned} q_1 &= V_0 - \frac{1}{\tau_1} X_1 \\ q_2 &= T_1 \\ q_3 &= V_1 \\ q_4 &= T_2 \\ q_5 &= V_2 + \left(\frac{1}{\tau_2} - \frac{1}{\tau_1} \right) X_1 \end{aligned}$$

Assuming that the bearing friction in the idle rollers is negligible, the state space form of the dynamics in the transformed variables is given by

$$\begin{aligned} \begin{bmatrix} \dot{q}_1 \\ \dot{q}_2 \\ \dot{q}_3 \\ \dot{q}_4 \\ \dot{q}_5 \end{bmatrix} &= \begin{bmatrix} 0 & \frac{1}{\beta} & 0 & 0 & 0 \\ -\frac{\alpha}{\tau_1} & -\frac{1}{\tau_1} & \frac{\alpha}{\tau_1} & 0 & 0 \\ 0 & -\frac{1}{\beta} & -\frac{\alpha}{\beta} & \frac{1}{\beta} & 0 \\ 0 & \frac{1}{\tau_2} & -\frac{\alpha}{\tau_2} & -\frac{1}{\tau_2} & \frac{\alpha}{\tau_2} \\ 0 & 0 & 0 & -\frac{1}{\beta} & 0 \end{bmatrix} \begin{bmatrix} q_1 \\ q_2 \\ q_3 \\ q_4 \\ q_5 \end{bmatrix} + \begin{bmatrix} -\frac{1}{\tau_1} \\ \frac{\alpha}{\tau_1} \\ 0 \\ \frac{\alpha}{\tau_2} \\ \frac{1}{\tau_2} - \frac{1}{\tau_1} \end{bmatrix} U(t) + \begin{bmatrix} -\frac{1}{\beta} & 0 \\ \frac{1}{\tau_1} & 0 \\ 0 & 0 \\ 0 & 0 \\ 0 & \frac{1}{\beta} \end{bmatrix} \begin{bmatrix} T_0(t) \\ T_3(t) \end{bmatrix} \\ y(t) &= \begin{bmatrix} 0 & 0 & 0 & 1 & 0 \end{bmatrix} \begin{bmatrix} q_1 \\ q_2 \\ q_3 \\ q_4 \\ q_5 \end{bmatrix} + \begin{bmatrix} 0 \end{bmatrix} U(t) + \begin{bmatrix} 0 & 1 \end{bmatrix} \begin{bmatrix} T_0(t) \\ T_3(t) \end{bmatrix} \end{aligned} \quad (2.19)$$

Notice that the above model contains both $T_0(t)$ and $T_3(t)$, both of which can be considered as disturbances. The above model can be represented compactly in matrix form as

$$\begin{aligned}\dot{Q}(t) &= \mathbf{A}Q(t) + \mathbf{B}_u U(t) + \mathbf{B}_w W(t) \\ y(t) &= \mathbf{C}Q(t) + \mathbf{D}_u U(t) + \mathbf{D}_w W(t)\end{aligned}\quad (2.20)$$

where $Q(t) = [q_1(t), q_2(t), q_3(t), q_4(t), q_5(t)]^\top$ and $W(t) = [T_0(t), T_3(t)]^\top$.

2.2 Analysis of the Input/Output Model

Analysis of the input/output active dancer model given by (2.12) is conducted by varying the parameters: L_1, L_2, E, A, J, R and v_r . Since most feedback control algorithms for the dancer input involve some type of proportional action, the analysis of the basic analysis of the active dancer system is conducted with proportional control. The closed-loop characteristic equation with proportional feedback control, i.e., $U(s) = -K_p T_2(s)$, is

$$1 + K_p \frac{D_{ad}(s)}{C_{ad}(s)} = 0, \quad (2.21)$$

where K_p is the proportional gain. To investigate the effect of the four constants, η, β, τ_1 and τ_2 , on the choice of the proportional gain, the root-locus method is employed.

Effect of span lengths: L_1, L_2

First, locus of the closed-loop poles for varying K_p is plotted for various values of L_1 and L_2 . Other physical parameters of the web and the rollers are kept constant and the values used are given in the following table.

v_r	E	A	J	R
330 FPM	6×10^5 PSI	1.27×10^{-4} in ²	96.21 lb in ²	2.5 in

Table 2.1: Web and roller parameters for root-locus

Recall from classical control theory (root-locus method) that the closed-loop poles approach the open-loop zeros as K_p is increased. Root locus for the following cases are considered in the investigation.

- $L_1 > L_2$

Fig. 2.2 shows the root-locus plot for the case when $L_1 = 36$ in and $L_2 = 9$ in. The open-loop poles and zeros of the plant transfer function are given in table 2.2.

Zeros	Poles
$-1.70 + 251.08i$	$-2.74 + 424.93i$
$-1.70 - 251.08i$	$-2.74 - 424.93i$
-2.98	$-0.45 + 171.18i$
	$-0.45 - 171.18i$

Table 2.2: Open-loop zeros and poles for $L_1 = 36$ in and $L_2 = 9$ in

Fig. 2.2 shows that the proportional gain K_p can be chosen as large as possible. Thus, the disturbance effect on the span downstream to an active dancer can be suppressed to as small a value as possible. Notice that after a certain value any increase in K_p results in moving the closed-loop poles towards the imaginary axis. So, a very small gain and a very large gain give similar set of closed-loop poles. Hence, appropriate choice of the gain K_p must be made such that the closed-loop poles are far away from the imaginary axis.

- $L_1 = L_2$

Fig. 2.3 shows the root-locus plot when $L_1 = L_2 = 9$ in. The open-loop poles and zeros of the plant transfer function are given in table 2.2.

In this case, there is a complex-conjugate pair of open-loop poles very close to a pair of complex-conjugate zeros. Thus, any choice of gain cannot move this pair of open-loop poles further to the left-half-plane away from the imaginary axis. The control flexibility and effectiveness is much reduced when the span lengths are equal.

Zeros	Poles
$-4.25 + 501.75i$	$-3.83 + 501.75i$
$-4.25 - 501.75i$	$-3.83 - 501.75i$
-1.70	$-1.28 + 289.68i$
	$-1.28 - 289.68i$

Table 2.3: Open-loop poles and zeros for $L_1 = 9$ in and $L_2 = 9$ in

- $L_1 < L_2/2$

The root-locus plot for this case is shown in Fig. 2.4 where $L_1 = 9$ in and $L_2 = 36$ in.

The open-loop poles and zeros of the plant transfer function are given in table 2.2.

Zeros	Poles
$-3.61 + 501.75i$	$-2.74 + 424.93i$
$-3.61 - 501.75i$	$-2.74 - 424.93i$
0.85	$-0.45 + 171.18i$
	$-0.45 - 171.18i$

Table 2.4: Open-loop poles and zeros for $L_1 = 9$ in and $L_2 = 36$ in

In this case, the root locus crosses the imaginary axis and enters the right-half plane when K_p exceeds a certain value. This implies that the disturbance can only be suppressed to a certain extent because large control input can make the closed-loop system unstable. When L_1 becomes smaller compared to L_2 , then the allowable controller gain K_p decreases. More specifically, as shown in Fig. 2.4, a branch of the root locus moves to the right-half plane for very small value of K_p . Thus the closed-loop system becomes unstable under feedback control for a very small control gain.

Effect of web material and roller properties: E, A, J, R

Each of the constants E, A, J, R affect the constant parameter $\eta = (Jv_r)/(EAR^2)$ in the input/output model. So, varying the value of η in the model reflects variations of E, A, J, R . We have conducted a number of numerical simulations by varying these constants and noticed that the root-locus plot essentially has the same form. Thus the closed-loop poles of the dancer system are not generally affected as much by the constants E, A, J, R as it is affected by variation in upstream and downstream span lengths.

2.2.1 Time domain simulations

Simulation results in the time-domain using the state space model given by (2.19) with a proportional controller are discussed in this section. Tension measured on the roller downstream of the dancer roller is the measured output and the dancer velocity is the control input. It is assumed that a periodic tension disturbance is generated only in the upstream of the dancer, i.e., $T_0(t) = 10 \sin(20t)$ (lbf) and $T_3(t) = 0$. Simulations are conducted for different cases of span lengths while keeping the web and roller properties constant as given in table 2.1.

- $L_1 > L_2$

Fig. 2.5 shows simulation results when $L_1 = 36$ in and $L_2 = 9$ in. Results show good tension disturbance attenuation with active dancer control.

- $L_1 = L_2$

Fig. 2.6 shows simulation results when $L_1 = L_2 = 9$ in. Results are similar to the simulations obtained from the previous case.

- $L_1 < L_2/2$

Fig. 2.7 shows simulation results when $L_1 = 9$ in and $L_2 = 36$ in. Results show that the dancer system is unstable, which was concluded also from the root-locus

analysis.

2.2.2 Interpretation of the effect of span lengths on tension control

Assuming that the web is mostly elastic, it is common practice in the web handling community to model a web span as an elastic spring with spring constant $K_n = E_n A_n / L_n$. The spring constants of the upstream and the downstream web spans to the dancer roller are $K_1 = EA/L_1$ and $K_2 = EA/L_2$, respectively.

When $L_1 \geq L_2$, $K_1 \leq K_2$, that is the upstream spring constant is smaller than the downstream spring constant. So, any motion of the dancer roller gives larger tension variation in tension T_2 than in T_1 . Thus, rejection of periodic disturbances from the spans upstream of the dancer into the spans downstream of the dancer is possible in this case.

When $L_1 < L_2/2$, $K_1 < K_2/2$, that is the upstream spring constant is larger than the downstream spring constant. Periodic dancer motion induces larger tension disturbances into the upstream span than it rejects in the downstream span due to feedback of tension T_2 .

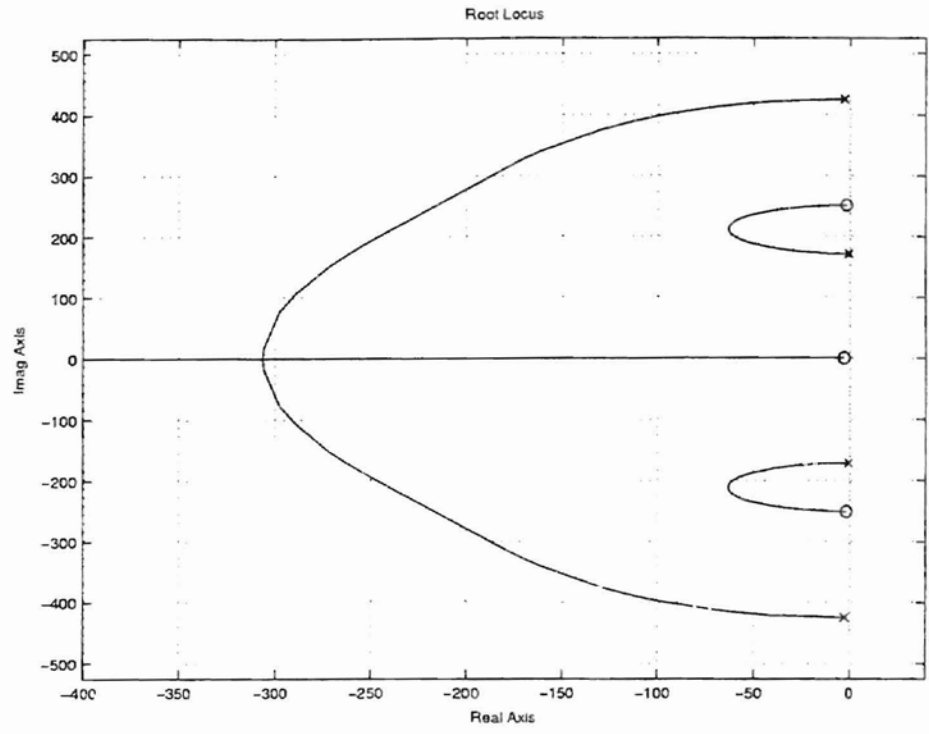


Figure 2.2: Root locus plot for $L_1 > L_2$

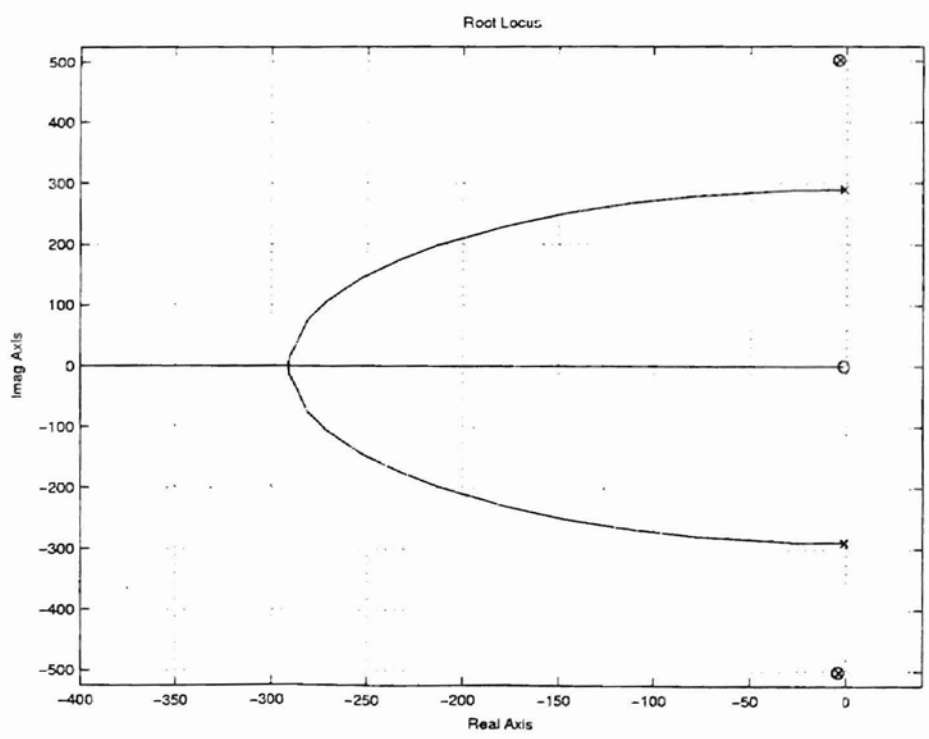


Figure 2.3: Root locus plot for $L_1 = L_2$

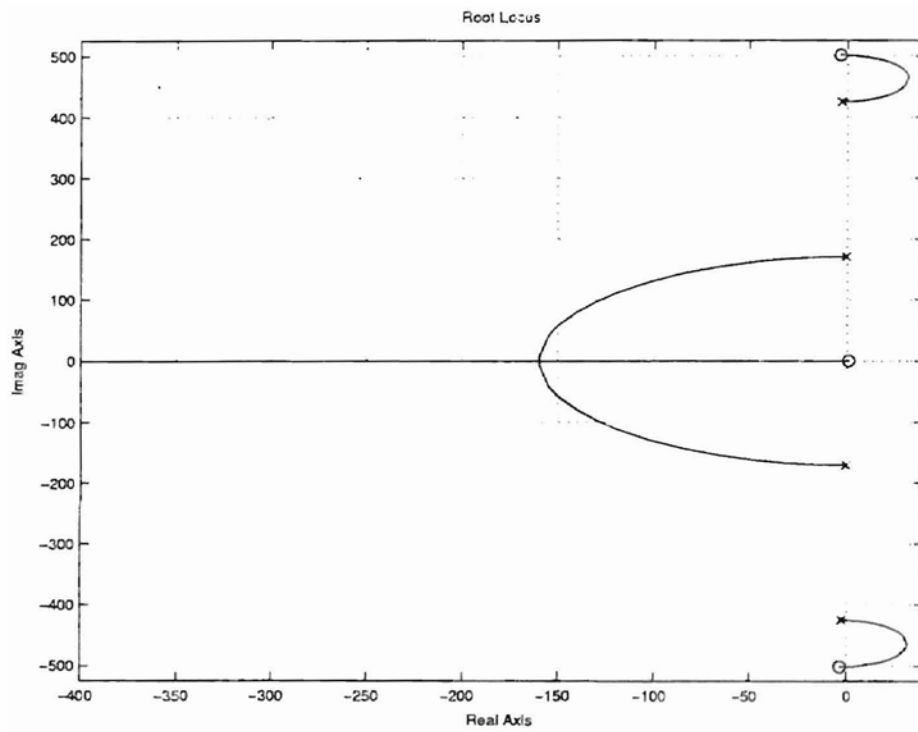


Figure 2.4: Root locus plot for $L_1 < L_2/2$

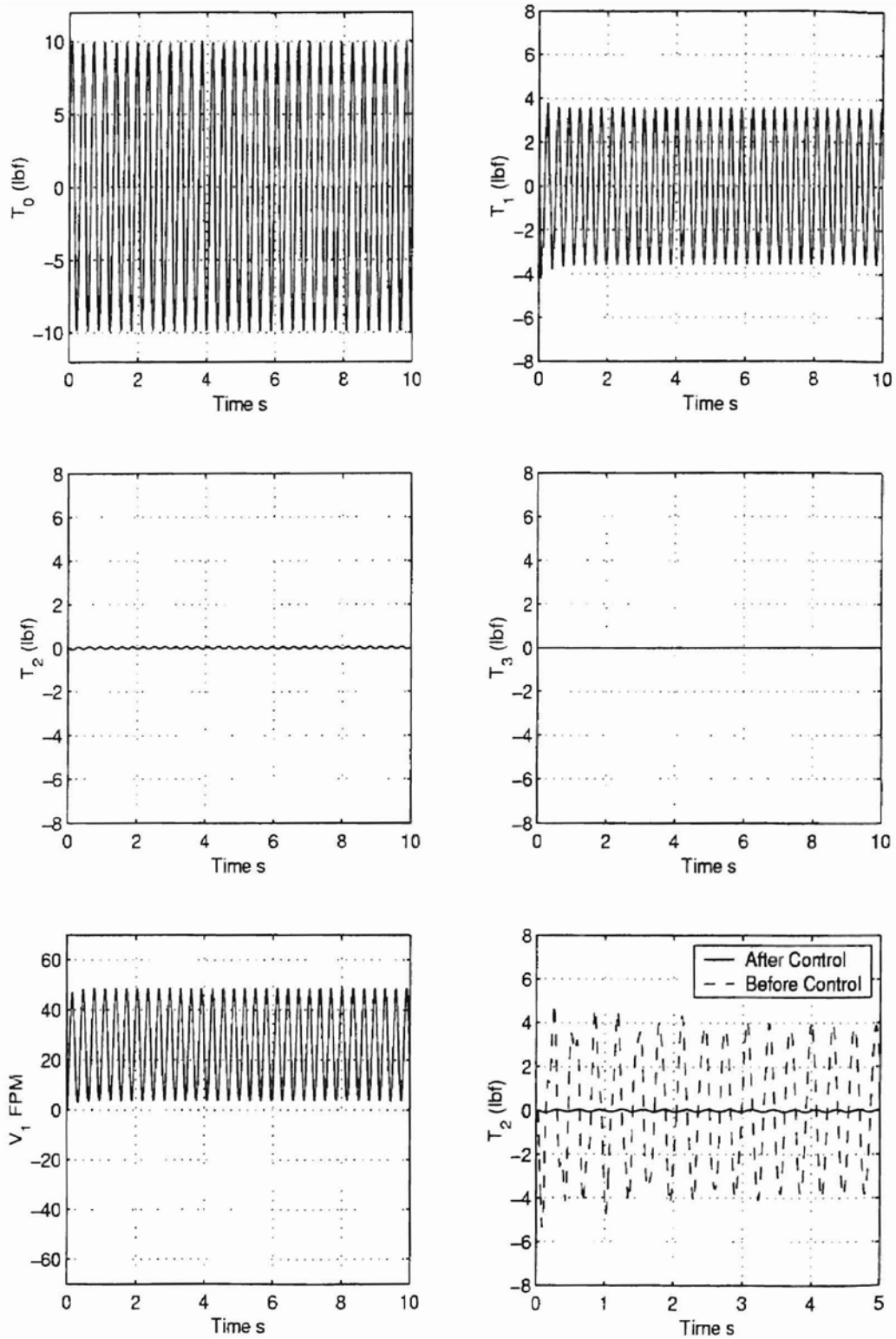


Figure 2.5: Web tension for $L_1 > L_2$ with proportional control

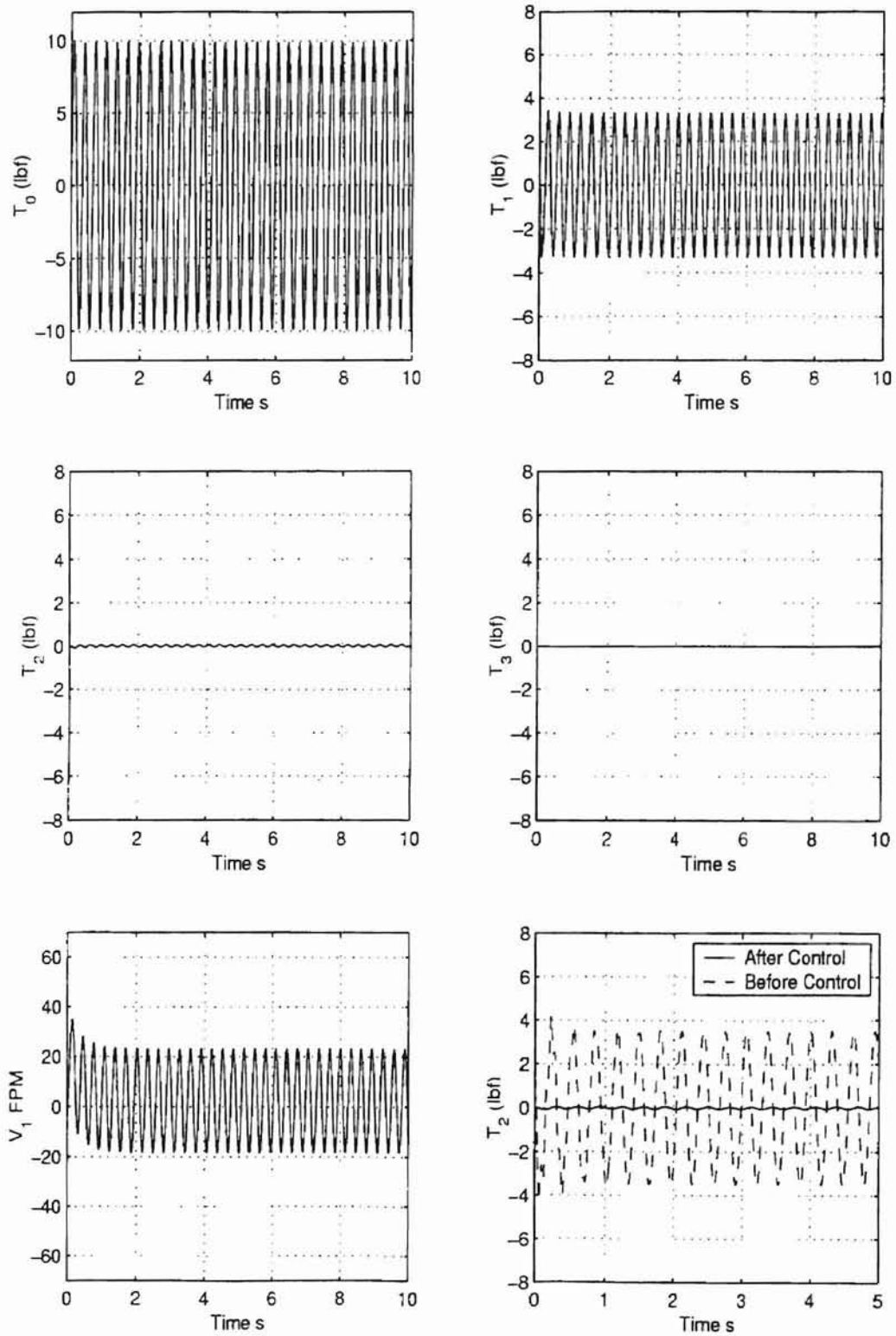


Figure 2.6: Web tension for $L_1 = L_2$ with proportional control

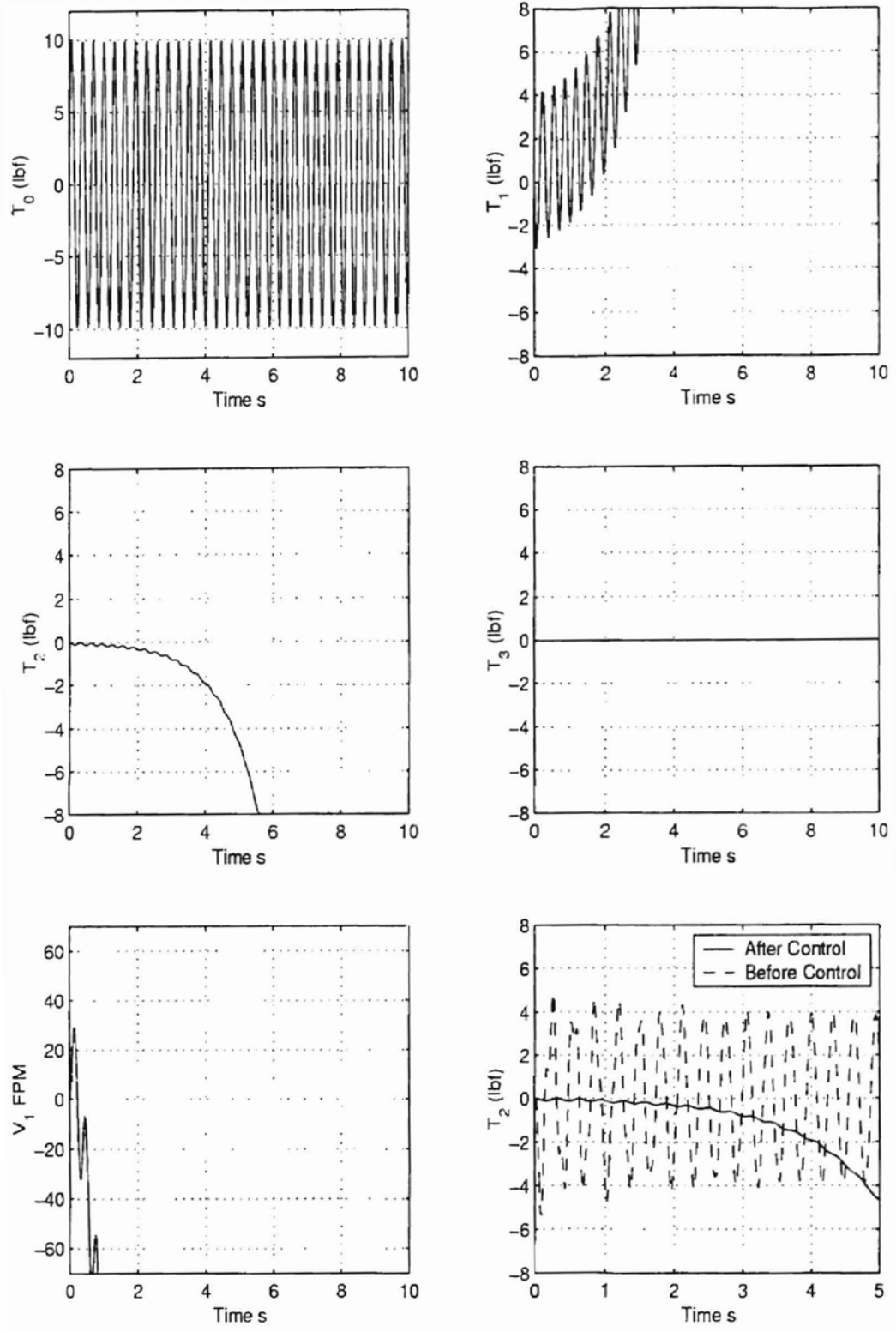


Figure 2.7: Web tension for $L_1 < L_2/2$ with proportional control

CHAPTER 3

EXPERIMENTAL WEB PLATFORM

This chapter describes the open-architecture experimental web platform developed for conducting experiments in tension control. The platform mainly consists of an endless web line with tensions control and lateral control systems as shown in Fig. 3.1. The term endless web line refers to a web line without unwind and rewind rolls. This type of platform mimics most of the features of a process section of a web processing line.

The experimental platform can be divided into two sections: Hardware and Software. The hardware section consists of the endless web line, active dancer system, web guide system, passive dancer system, sensors, data acquisition board, and a computer for implementing control algorithms in real-time. Software part consists of an open architecture real-time program written in C++ programming language.

A brief description of the hardware and software elements of the experimental platform is given in the following sections. The chapter outline is as follows: Section 3.1 deals with the hardware part of the experimental platform. Subsection 3.1.1 presents the experimental setup for active dancer subsystems. Similarly web guide system present in subsection 3.1.2. Sensors and sensor calibration information present in subsection 3.2.3. In subsection 3.1.4, computer system with digital data acquisition system are considered. Finally, section 3.2 presents the software structure designed for the real-time tension control experiments.

3.1 Hardware

The experimental web platform is shown in Fig. 3.1. Mechanical components used in this platform include sixteen rollers, one large master speed roller with a nip roller, an electric

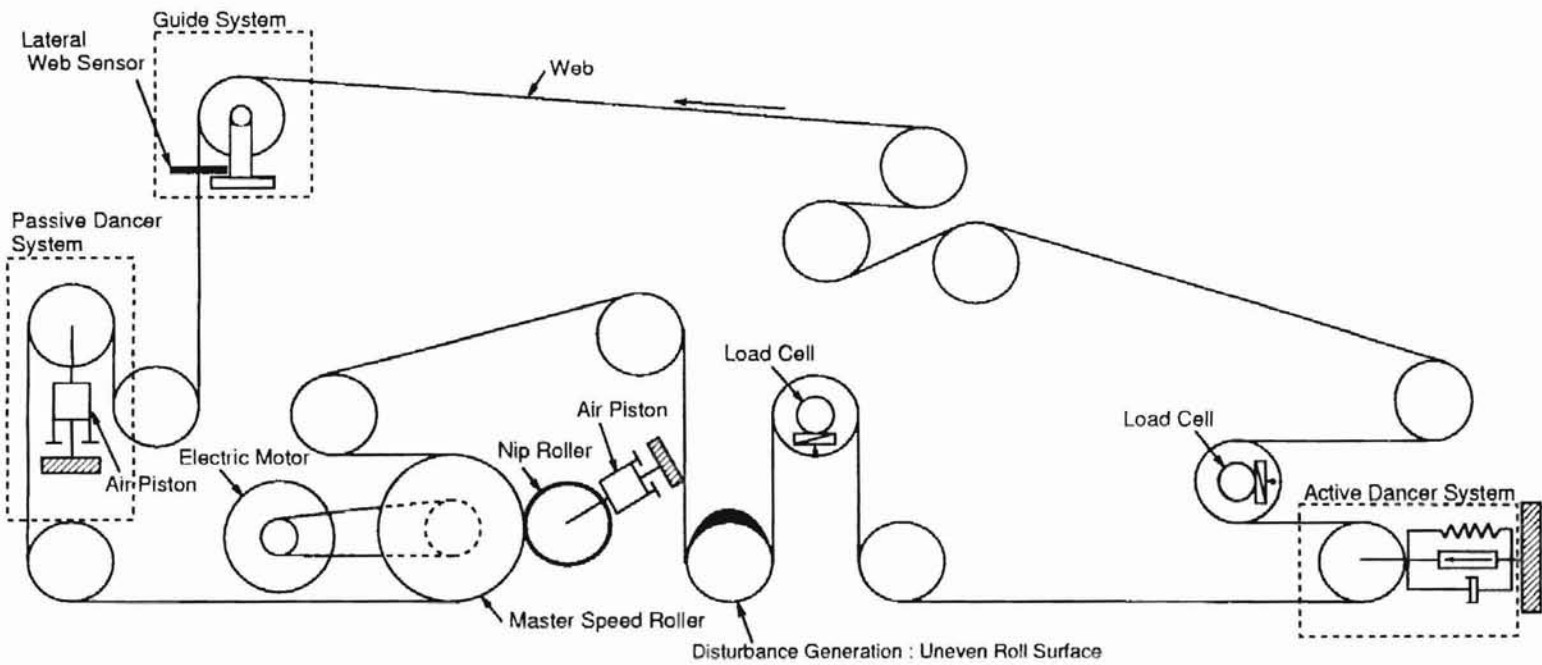


Figure 3.1 : Sketch of the experimental web platform

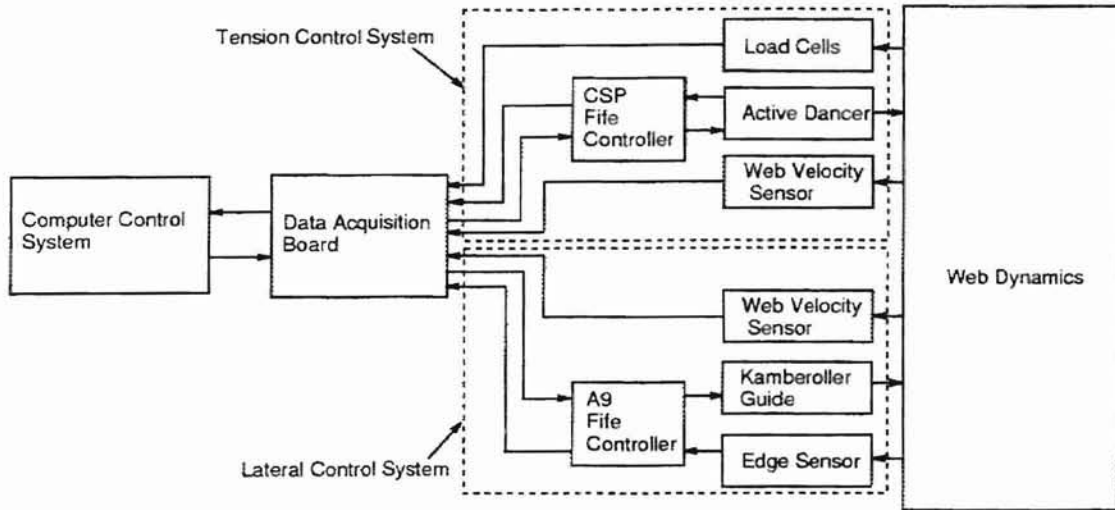


Figure 3.2: Functional block of the experimental web platform

motor, and a passive dancer system. The main control elements are a Fife remotely pivoted guide and an active dancer mechanism as shown in Fig. 3.1. Since the width of each roller is 8 inches, the maximum web width that can be used in the web line is limited to about 6 inches. The diameter of each roller is 5 inches, except for the master speed roller, which has a diameter of 10 inches. A nip roller for the master speed roller is used to reduce slip during start-up. An analog controller for the master speed roller is available to obtain the desired transport velocity of the web. Similarly an analog controller for air pressure in passive dancer system is available to obtain desired reference tension in endless web line.

The passive dancer mechanism is shown in Fig. 3.1. The primary function of the passive dancer mechanism is to generate adequate tension in the web during the start-up. The passive dancer connected to the analog main machine controller as shown in the Fig. 3.13. Main machine controller helps to adjust the air pressure in the passive dancer that helps to change the reference tensions in endless web line. The passive dancer mechanism can also be used to generate periodic tension disturbances when its roller has a non-uniform roll surface. The period of the tension disturbance generated this way depends on the velocity of the web, which is shown in the tension control experimental data. The endless web line

has two main control elements:

1. Active dancer system
2. Web guide system

3.1.1 Active Dancer System

Active dancer system consists of an actuator, CSP-01 signal processor and load cells immediately downstream of the dancer roller. A functional sketch of the experimental web platform for the active dancer is shown in Fig. 3.2.

A block diagram of the tension control system using an active dancer is shown in Fig. 3.3. The main objective of the active dancer system is to reject the tensions disturbances generated in the processing line. The web dynamics has the features of a low-pass filter. Hence, the common disturbances are low frequency periodic plant disturbance and high frequency sensor noise. A low-pass filter can be used to kill the high frequency sensor noise and the active dancer can be employed to kill the low frequency plant disturbances. In our experimental setup the low frequency plant disturbance is generated by a roller with uneven surface as shown in Fig. 3.1. A description of the components in the active dancer system is given below:

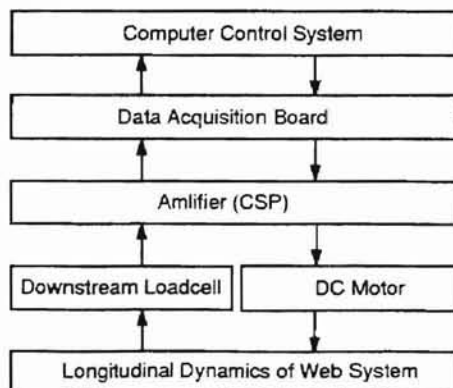


Figure 3.3: Schematic of active dancer tension control system

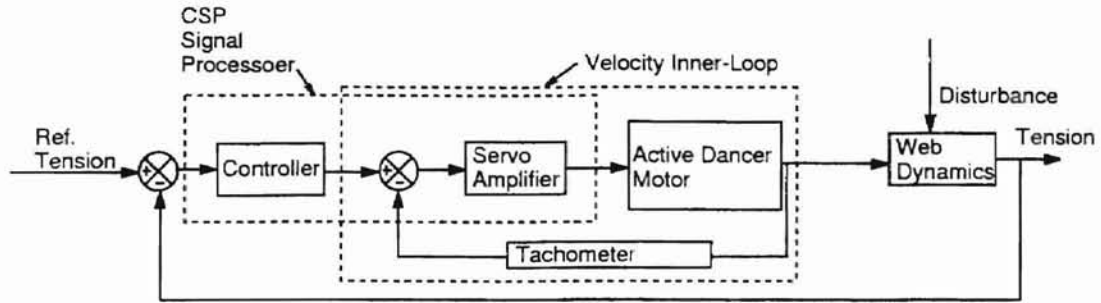


Figure 3.4: Block diagram of the tension control system

- **Fife Actuator**

The dancer roller is mounted on the Fife actuator. The Fife CSP-01 signal processor is just used as an amplifier to the DC motor. DC motor drives the dancer roller to attenuate the tension disturbances in web process line. The motor velocity is based on the control signal from the computer. The feedback web tension disturbances measured from the downstream load cell. The DC motor velocity proportional to the input voltage and Fig. 3.12 shows calibration data for motor tachometer.

- **Load Cells**

The web line has load cells downstream and upstream of the actuator to measure tension disturbances. Cleveland-Kidder Tensi-Master stationary shaft transducers are mounted in downstream to the dancer roller. The wrap angle in the roller that load cells mounted is 180° to measure the highest tension and reduce the slippage in-between roller and web span. In this experiment two load cells are used to get accurate linear tension data. The two transducers make the complete Winston-bridge that measures the force independent of the position of its application.

- **Amplifier**

The active dancer contains Cleveland-Kidder Tensi-Master Din-Rail Amplifier as a part of load cells. The initial output signals of the load cells in the dancer structure

are very small. This amplifier helps us to get the higher voltage signal from the downstream load cells.

- **CSP-01**

CSP-01 signal processor used for longitudinal tension control in Fife Corporation. In this project only the amplifier in CSP-01 is used to send signal to the DC motor of the active dancer. As can be seen from Fig. 3.4, the CSP-01 processor has its own inner loop with the controller. CSP-01 is designed with internal PID controller. In our experiments internal control is by-passed and proposed controller algorithms are implemented. A block diagram of the tension control system using CSP-01 is shown in Fig. 3.2

The front panel of the CSP-01 consists of jog left/right, sensitivity adjustment, guide point adjust, null led, mode selector switch (for dancer controller in auto, manual, servo center), sensor select switch, dead band adjustment and lock led.

3.1.2 Web Guide System

Guide system is accomplished by a remotely pivoted Fife steering guide as shown in Fig. 3.1. The guide mechanism consists of a guide roller on a base which is actuated by a DC motor (not shown in the figure). An edge sensor downstream of the guide roller gives the web lateral position. From a control point of view, the Fife analog control system is given by the sketch shown in Fig. 3.5.

The Fife guide mechanism consists of an actuator and an edge sensor immediately downstream of the guide roller. Lateral control of the web in the line is accomplished using the Fife guide. A functional sketch of the experimental web platform is shown in Fig. 3.2. The physical elements of the Fife guide and their interaction is shown in Fig. 3.6. The analog lateral control system includes:

- **Fife analog signal processor(A9)**

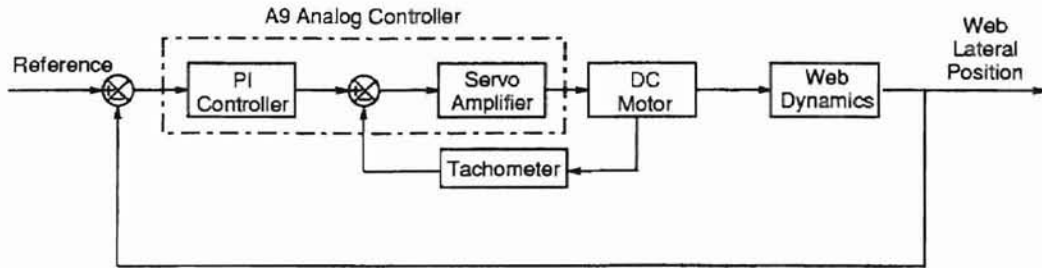


Figure 3.5: Fife analog lateral control system

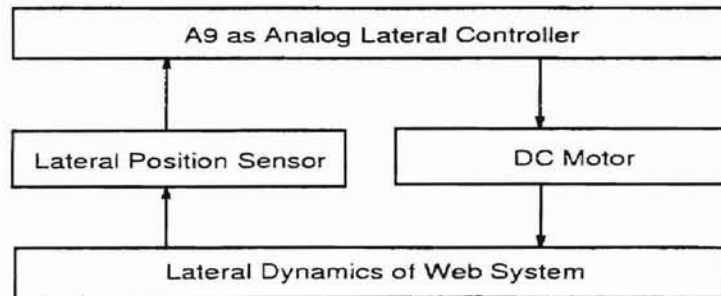


Figure 3.6: Schematic of analog lateral control system

The signal processor(A9) serves as an amplifier and an on-board analog controller. It implements a velocity inner-loop and a position outer-loop as shown in Fig. 3.5. The velocity inner-loop is used to regulate motor velocity by applying proportional control. The position outer-loop is formed by feedback of the web lateral position from the edge sensor. The outer position loop regulates the web lateral position by applying proportional control.

- **Sensors (edge sensor, tachometer)**

The edge sensor is a Fife optical position sensor which measures the lateral displacement of the web. It gives a DC voltage signal proportional to the lateral displacement of the web. The tachometer used in the velocity inner-loop gives a DC voltage proportional to the RPM of the motor.

- **The DC motor**

This motor moves the guide roller to adjust the lateral position of the web based on the control signal from the signal processor(A9).

To obtain an open-architecture computer control system, the analog controller of the A9 processor is bypassed and instead the control algorithm implemented in the computer is used. So, when the computer control system is used, Fife A9 processor simply serves as an amplifier. This arrangement allows implementation of any desired control algorithm. A schematic of physical elements and their interaction in computer control system is shown in Fig. 3.7. The main component of a Fife guide system is the DC motor. A velocity

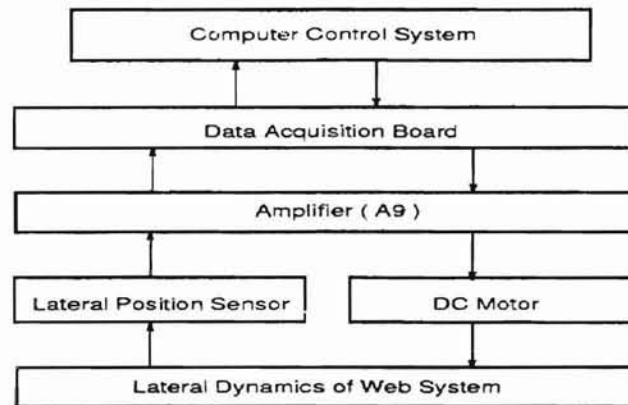


Figure 3.7: Schematic of lateral computer control system with velocity inner-loop

inner-loop is typically used to stabilize the DC motor. This requires measurement of motor velocity using a tachometer. It is typical that the tachometer may cost up to 25 percent of the cost of the DC motor setup. Considerable reduction in cost can be achieved if other means can be employed for generating a stable inner-loop without using tachometer to measure velocity. An observer is used to estimate the motor velocity [25].

3.1.3 Sensor Calibration

The sensors used in the control system typically give a voltage output. Before we use the output of the sensor in any feedback loop it is necessary to calibrate these sensors with known inputs. The open-architecture experimental platform includes the following sensors:

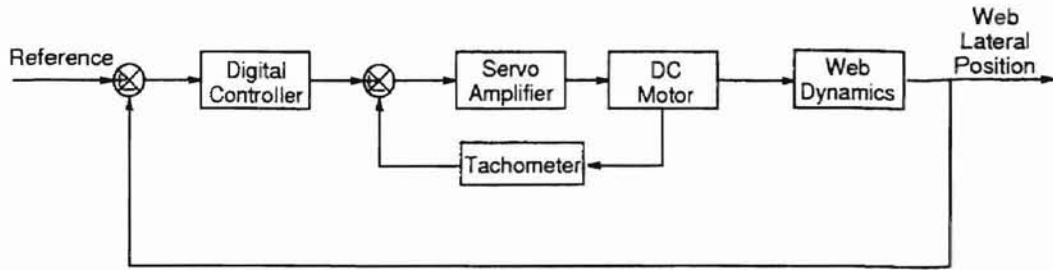


Figure 3.8: Lateral computer control system with tachometer velocity feedback

- Edge sensor: measures the lateral displacement
- Lateral motor tachometer: measures the velocity of the lateral motor
- Web velocity sensor: measures the velocity of the web
- Upstream load cell: measures the web tension upstream of the active dancer
- Downstream load cell: measures the web tension downstream of the active dancer
- Active dancer motor tachometer: measures the velocity of the active dancer motor

The web velocity sensor outputs square wave signal with its frequency proportional to the web velocity. A frequency to voltage converter chip is used to get the DC voltage output in this platform. Fig. 3.9 shows the schematic circuit.

The calibration results for the web velocity sensor, load cell, and active dancer motor tachometer are shown in Fig. 3.10, Fig. 3.11 and Fig. 3.12.

3.1.4 Computer System

The computer system is a 450 MHz Pentium computer with a digital data acquisition board. The data acquisition board is a Keithley DAS 1601, which consists of eight A/D and two D/A channels. The two D/A channels are used to send control input to the amplifiers of the guide actuator and the active dancer motor. The eight A/D channels are used to acquire the sensor signals. The distribution of the A/D and D/A channels are given in the following.

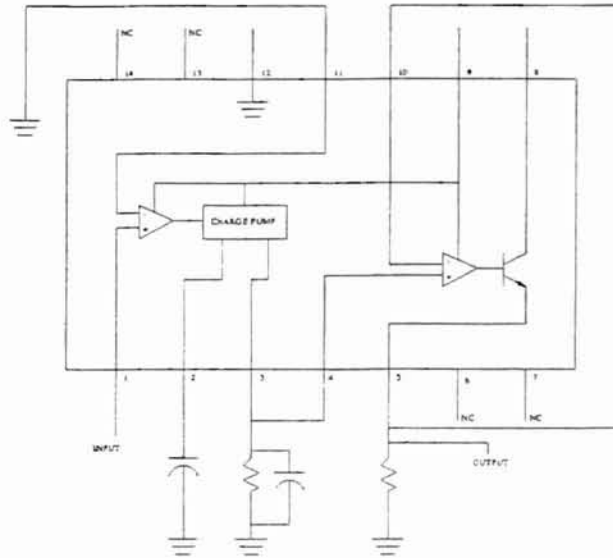


Figure 3.9: Schematic diagram for processing web velocity output

A/D Channel Configuration

The A/D channel configuration is shown in Fig. 3.13

- Channel 0 : Web Velocity Sensor
- Channel 1 : Lateral Control Motor Tachometer
- Channel 2 : None
- Channel 3 : Upstream Load-cell
- Channel 4 : Dancer Motor Tachometer
- Channel 5 : Downstream Load-cell
- Channel 6 : Upstream Load-cell
- Channel 7 : Edge Sensor

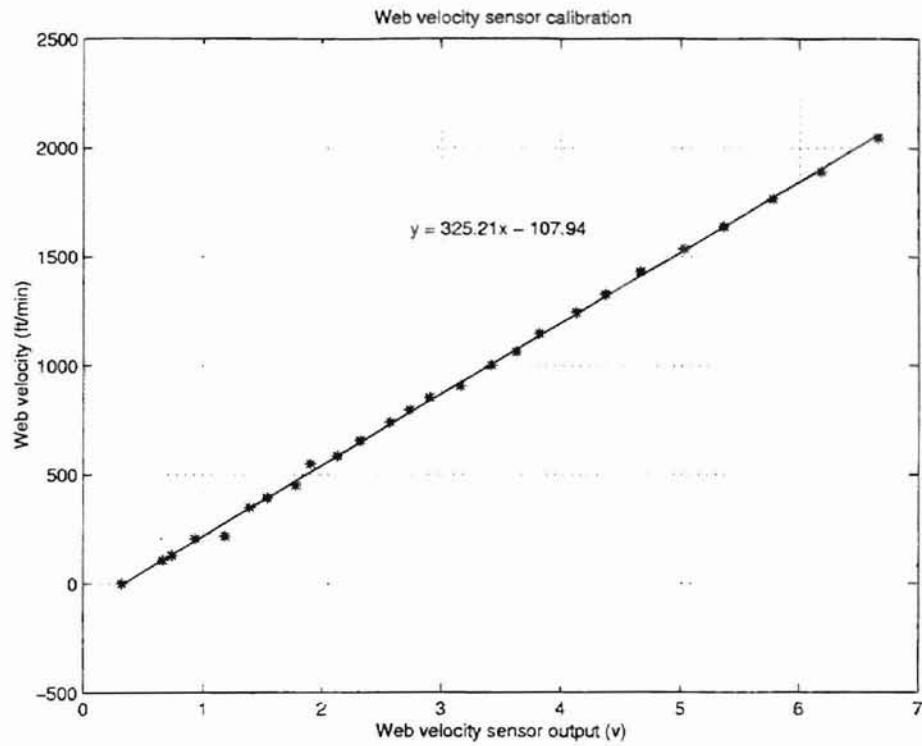


Figure 3.10: Calibration of web velocity sensor

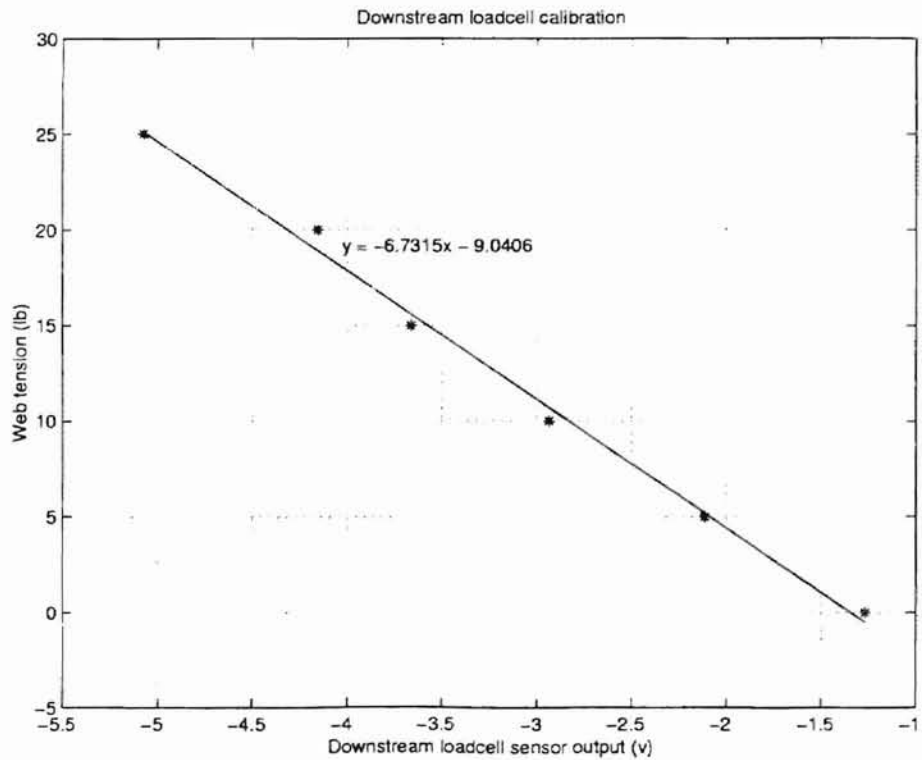


Figure 3.11: Calibration of loadcell

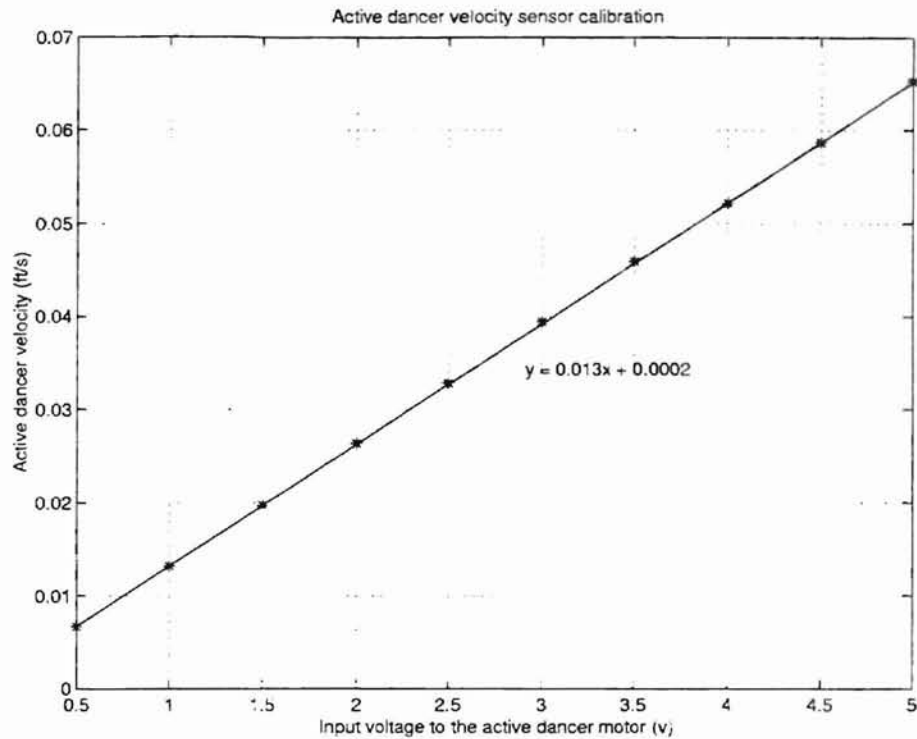


Figure 3.12: Calibration of active dancer velocity input

D/A Channel Configuration

The D/A channel configuration is also shown in Fig. 3.13

- Channel 0 : Dancer Motor
- Channel 1 : Lateral Control Motor

3.2 Software Structure

The software for real-time control and data analysis is written in C++ programming language, and can be divided into off-line software and real-time software as shown in Fig. 3.14. MATLAB software and C++ programming language are used for data analysis and off-line simulation. The real-time software, which is written in C++ based on Windows platform, implements the following functions in a modular way:

1. data acquisition and processing

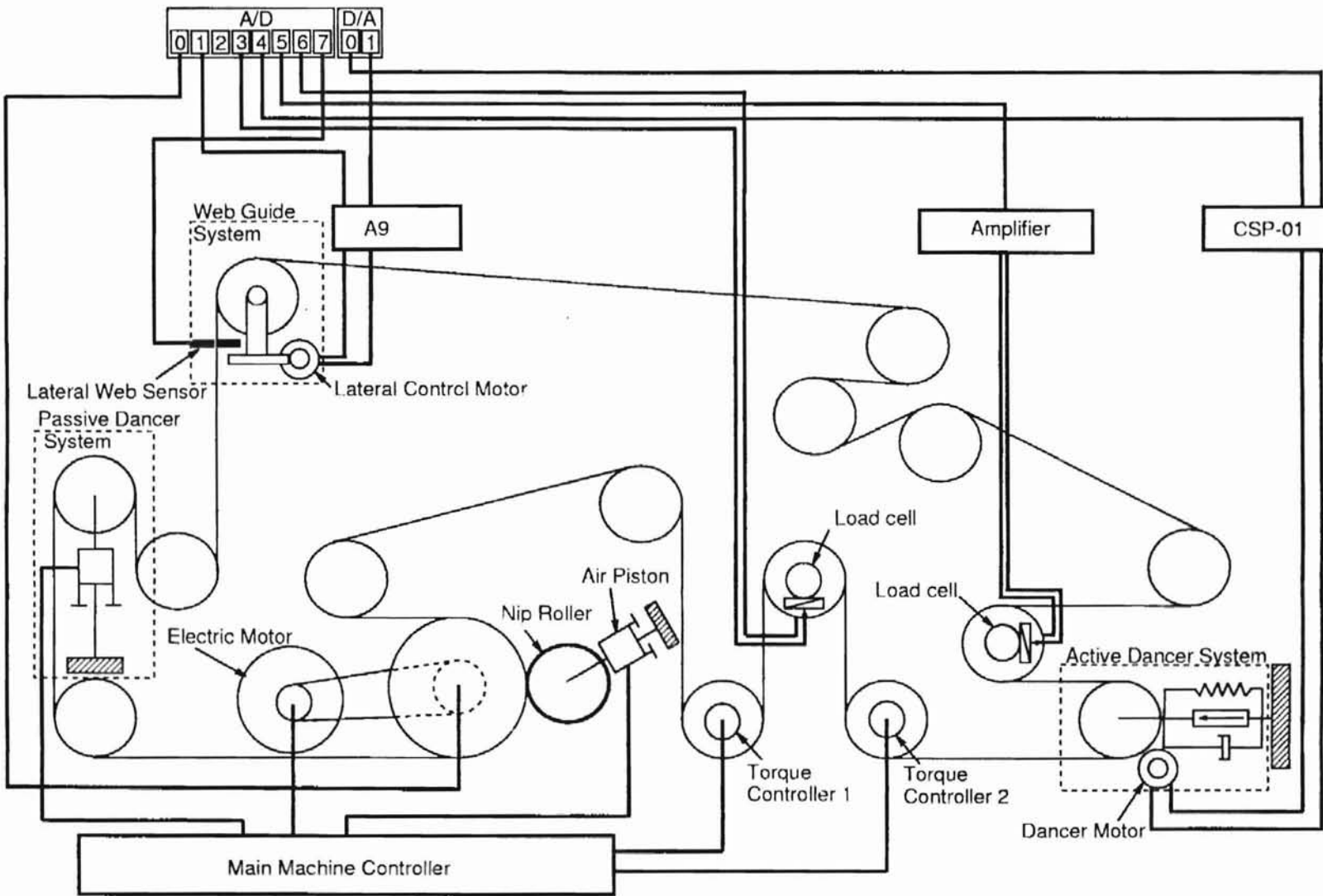


Figure 3.13: A/D and D/A channel configuration

2. real-time data display and plotting
3. control algorithm
4. state observer algorithm
5. control signal output
6. timer interrupt
7. human-machine interface
8. database maintenance

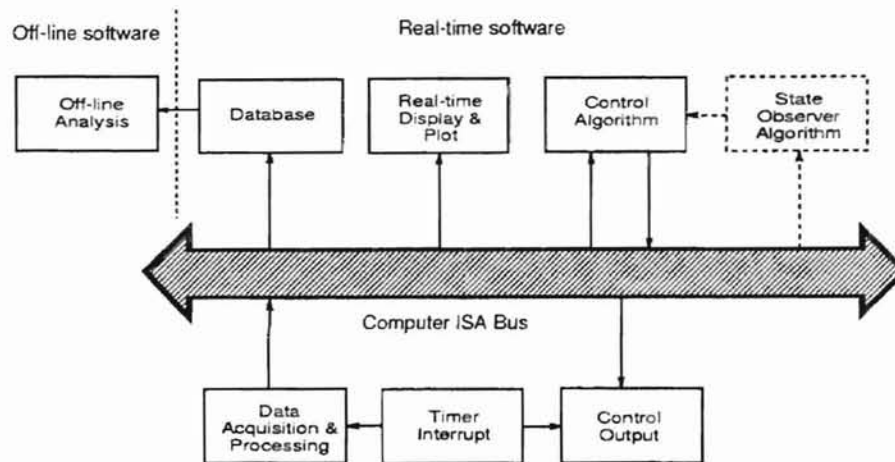


Figure 3.14: Software structure

3.2.1 Real-time Software

The individual blocks of the real-time software shown in Fig. 3.14 are explained in the following sections:

1. Data acquisition and processing

At each sampling time, current information on web lateral position (for lateral control) and web tension (for tension control) are read from A/D channels on the digital

data acquisition board. More specifically, the information collected includes: the lateral positional signal from edge sensor, the tachometer signal from the DC motor of Kamberoller guide, tension information from upstream load cell and downstream load cell, tachometer signal from the DC motor of the active dancer mechanism, and web velocity from the velocity sensor. The supporting software for this function module is DAS-1600/1400 series standard software package, which is shipped with the data acquisition board. This software package includes support functions for Microsoft Windows and function libraries for writing application programs under *WindowsTM* in Visual C++.

2. Real-time display and plot

Based on the data acquired through data acquisition board, real-time information on web tension and lateral position is plotted so that the users can have a direct sense on the performance of the control designs. Other parameters such as controller gains are displayed on computer screen, and can be modified in real time.

3. Control algorithm

This block implements the control algorithm via a control function. The function can be modified based on the design of the controller.

4. State Observer Algorithm

This block contains function for implementation of a minimum-order observer to estimate the motor velocity. The inputs to this function at each sampling period are the web lateral position and the control input to the DC motor. The motor velocity is estimated in real-time in this functional block.

5. Control signal Output

During each sampling period, after the control algorithm is evaluated, the control signals are output through D/A channels on the digital data acquisition board, and

then sent out to DC motors after amplification to drive the active dancer (for tension control) and Kamberoller guide (for lateral control).

6. Timer interrupt

Timer interrupt serves as the "clock" of the real-time control system. As shown in Fig. 3.14, timer interrupt determines both the sampling period and the control period of the computer-control system. For all the control experiments, the sampling period and the control period are the same, and is taken to be 5 milliseconds. It is well known that when a continuous-time system is discretized, if the sampling frequency is not fast enough, then discretized control system can become unstable. From the well known Shannon sampling condition, we know that the sampling frequency should be at least twice the highest frequency content of the measured signal. Considering the dynamic characteristics of the web system, the chosen sampling frequency of 200 Hz is fast enough. Moreover, since computer control is used, the sampling period can be set at any value by just a change of the variable in the real-time control program.

7. Database Maintenance

Data from the sensor signals acquired from A/D channels is written into a database for later off-line analysis, which is mainly performed using MATLAB.

CHAPTER 4

CONTROL DESIGN AND EXPERIMENTAL RESULTS

This chapter discusses the control designs for the active dancer system and experimental results. Three different controllers are considered for the active dancer experiment. These are: (1) Proportional-Integral-Derivative (PID) Controller, (2) Internal Model Controller (IMC), and (3) Linear Quadratic Optimal Controller (LQR). PID control is very well known in industry and is extensively used. The Internal Model Controller is a modified version of PID controller, wherein an internal model of the disturbance is embedded into the controller. The Linear Quadratic Optimal Controller is a state feedback controller that is based on minimizing a quadratic performance index. The performance index places constraints on both the state variables of interest and the input variable. LQR type of controllers are becoming popular as they provide some inherent robustness to the closed-loop system, such as providing some guaranteed phase and gain margins.

The outline of this chapter is follows. Section 4.1 presents the controller design. Subsection 4.1.1 deals with the state space model considered for the controller design. PID controller is discussed in subsection 4.1.2 and IMC and LQR controllers are presented in subsection 4.1.2 and 4.1.3, respectively. Section 4.2 presents the experimental results. Subsection 4.2.1 deals with the effects of dancer movement. Results of the controller implemented on the web line are presented on section 4.2.2. Finally, section 4.2.3 presents a comparison of the three controllers.

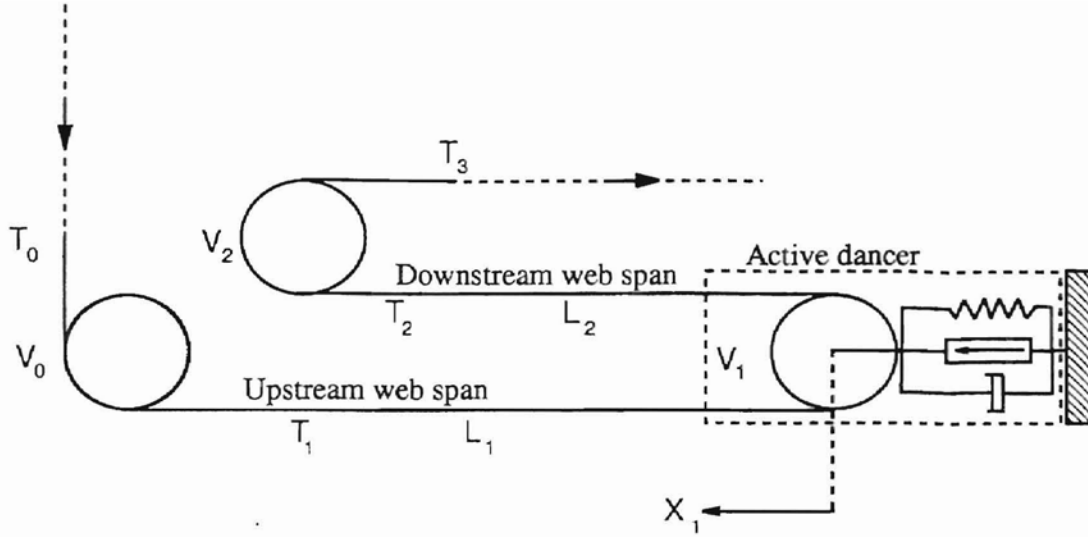


Figure 4.1: Active dancer system

4.1 Controller Design

4.1.1 State-space Model for Active Dancer System

From the previous chapter the state space model of the dancer system is

$$\dot{Q}(t) = \mathbf{A}Q(t) + \mathbf{B}_u U(t) + \mathbf{B}_w W(t) \quad (4.1)$$

$$y(t) = \mathbf{C}Q(t) + \mathbf{D}_u U(t) + \mathbf{D}_w W(t) \quad (4.2)$$

where

$$\mathbf{A} = \begin{bmatrix} 0 & \frac{1}{\beta} & 0 & 0 & 0 \\ -\frac{\alpha}{\tau_1} & -\frac{1}{\tau_1} & \frac{\alpha}{\tau_1} & 0 & 0 \\ 0 & -\frac{1}{\beta} & -\frac{\gamma}{\beta} & \frac{1}{\beta} & 0 \\ 0 & \frac{1}{\tau_2} & -\frac{\alpha}{\tau_2} & -\frac{1}{\tau_2} & \frac{\alpha}{\tau_2} \\ 0 & 0 & 0 & -\frac{1}{\beta} & 0 \end{bmatrix} \quad \mathbf{B}_u = \begin{bmatrix} -\frac{1}{\tau_1} \\ \frac{\alpha}{\tau_1} \\ 0 \\ \frac{\alpha}{\tau_2} \\ \frac{1}{\tau_2} - \frac{1}{\tau_1} \end{bmatrix} \quad \mathbf{B}_w = \begin{bmatrix} \frac{1}{\beta} & 0 \\ \frac{1}{\tau_1} & 0 \\ 0 & 0 \\ 0 & 0 \\ 0 & \frac{1}{\beta} \end{bmatrix} \quad (4.3)$$

$$\mathbf{C} = \begin{bmatrix} 0 & 0 & 0 & 1 & 0 \end{bmatrix} \quad \mathbf{D}_u = \begin{bmatrix} 0 \end{bmatrix} \quad \mathbf{D}_w = \begin{bmatrix} 0 & 1 \end{bmatrix} \quad (4.4)$$

Notice that the state-space model for the active dancer system is obtained by assuming that load cells measure the sum of the tensions $T_2(t)$ and $T_3(t)$.

4.1.2 PID Controller

PID controller is one of the most widely used controllers in industry whose form in continuous-time domain is given by

$$U(t) = K_p E(t) + K_i \int_0^t E(t) dt + K_d \frac{dE(t)}{dt} \quad (4.5)$$

where $U(t)$ is the control input to the plant and $E(t)$ is the feedback error signal. The constants K_p , K_i and K_d are chosen appropriately to provide the desired behavior. The discrete-time version of the PID controller is

$$U(k) = K_p E(k) + K_i T_s \sum_{j=1}^k E(j) + K_d \left(\frac{E(k) - E(k-1)}{T_s} \right) \quad (4.6)$$

where T_s is the sampling period. The controller can be expressed in z-domain as

$$U(z) = \left(K_p + K_i \frac{T_s z}{z-1} + \frac{K_d (z-1)}{T_s z} \right) E(z) \quad (4.7)$$

The control algorithm for real-time implementation can be written as

$$U(k) = U(k-1) + \left(K_p + K_i T_s + \frac{K_d}{T_s} \right) E(k) - \left(K_p + 2 \frac{K_d}{T_s} \right) E(k-1) + \frac{K_d}{T_s} E(k-2) \quad (4.8)$$

4.1.3 IMC Controller

In this type of controller, a PI or PID type controller is augmented with an internal model of the disturbance. IMC controller is useful when the disturbance is partially or completely known. For example, this type of controller can be used to reject/attenuate periodic tension disturbances whose amplitude is unknown but whose frequency is known. The motivation for adding an internal model of the disturbance is given in the following. Consider a periodic tension disturbance of the form,

$$d(t) = A_d \sin(\vartheta t + \phi) \quad (4.9)$$

where A_d and ϕ are unknown. Figure 4.2 represents a closed-loop system with $G_p(s)$ as the plant and $G_c(s)$ as the controller. The control objective is to choose $G_c(s)$ such that periodic disturbances of the form $d(t)$ do not appear in the output. The closed-loop transfer

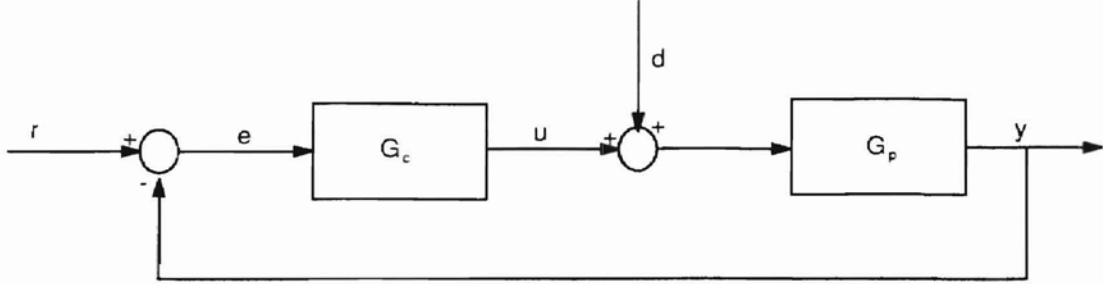


Figure 4.2: Active dancer tension control system

function from $D(s)$ to $E(s)$ is given by

$$\frac{E(s)}{D(s)} = -\frac{G_p(s)}{1 + G_c(s)G_p(s)} \quad (4.10)$$

Substituting $s = j\varpi$, we obtain

$$E(j\varpi) = -\frac{G_p(j\varpi)}{1 + G_c(j\varpi)G_p(j\varpi)}D(j\varpi) \quad (4.11)$$

To reject a disturbance at particular frequency $\varpi = \vartheta$, we should have $E(j\vartheta) = 0$. Therefore, the choice of the controller is such that $G_c(j\vartheta) = \infty$, i.e., $G_c(s)$ has a pair of poles at $s = \pm j\vartheta$. A discrete-time equivalent to the above continuous-time disturbance is

$$D(k) = A_d \sin(\varpi k T_s) \quad (4.12)$$

where T_s is the sampling period. The disturbance $D(k)$ in the z-domain is

$$D(z) = \frac{z^{-1}A_d \sin(\varpi T_s)}{1 - 2z^{-1} \cos(\varpi T_s) + z^{-2}} \quad (4.13)$$

To reject this periodic disturbance, $G_c(z)$ should include the model of the disturbance. Let $G_p(z)$ be the discrete equivalent of $G_p(s)$, then

$$Y(z) = G_p(z)(D(z) + G_c(z)E(z)) \quad (4.14)$$

Assuming the reference to be zero gives $E(z) = -Y(z)$. The transfer function from the disturbance input to the error is given by the following:

$$E(z) = -\frac{G_p(z)}{1 + G_p(z)G_c(z)}D(z). \quad (4.15)$$

Consider the following controller

$$G_c(z) = \frac{K_p + z^{-1}K_{imc} \sin(\varpi T_s)}{1 - 2z^{-1} \cos(\varpi T_s) + z^{-2}} \quad (4.16)$$

where K_p is the proportional gain and K_{imc} is the tunable gain to compensate for the amplitude of the sinusoidal disturbance. With the choice of $G_c(z)$ as given in (4.16), $G_c(z) = \infty$ when $z = \cos(\vartheta T_s) + j \sin(\vartheta T_s)$. Since $U(z) = G_c(z)E(z)$. The control algorithm for real-time implementation is

$$U(k) = [2 \cos(\varpi T_s)]U(k-1) - U(k-2) + K_{imc}[\sin(\varpi T_s)]E(k-1) + K_p E(k) \quad (4.17)$$

4.1.4 LQR Controller

Recall the continuous-time state space model given by (2.20)

$$\dot{Q} = \mathbf{A}Q + \mathbf{B}_u U + \mathbf{B}_w W \quad (4.18)$$

A discrete-time system equivalent to the above continuous-time system is

$$\xi(k+1) = \mathbf{G}\xi(k) + \mathbf{H}_u U(k) + \mathbf{H}_w W(k) \quad (4.19)$$

where

$$\mathbf{G} = e^{\mathbf{A}T_s}, \quad \mathbf{H}_u = \int_0^{T_s} e^{\mathbf{A}\varpi} \mathbf{B}_u d\varpi, \quad \text{and,} \quad \mathbf{H}_w = \int_0^{T_s} e^{\mathbf{A}\varpi} \mathbf{B}_w d\varpi$$

where T_s is the sampling period.

The traditional stationary linear quadratic (LQ) problem is to find the control input that minimizes the performance index,

$$\mathbf{J} = \frac{1}{2} \sum_{k=0}^{\infty} [\xi^*(k) \mathbf{Q}_{lqr} \xi(k) + U^*(k) \mathbf{R}_{lqr} U(k)] \quad (4.20)$$

where \mathbf{Q}_{lqr} and \mathbf{R}_{lqr} , which are chosen to place constraints on a choice of state variables and input variable, respectively. The control input that results from minimizing the above performance index is a state feedback controller of the form,

$$U(k) = -\mathbf{K}\xi(k) \quad (4.21)$$

where \mathbf{K} is the optimal gain vector given by

$$\mathbf{K} = (\mathbf{R}_{lqr} + \mathbf{H}_u^* \mathbf{P}_\infty \mathbf{H}_u)^{-1} \mathbf{H}_u^* \mathbf{P}_\infty \mathbf{G}$$

and \mathbf{P}_∞ is the solution of the following Algebraic Ricatti equation,

$$\mathbf{P}_\infty = \mathbf{Q}_{lqr} + \mathbf{G}^* \mathbf{P}_\infty \mathbf{G} - \mathbf{G}^* \mathbf{P}_\infty \mathbf{H}_u (\mathbf{R}_{lqr} + \mathbf{H}_u^* \mathbf{P}_\infty \mathbf{H}_u)^{-1} \mathbf{H}_u^* \mathbf{P}_\infty \mathbf{G}$$

Notice that the LQR controller requires measurement of all the state variables to implement the control input given by (4.21). If all the state variables are not measured, which is typically the case, an observer can be designed to estimate the state variables. In the case of the active dancer system, measurement of the dancer rotational velocity (V_2) and the downstream web tension (T_2) would render the system observable. An observer can be designed to estimate the state variables based on the measured variables. Consider the measurements given by the following equation,

$$y(k) = \mathbf{C}\xi(k) \quad (4.22)$$

Based on the measurements, a Luenberger observer is proposed to estimate the state variables:

$$\hat{\xi}(k+1) = \mathbf{G}\hat{\xi}(k) + \mathbf{H}_u U(k) + \mathbf{L}(y(k) - \hat{y}(k)) \quad (4.23)$$

where $\hat{\xi}(k)$ is the estimated state and

$$\hat{y}(k) = \mathbf{C}\hat{\xi}(k) \quad (4.24)$$

Estimated states can be used instead of the actual states in the controller given by (4.21), i.e., the control input is modified to

$$U(k) = -\mathbf{K}\hat{\xi}(k) \quad (4.25)$$

To answer the question of whether estimated states can be used instead of the actual states, we proceed to find the closed-loop error dynamics consisting of the plant, controller, and the observer. Substituting (4.22) and (4.24) into (4.23), we obtain

$$\hat{\xi}(k) = \mathbf{G}\hat{\xi}(k) + \mathbf{H}_u U(k) + \mathbf{L}\mathbf{C}(\xi(k) - \hat{\xi}(k)) \quad (4.26)$$

where \mathbf{L} is the observer gain. Define the estimation error as $\hat{E}(k) = \xi(k) - \hat{\xi}(k)$. Then, the estimation error dynamics is given by

$$\hat{\xi}(k+1) = (\mathbf{G} - \mathbf{L}\mathbf{C})\hat{\xi}(k) + \mathbf{H}_w W(k) \quad (4.27)$$

where the eigenvalues of the matrix $\mathbf{G} - \mathbf{L}\mathbf{C}$ are the observer poles and can be placed anywhere within the unit circle in the complex z-plane by choosing the observer gain \mathbf{L} . The control input in terms of the estimation error is given by

$$U(k) = -\mathbf{K}\hat{\xi}(k) = -\mathbf{K}\xi(k) + \mathbf{K}\hat{E}(k) = \begin{bmatrix} -\mathbf{K} & \mathbf{K} \end{bmatrix} \begin{bmatrix} \xi(k) \\ \hat{E}(k) \end{bmatrix} \quad (4.28)$$

The closed-loop error dynamics can be written in matrix form as

$$\begin{bmatrix} \xi(k+1) \\ \hat{E}(k+1) \end{bmatrix} = \begin{bmatrix} \mathbf{G} - \mathbf{H}_u \mathbf{K} & \mathbf{H}_u \mathbf{K} \\ 0 & \mathbf{G} - \mathbf{L}\mathbf{C} \end{bmatrix} \begin{bmatrix} \xi(k) \\ \hat{E}(k) \end{bmatrix} + \begin{bmatrix} \mathbf{H}_w \\ \mathbf{H}_w \end{bmatrix} W(k) \quad (4.29)$$

Notice that the observer poles can be chosen independent of the controller poles in the above closed-loop error dynamics. The MATLAB program for LQR controller and Luenberger observer is given in appendix D.

4.2 Experimental Results

In the previous chapter, open architecture experimental web platform was described. This section presents the experimental results collected on the platform. Three types controllers

described in the previous section were implemented. The controllers were implemented with a control sampling period of 5 milli-seconds. Periodic tension disturbance upstream of the dancer is created by introducing an uneven roll surface into an idle roller in the web line. The roller with out-of-round roll surface is shown in Fig. 4.3. A load cell on the roll immediately downstream of the out-of-round idle roller measures the amount of tension disturbance that is being generated. The fundamental frequency of the periodic tension disturbance for a given out-of-round roll surface increases with increase in web speed. In some cases periodic tension disturbance is also generated using an out-of-round roll surface on the passive dancer roller shown in Fig. 4.3. A representative sample of the experimental results from both the cases of tension disturbance generation are shown and discussed in the following.

For the case of tension disturbance generation by the out-of-round passive dancer roller, a summary of the amount of tension disturbance magnitude reduction for PID and IMC controllers for three different web speeds (300 FPM, 350 FPM, and 400 FPM) is shown in Fig. 4.4. Results of each individual experiment are shown in Fig. 4.5 through Fig. 4.10. In all the plots, the top two graphs pertain to measured tension and its fast fourier transform (FFT) downstream of the active dancer roller when the active dancer is not actuated; and the bottom two plots correspond to the measured tension and its FFT with the particular controller shown for the active dancer roller. From the summary shown in Fig. 4.4 it can be observed that substantial attenuation of the tension disturbance is achieved using the active dancer for both PID and IMC controllers. The IMC controller performs better; this is due to the inclusion of the knowledge of the disturbance frequency into the IMC controller.

For the case of tension generation by the out-of-round idle roller in the web line, a summary of the amount of tension disturbance magnitude reduction for PID, IMC and LQR controllers for four different web speeds (200 FPM, 250 FPM, 300 FPM, and 350 FPM) is shown in Fig. 4.11. Results of each individual experiment are shown in Fig. 4.12 through Fig. 4.15. Summary shown in Fig. 4.11 indicates that all three controllers gave

substantial attenuation of the tension disturbance using the active dancer. Notice that at the low speed of 200 FPM, the attenuation level of all three controllers is similar but as the speed is increased the attenuation level is more for the IMC and the LQR controllers.

Since the experimental web platform contains an endless web line, it is uncertain as to how much of the tension reflected by the load cell downstream of the active dancer due to back propagation of the tension. In the case of tension disturbance generation by the out-of-round passive dancer roller, there are fewer spans between the active dancer load cell roller and the disturbance generating roller. In the case of tension disturbance generation by the out-of-round idle roller, there are more spans between the active dancer load cell roller and the idle roller going downstream from the load cell roller; so back propagation of tension disturbance may not be an issue; further the driven roller prevents such type of back propagation.

Also, notice that the experimental results indicate that the active dancer does not reject any periodic disturbances above the 10 Hz level; this is due to the bandwidth limitation of the actuator. Further, the actuator saturates above a certain value of the controller gains in each case, which negates any further tension attenuation.

In summary, experimental results show that the active dancer system is highly effective in tension disturbance attenuation. The disturbance rejection capability of the active dancer system is limited only by the bandwidth limitation of the actuator as opposed to the passive dancer or an inertia compensated dancer which have considerable resonance problems.

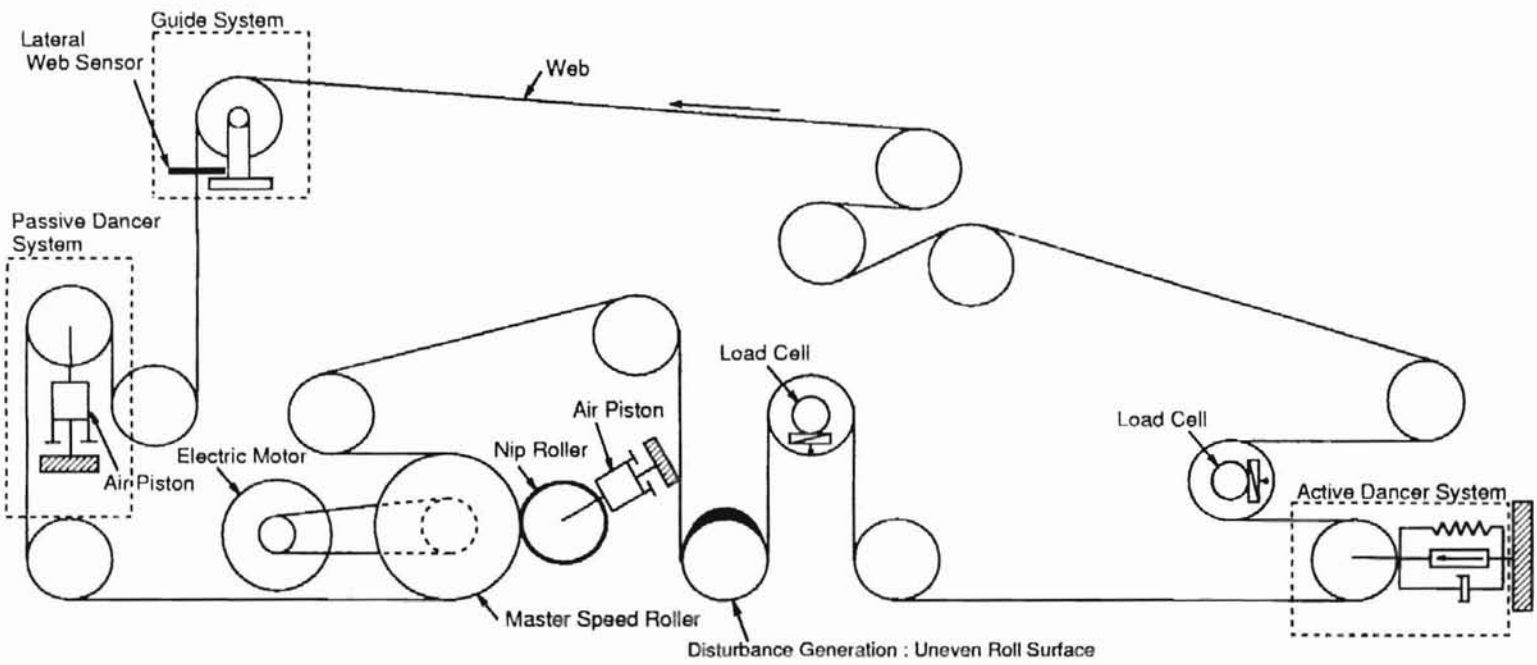


Figure 4.3: Experimental web platform with uneven roll surface

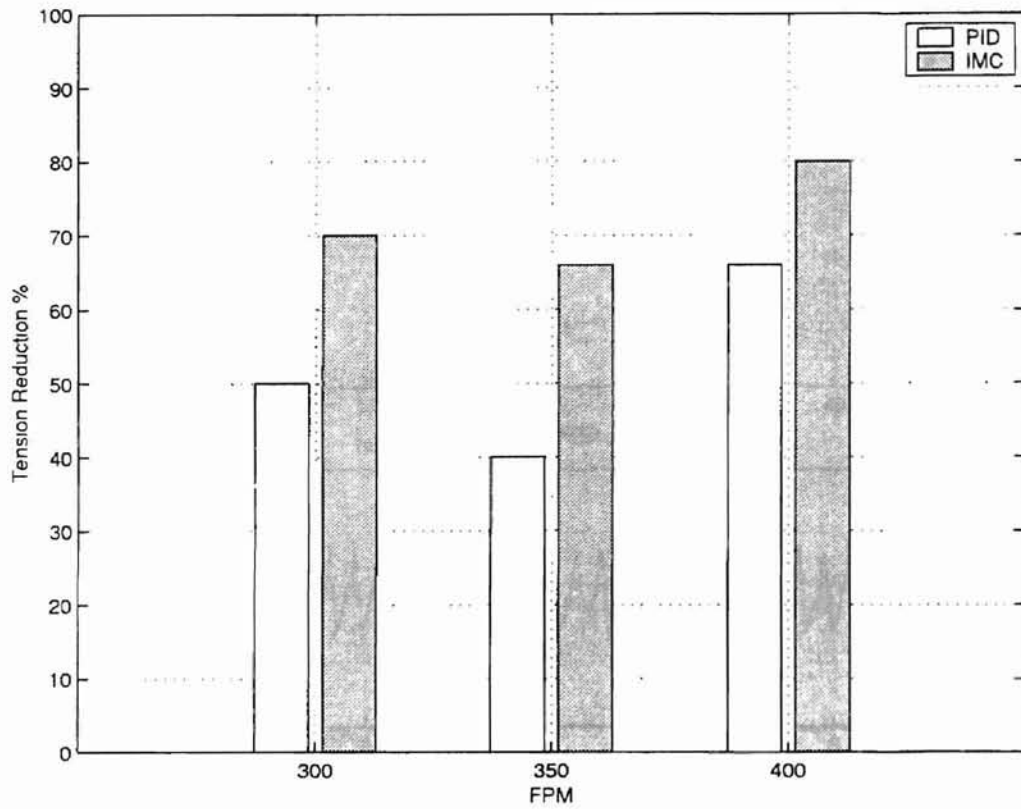


Figure 4.4: Summary of tension disturbance reduction with PID and IMC controllers; out-of-round passive dancer roller

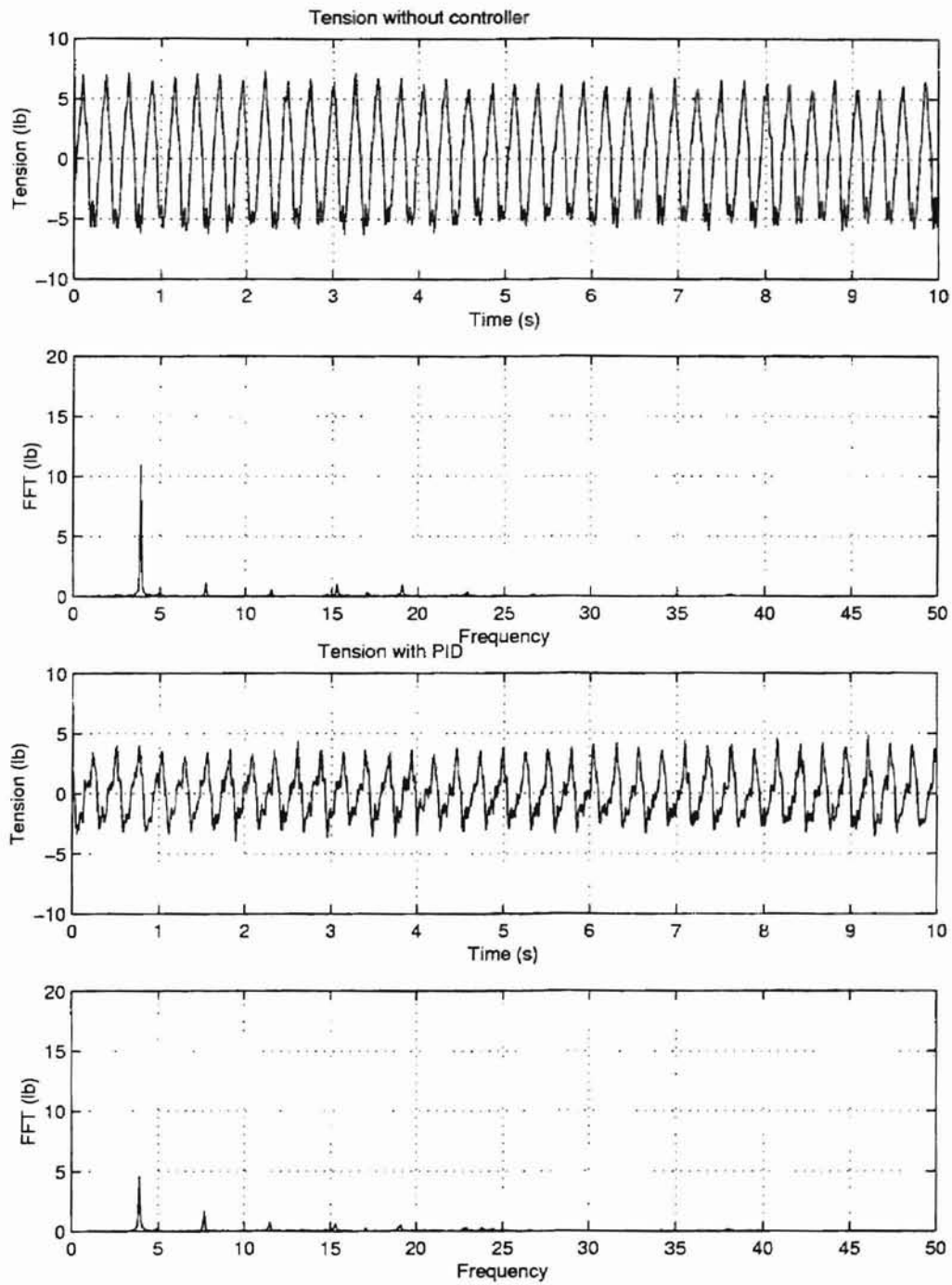


Figure 4.5: Tension with active dancer PID control; $v_r = 300$ FPM, $t_r = 18$ lb

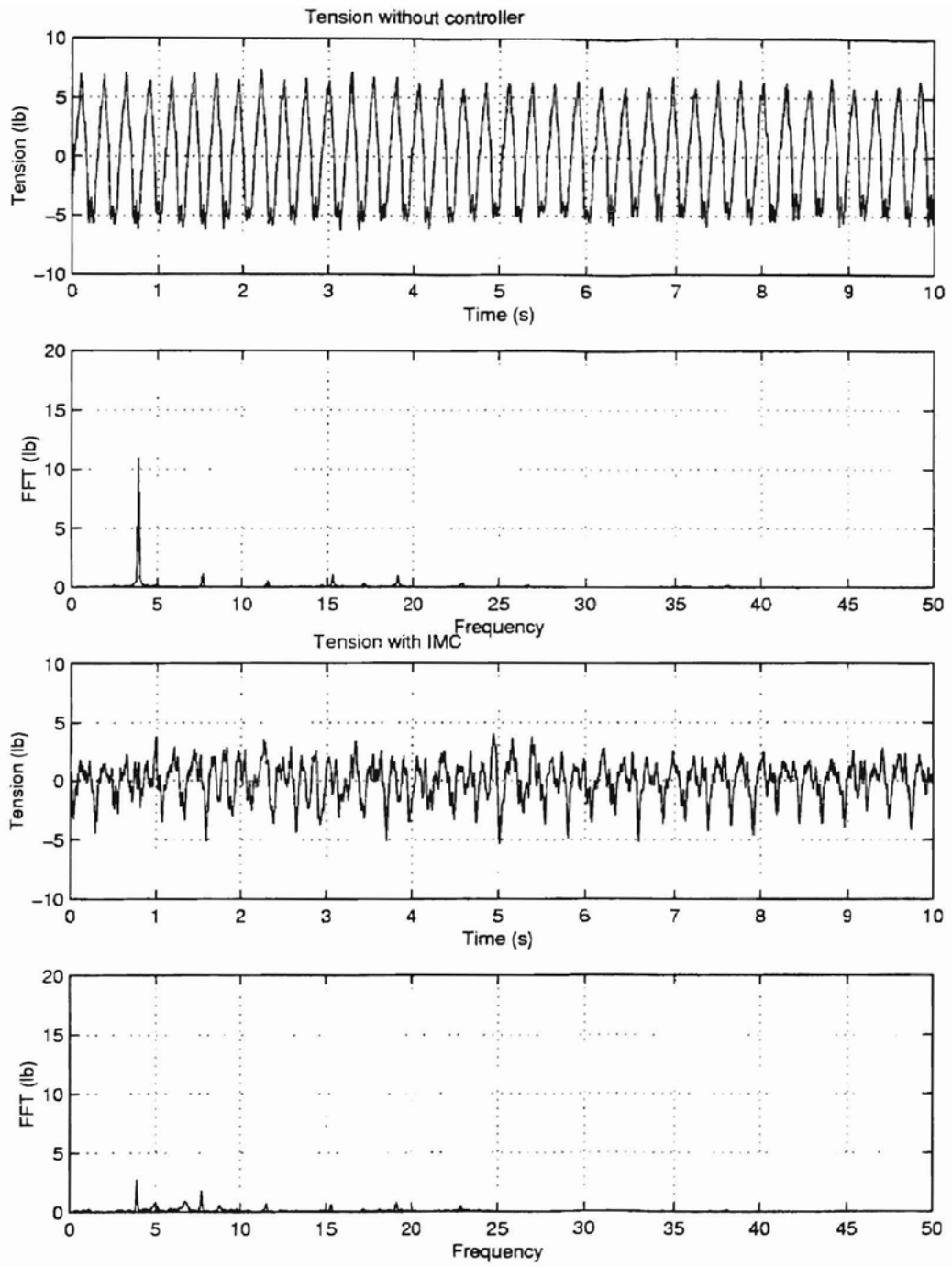


Figure 4.6: Tension with active dancer IMC control; $v_r = 300$ FPM, $t_r = 18$ lb

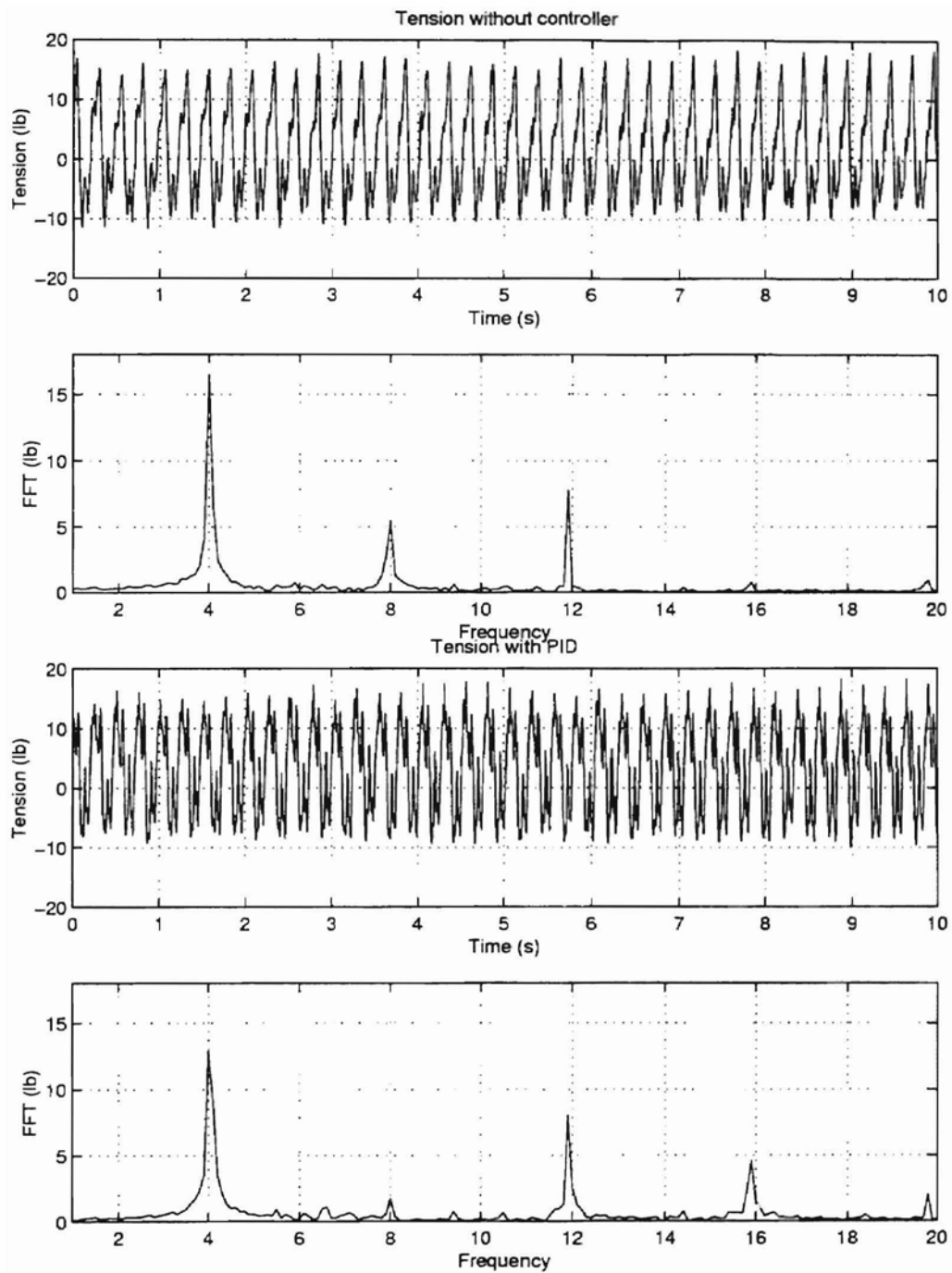


Figure 4.7: Tension with active dancer PID control; $v_r = 350$ FPM, $t_r = 25$ lb

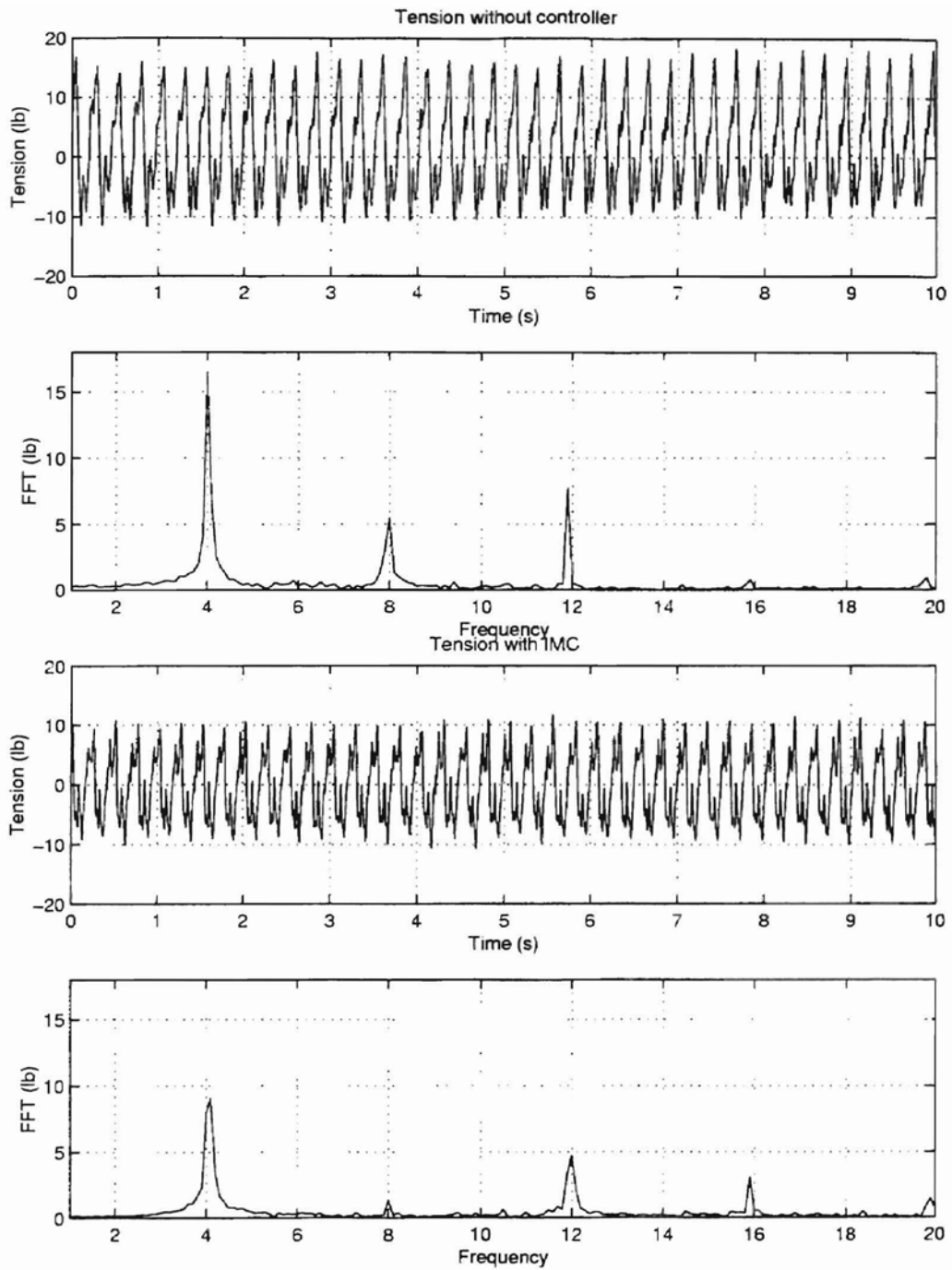


Figure 4.8: Tension with active dancer IMC control; $v_r = 350$ FPM, $t_r = 25$ lb

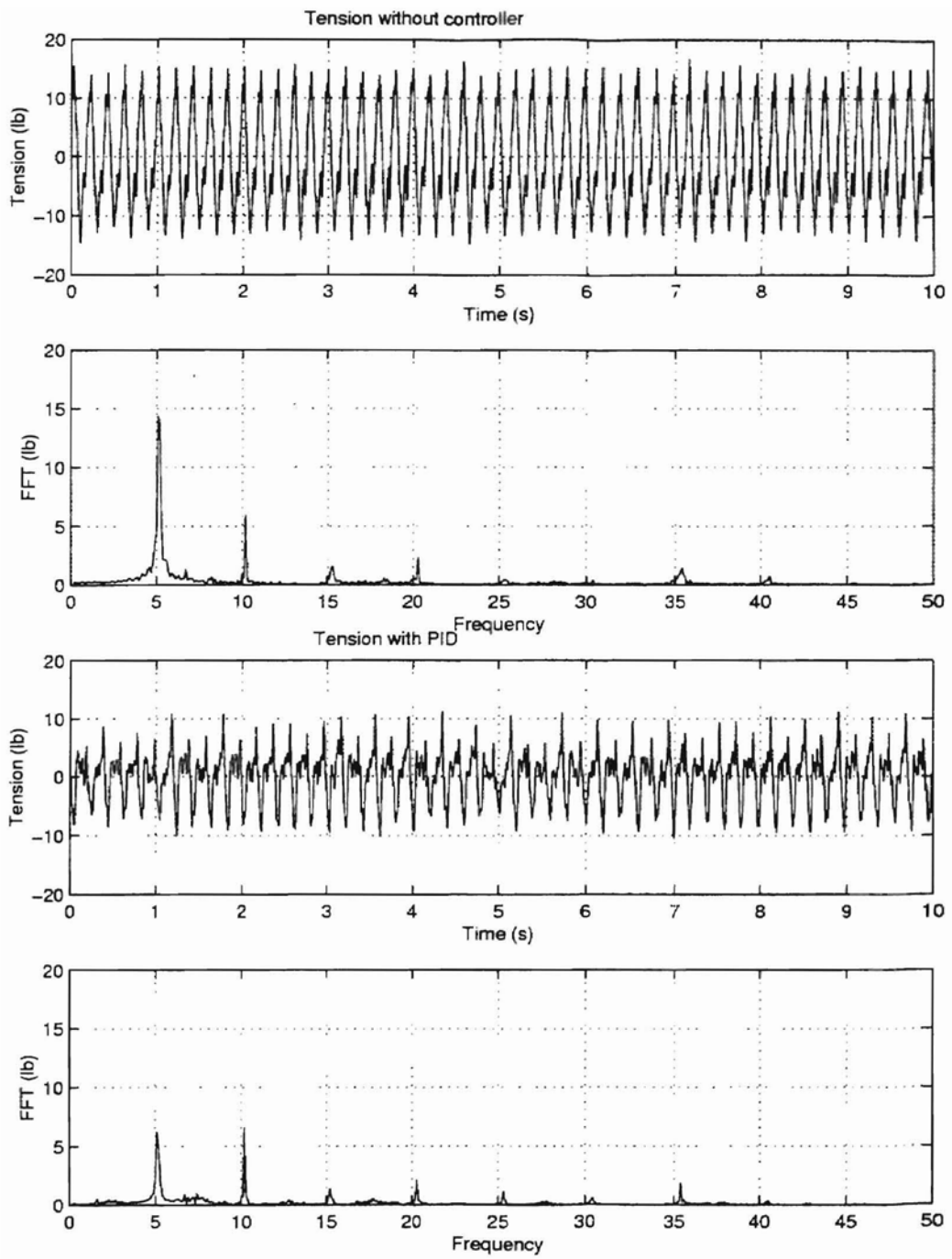


Figure 4.9: Tension with active dancer PID control; $v_r = 400$ FPM, $t_r = 26$ lb

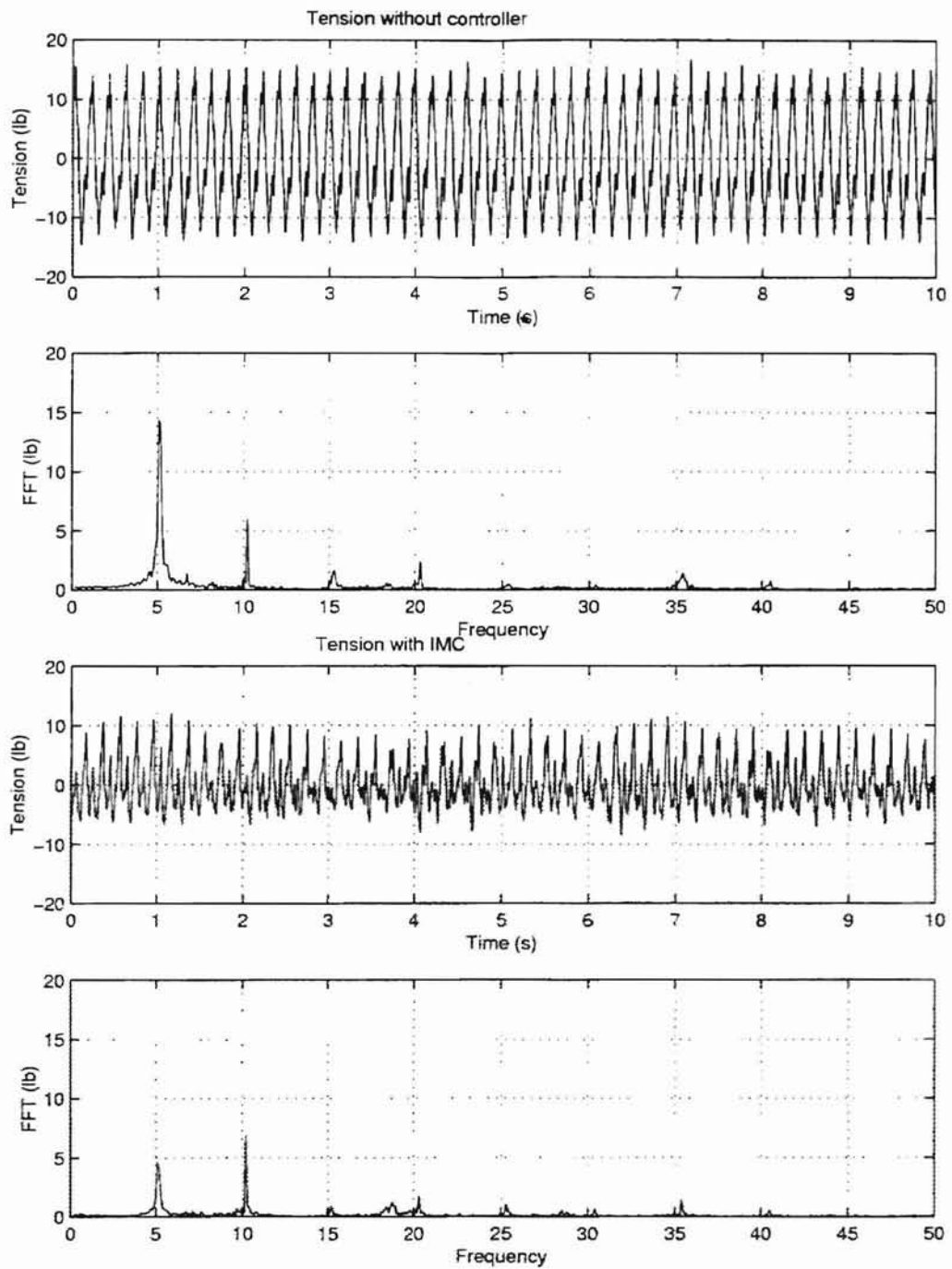


Figure 4.10: Tension with active dancer IMC control; $v_r = 400$ FPM, $t_r = 26$ lb

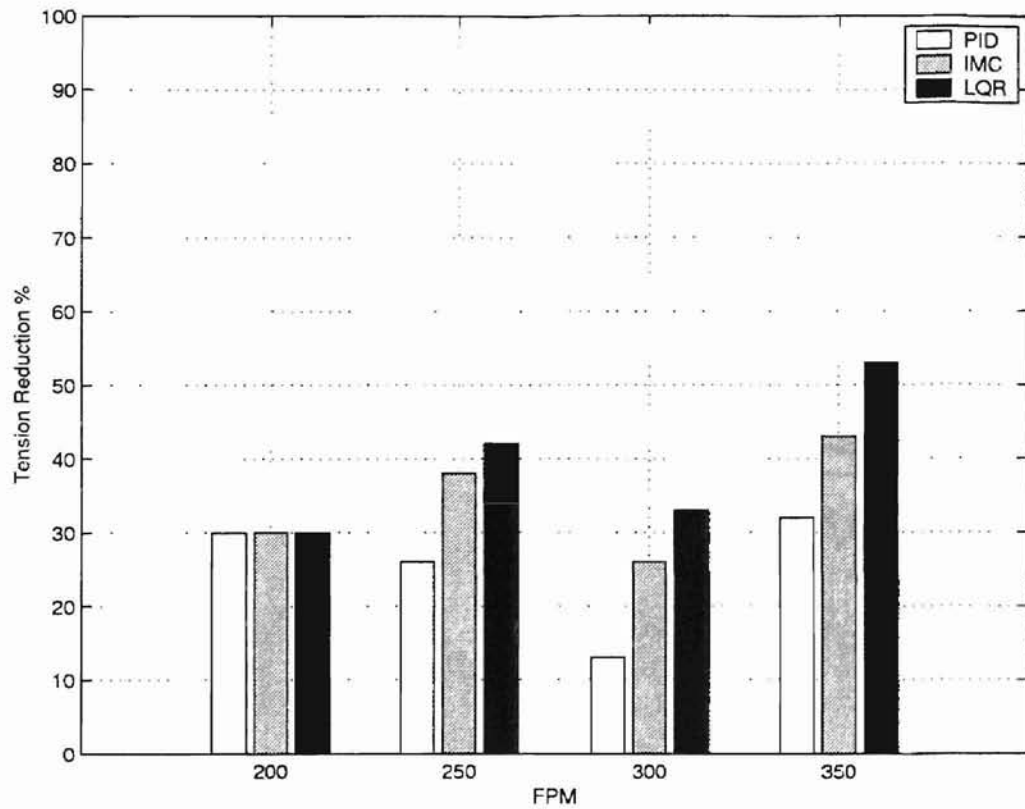


Figure 4.11: Summary of tension disturbance reduction with PID, IMC, LQR controllers; out-of-round idle roller

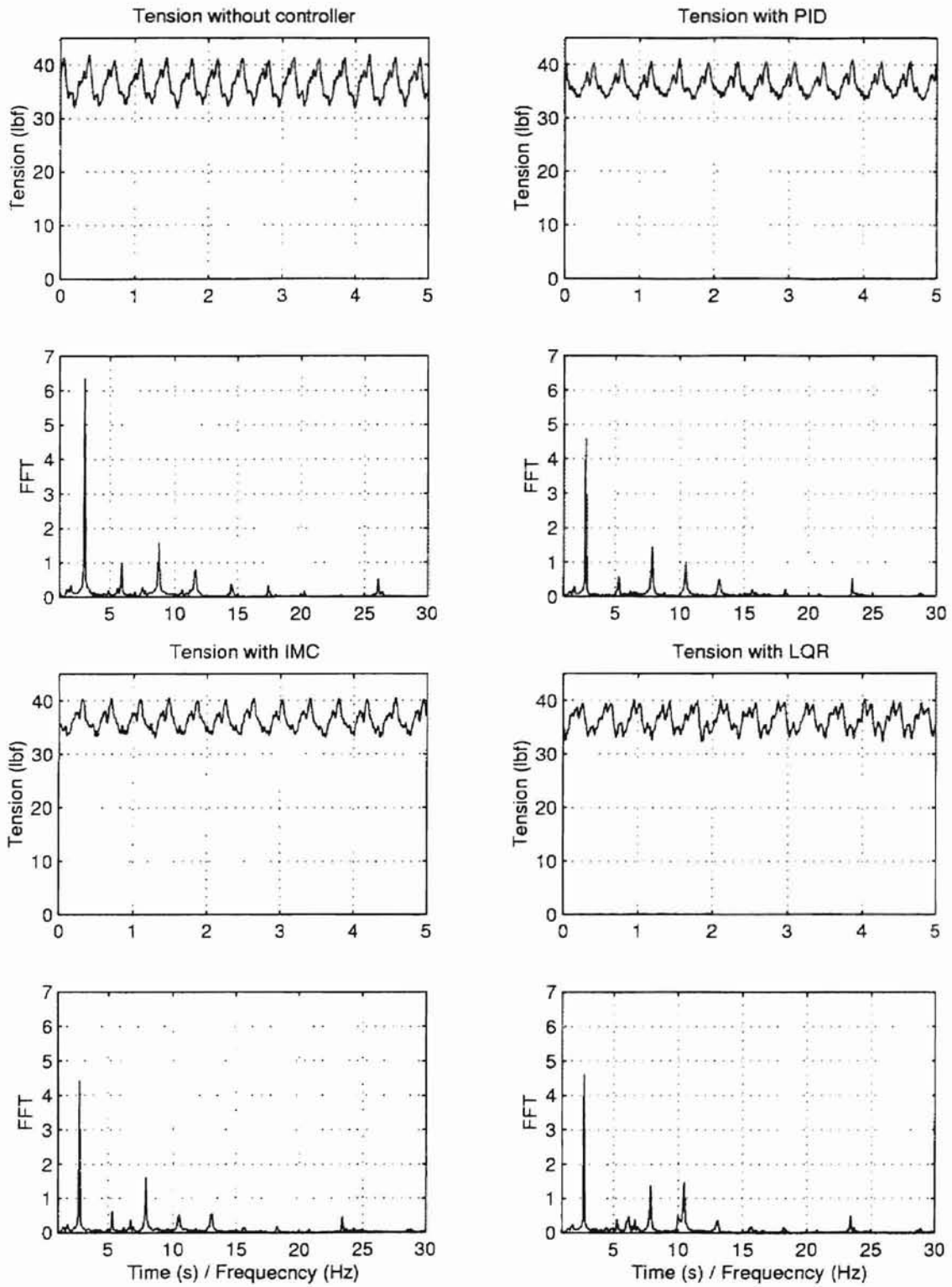


Figure 4.12: Tension with out-of-round idle roller; $v_r = 200$ FPM, $t_r = 36$ lb

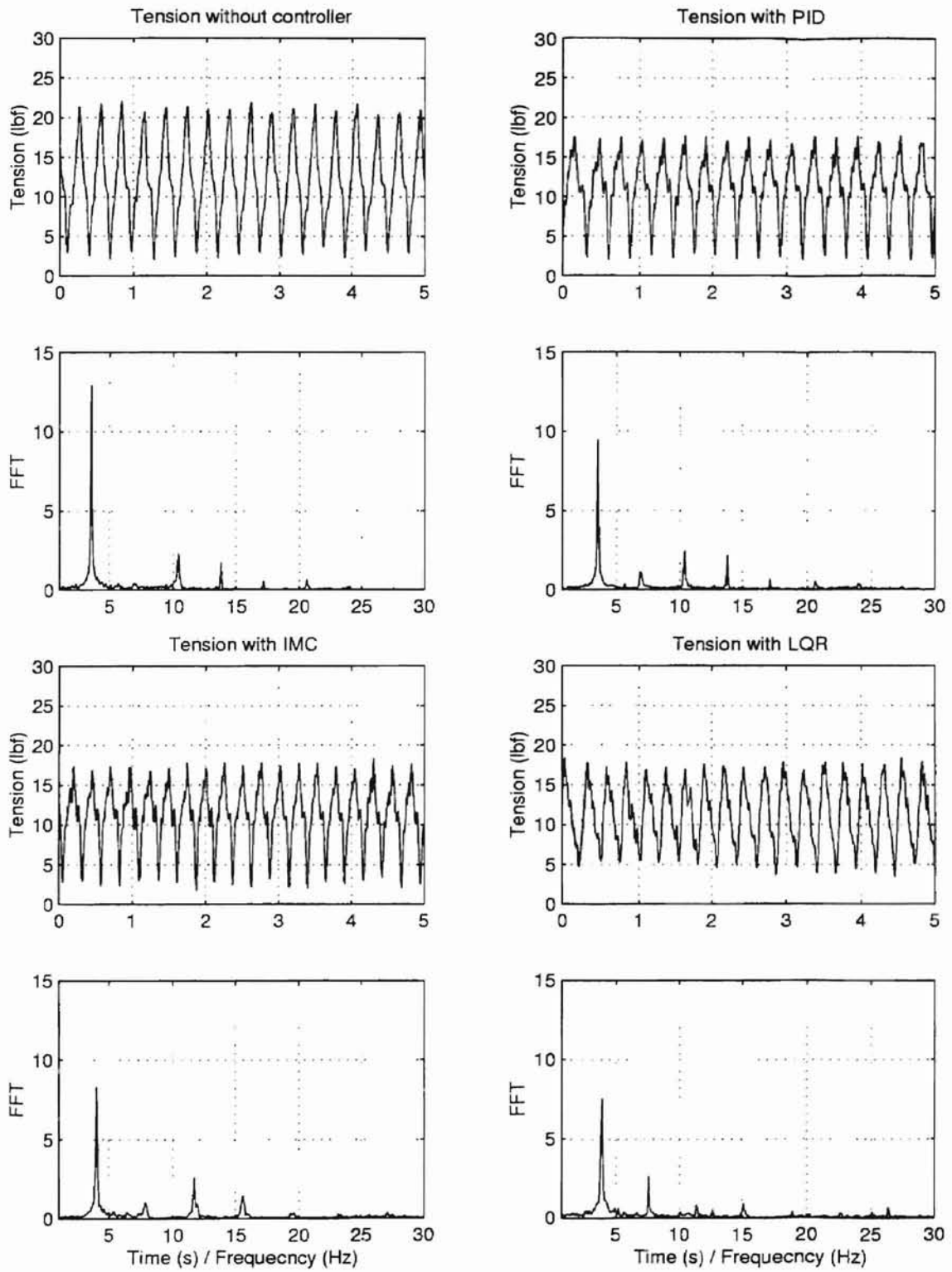


Figure 4.13: Tension with out-of-round idle roller; $v_r = 250$ FPM, $t_r = 10$ lb

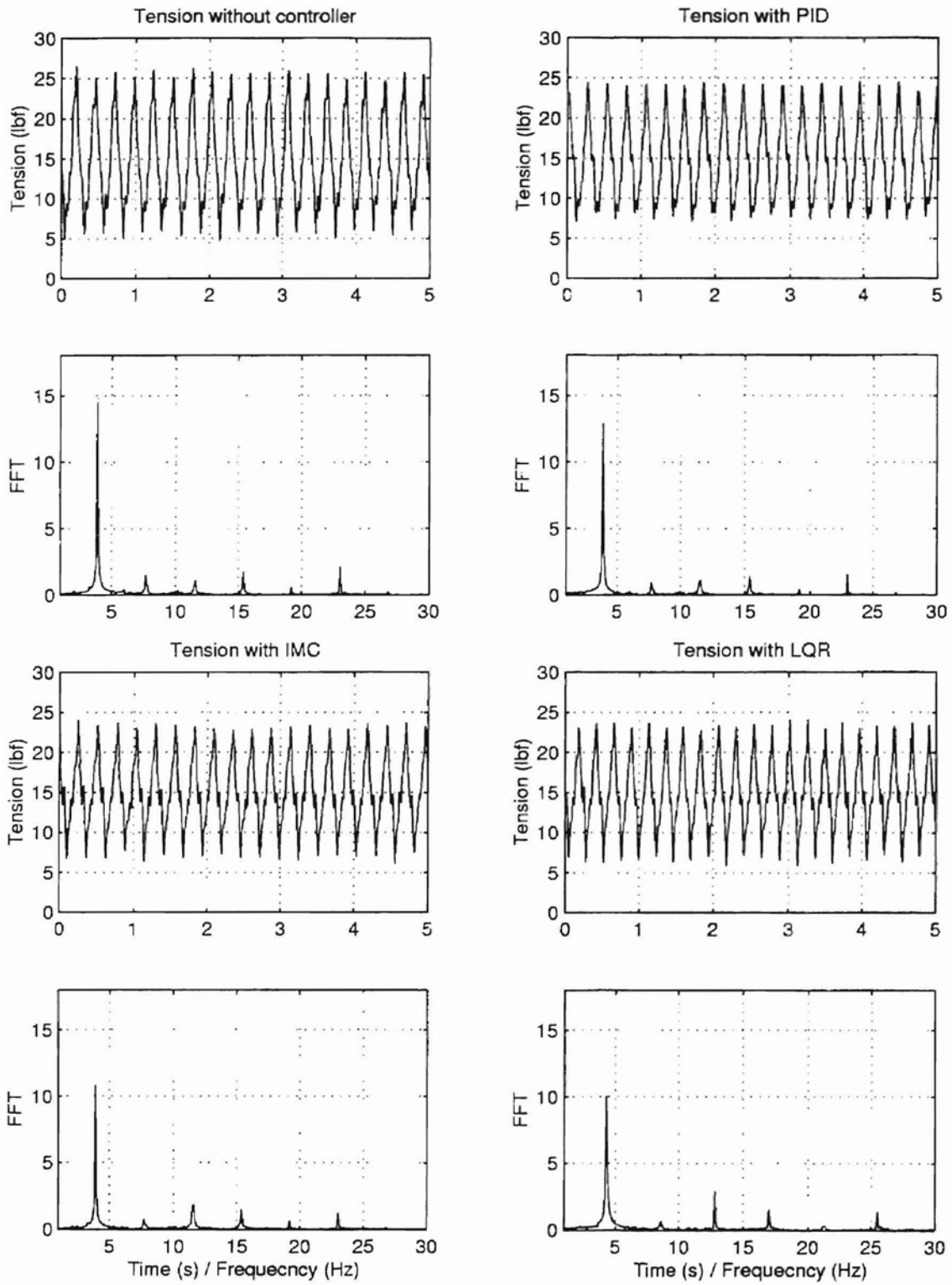


Figure 4.14: Tension with out-of-round idle roller; $v_r = 300$ FPM, $t_r = 15$ lb

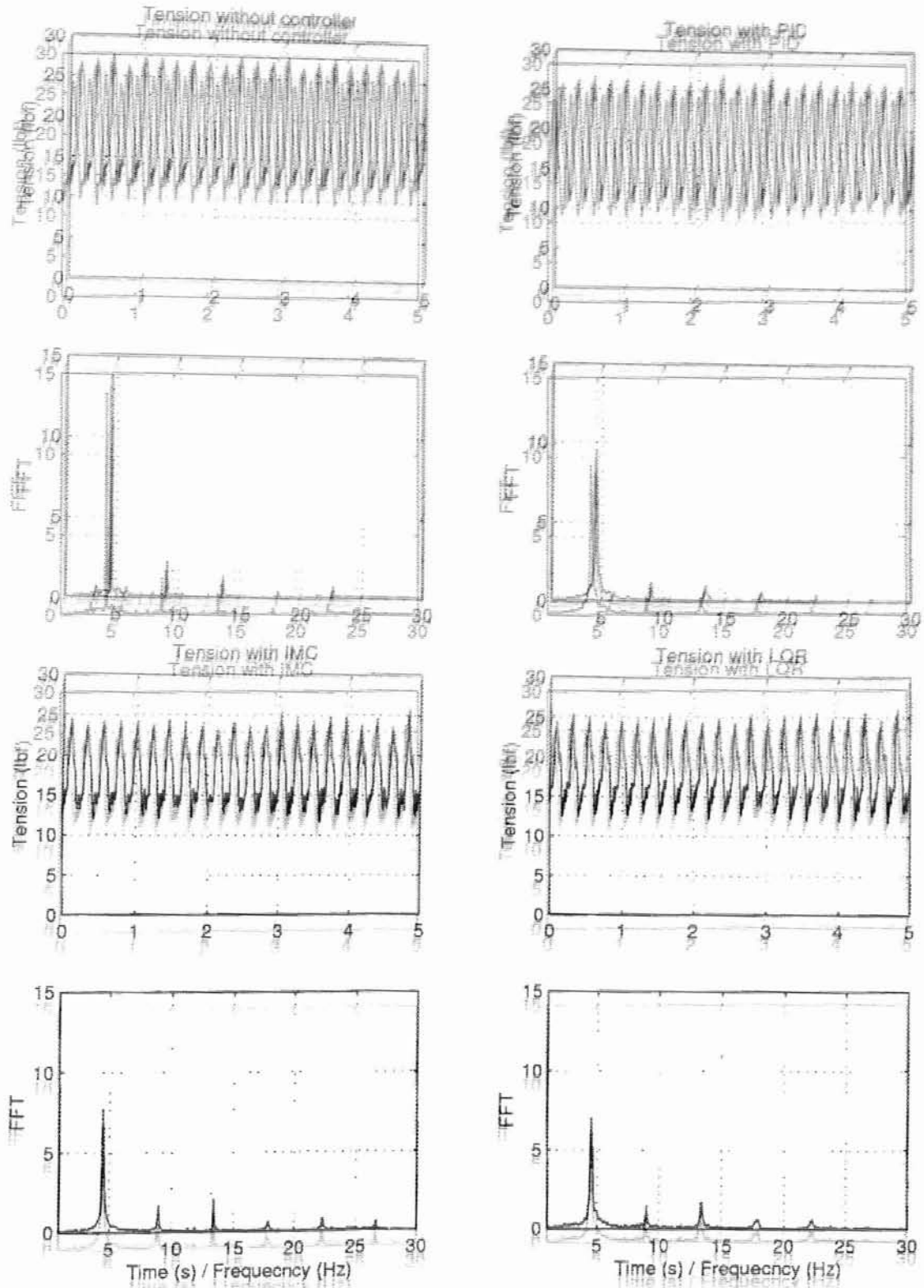


Figure 4.15: Tension with out-of-round idle roller; $v_r = 350$ FPM, $t_r = 20$ lb

CHAPTER 5

CONCLUSIONS AND FUTURE RESEARCH

5.1 Conclusions

The main goal of this project was to determine the effectiveness of the active dancers in tension disturbance attenuation. Towards achieving this goal the following items were reported in this report.

- Investigation and improvements to the existing models.
- Development of a general mathematical model for the active dancer system.
- Investigation of the active dancer model for effective tension disturbance attenuation.
- Design and development of an experimental web platform for conducting tension control experiments with an active dancer system.
- Design and development of an open-architecture real-time software system for implementation of tension control strategies on the experimental platform.
- Experimental evaluations of the three types of controllers, i.e., PID, IMC, and LQR, for the active dancer system.

A compact model of the active dancer system was developed; the model depends on four parameters, $\eta = Jv_r/EAR^2$, $\beta = J/R^2$, $\tau_1 = L_1/v_r$, and $\tau_2 = L_2/v_r$.

An investigation of the active dancer model shows that the ratio of the upstream span length (L_1) to the downstream span length (L_2) with respect to the active dancer roller plays a critical role in the effectiveness of tension disturbance attenuation using an active dancer.

It is shown that when $L_2/L_1 > 2$ feedback control of the active dancer roller velocity with downstream tension as the measured feedback renders the system unstable, i.e., the motion of the active dancer induces tension variations into the web instead of rejecting the tension disturbance. Further, for better performance of the active dancer, the ratio L_2/L_1 must be smaller than one.

Experimental results show that very good attenuation of the tension disturbance is possible using an active dancer. Three controllers, i.e., PID, Internal model based (IMC), and linear quadratic optimal (LQR), were used in the investigation. All the three controllers that were used in the experimental evaluation show good attenuation levels but the IMC and LQR controllers give better attenuation at higher web speeds than the PID controller. The disturbance rejection capability of the active dancer system is limited only by the bandwidth limitation of the actuator as opposed to the passive dancer or an inertia compensated dancer which have been reported in literature to have considerable resonance problems even at low frequencies.

5.2 Future Research

In this report, experimental investigations were on an endless web line. Propagation of tension disturbances into upstream and downstream directions can lead to problems in terms of what is truly being reflected by the load cell measurements. Investigation of the active dancer system in an unwind/rewind web line should be done.

It is assumed in this research that the load cell is very rigid. Although the resonant frequency of the load cell is high, it is a factor when high frequency disturbances are to be rejected using an active dancer.

Future research should also focus on developing self-tuning control designs for the active dancer system. The expectation is that a self-tuning mechanism built in the controller will identify the amplitude and frequency of periodic disturbances and tune the controller gains to give the required performance.

Currently, the active dancer mechanism contains an electro-mechanical actuator. The bandwidth of this actuator is limited. Further, it cannot attenuate large tension disturbances because of actuator saturation. In collaboration with Fife, plans are underway to secure a servo-hydraulic actuator with a fast servo-valve for the active dancer mechanism. Tension control experiments to attenuate large tension disturbances in the web line will be explored after retrofitting the active dancer mechanism with a new actuator.

Mishkanna Chitra / Inisranta / IITBOM

BIBLIOGRAPHY

- [1] C. A. Norman, *Experiments on Belt-Drive Fundamentals*. Columbus: The Ohio State University, The Engineering Experiment Station, January 1949. Bulletin No 135.
- [2] D. P. Campbell, *Dynamic Behavior of the Production Process, Process Dynamics*. New York: John Wiley and Sons, Inc., 1 ed., 1958.
- [3] K. P. Grenfell, "Tension control on paper-making and converting machinery," *IEEE 9 th Annual Conference on Electrical Engineering in the Pulp and Paper Industry, Boston, Mass.*, pp. 20–21, June 1963.
- [4] D. King, "The mathematical model of a newspaper press," *Newspaper Techniques*, pp. 3–7, December 1969.
- [5] G. Brandenburg, "New mathematical models for web tension and register error," *International IFAC Conference on Instrumentation and Automation in the Paper, Rubber, and Plastics Industry, 3 rd Proc.*, vol. 1, pp. 411–438, 1977.
- [6] D. P. D. Whitworth and M. C. Harrison, "Tension variation in pliable material in production machinery," *Appl. Math. Modelling*, vol. 7, pp. 189–196, 1983.
- [7] K. H. Shin, *Tension Control in a Moving Web*. Master's thesis, Oklahoma State University, Stillwater, OK, December 1986.
- [8] K. N. Reid and K. H. Shin, "Variable-gain control of longitudinal tension," *Proceedings of the First International Conference on Web Handling*, pp. 220–233, June 1991.

- [9] P. Lin and M. S. Lan, "Effects of pid gains for controller design with dancer mechanism on web tension," *Proceedings of the Second International Conference on Web Handling*, pp. 66–76, June 1993.
- [10] K. Kuribayashi and K. Nakajima, "An active dancer roller system for tension control of wire and sheet," *Proceedings of 9 th Triennial World Congress of IFAC, Budapest Hungary*, pp. 1747–1752, 1984.
- [11] W. Wolfermann and D. Schroder, "Application and decoupling and state space control in processing machine with continuous moving webs.," *Proceedings of International Federation of Automatic Control*, vol. III, pp. 100–105, 1987.
- [12] W. Wolfermann, "Tension control of webs, a review of the problems and solutions in the present and future," *Proceedings of the Third International Conference on Web Handling*, pp. 198–229, June 1995.
- [13] G. J. Rajala, *Active Dancer Control for Web Handling Machine*. Master's thesis, University of Wisconsin-Madison, Wisconsin, August 1995.
- [14] K. Zhou and J. C. Doyle, *Essentials of Robust Control*. Upper Saddle River, New Jersey: Prentice Hall, 1998.
- [15] K. N. Reid, J. J. Shelton and K. C. Lin, "Distributed control of tension in a web transport system, whrc project report," tech. rep., Oklahoma State University, Stillwater, Oklahoma, May 1992.
- [16] K. N. Reid and K. C. Lin, "Dynamic behavior of dancer subsystems in web transport systems," *Proceedings of the Second International Conference on Web Handling*, pp. 135–146, June 1993.
- [17] K. H. Shin, *Distributed Control of Tension in Multi-span Web Transport Systems*. PhD thesis, Oklahoma State University, Stillwater, Oklahoma, May 1991.

- [18] K. H. Shin, K. N. Reid and S. O. Kwon, "Non-interacting tension control in a multi-span web transport system," *Proceedings of the Third International Conference on Web Handling*, pp. 312–326, June 1995.
- [19] J. J. Shelton, "Dynamics of web tension control with velocity or torque control," *Proceedings of The American Control Conference, (IEEE), Seattle, WA*, pp. 1423–1427, June 1986.
- [20] K. Reid and K. Lin, "Control of longitudinal tension in multi-span web transport systems during start up," *Proceedings of the Second International Conference on Web Handling*, pp. 77–95, June 1993.
- [21] G. E. Young and K. N. Reid, "Lateral and longitudinal dynamic behavior and control of moving webs," *ASME Journal of Dynamic Systems, Measurement, and Control*, vol. 115, pp. 309–317, June 1993.
- [22] K. H. Shin and W. K. Hong, "Real-time tension control in a multi-stand rolling system," *Proceedings of the Third International Conference on Web Handling*, pp. 247–263, June 1995.
- [23] P. Dorato, C. Abdallah and V. Cerone, *Linear-Quadratic Control, An Introduction*. Englewood Cliffs, New Jersey: Prentice Hall, 1 ed., 1995.
- [24] J. J. Shelton, "Sensing of web tension by means of roller reaction forces, WHRC project report," tech. rep., Oklahoma State University, Stillwater, Oklahoma, July 1997.
- [25] S. S. Mandal, *Lateral Control of a Web using Velocity Feedback*. Master's thesis, Oklahoma State University, Stillwater, Oklahoma, July 2000.

APPENDIX A

DYNAMICS OF BASIC ELEMENTS OF WEB HANDLING SYSTEMS

This chapter presents the dynamics of basic elements of web handling systems. The dynamic equations are presented in the following order: (1) Unwind roller (2) Rewind roller (3) Free roller (Rotational dynamics) (4) Driven roller (Rotational dynamics) (5) Dancer roller (Translational dynamics) (6) General free web span (7) Web span upstream to the dancer roller (8) Web span downstream to the dancer roller (9) Web span next to unwind roller.

In this report, the term free web span is taken to mean that the span is not immediately downstream or upstream to the dancer roller. The nonlinear tension dynamics are reproduced from [17] here to make the report complete.

A.1 Assumptions for Mathematical Models

Considering the web handling elements shown in Figs. A.1 - A.4, certain assumptions are made in deriving the mathematical models. The assumptions are:

- (1) The strain distribution on each web is uniform along the web span.
- (2) The cross-sectional area of the web span is invariant.
- (3) The longitudinal web strain is very small compared to length of the web span.
- (4) The web is perfectly elastic.
- (5) There is no slippage between the roller and the web span.
- (6) The web thickness is very small compared to the radius of the rollers

- (7) The dynamics of the lead-in and lead-out of the web with the roller speed are negligible.
- (8) The contact region between the web and the roller is negligible compared to the length of the web span.
- (9) The density and the modulus of elasticity of the web are constant over the web span.
- (10) Physical properties of web do not change with ambient conditions.

A.2 Unwind Roller

Fig. A.1 shows an unwind roller and web span immediately next to it. Rotational dynamics

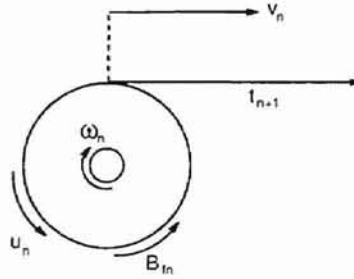


Figure A.1: Unwind roller

of n-th unwind roller can be written as

$$J_n(\tau_t)\dot{v}_n = -B_{fn}v_n - R_n(\tau_t)u_n + R_n^2(\tau_t)t_{n+1} \quad (\text{A.1})$$

The radius of the unwind roller decrease as the web is released into the process. The radius at time τ can be obtained from the following equation

$$R_n(\tau_t) = \sqrt{R_{n0}^2 - \frac{v_n h \tau_t}{\pi}} \quad (\text{A.2})$$

A.3 Rewind Roller

Fig. A.2 shows a rewind roller and a web span immediately before it. Rotational dynamics

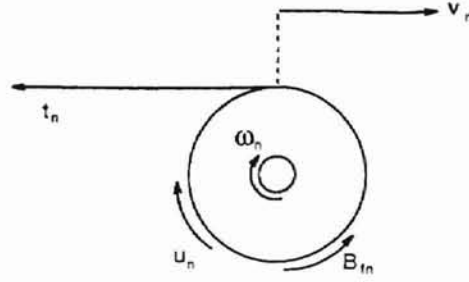


Figure A.2: Rewind Roller

for rewind roller can be written as

$$J_n(\tau_t)\dot{v}_n = -B_{fn}v_n + R_n(\tau_t)u_n - R_n^2(\tau_t)t_n \quad (\text{A.3})$$

The radius of the rewind roller increases as the web is wound onto the roller. The radius of rewind roller at time τ can be obtained from the following equation

$$R_n(\tau_t) = \sqrt{R_{n0}^2 + \frac{v_n h \tau_t}{\pi}} \quad (\text{A.4})$$

A.4 Free Roller (Rotational dynamics)

Fig. A.3 shows a free web span, a driven roller and a free roller. Rotational dynamics of

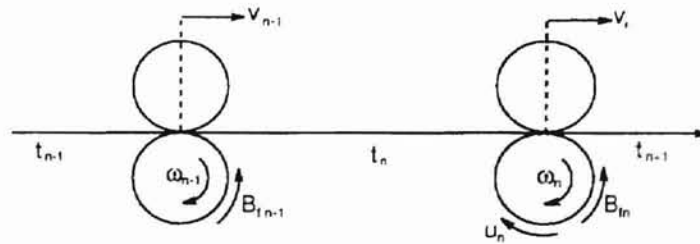


Figure A.3: General free span with driven roller

the (n-1)-th free roller can be written as

$$J_{n-1}\dot{\omega}_{n-1} = -B_{fn}\omega_{n-1} + R_{n-1}(t_n - t_{n-1}) \quad (\text{A.5})$$

Noting that $v_{n-1} = R_{n-1}\omega_{n-1}$, the above equation can be written as

$$J_{n-1}\dot{v}_{n-1} = -B_{fn}v_{n-1} + R_{n-1}^2(t_n - t_{n-1}) \quad (\text{A.6})$$

A.5 Driven Roller (Rotational Dynamics)

Rotational dynamics of the driven roller shown in Fig. A.3 can be written as

$$J_n\dot{v}_n = -B_{fn}v_n + R_n^2(t_{n+1} - t_n) + R_n u_n \quad (\text{A.7})$$

where u_n is the torque input to the driven roller

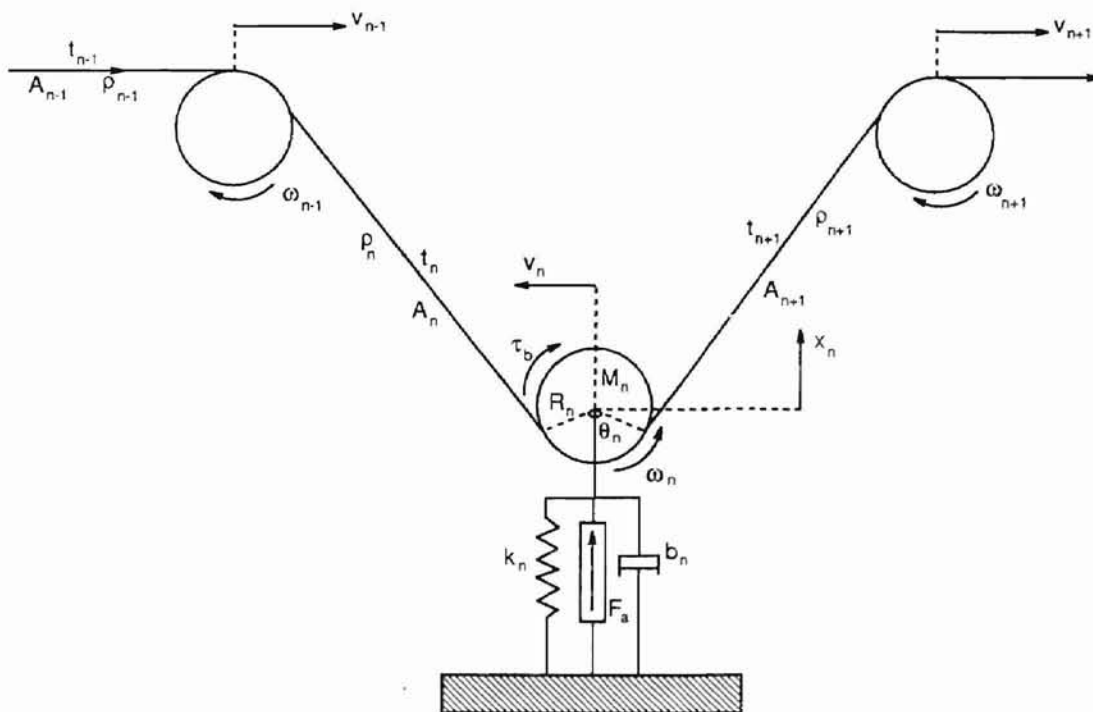


Figure A.4: Active dancer system

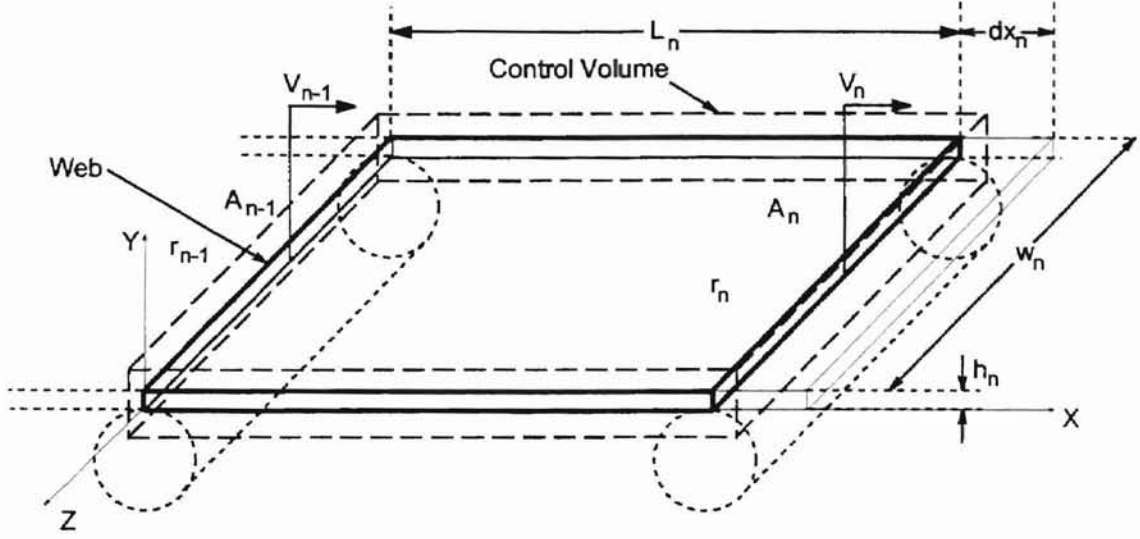


Figure A.5: Control volume of a web span

A.6 Dancer Roller (Translation Dynamics)

Active dancer system shown in Fig. A.4. Applying Newton's second law to the dancer roller in its translational direction

$$M_{n-1}\ddot{x}_{n-1} = -b\dot{x}_{n-1} - kx_{n-1} - (t_n + t_{n-1}) \sin\left(\frac{\theta_{n-1}}{2}\right) + F_a \quad (\text{A.8})$$

A.7 General Free Span

Tension dynamics of a general free span (i.e., one which is not immediately next to a dancer) is considered in this section. Applying the law of conservation of mass for control volume of the web span shown in Fig. A.5, we obtain

$$\frac{d}{dt} \left[\int_0^{L_n} \rho(x,t) A(x,t) dx \right] = \rho_{n-1} A_{n-1} v_{n-1} - \rho_n A_n v_n \quad (\text{A.9})$$

Now, consider the strain effect on the web in three directions as given by,

$$\begin{aligned} dx_n &= (1 + \varepsilon_n) dx_u \\ w_n &= (1 + \varepsilon_w) w_u \\ h_n &= (1 + \varepsilon_h) h_u \end{aligned} \quad (\text{A.10})$$

where subscript u indicates the unstretched state of the element, w and h denote the width and thickness of the web, respectively. Assuming that the elemental mass dm in the unstretched and stretched state is the same, we obtain

$$dm = \rho_n dx_n w_n h_n = \rho_u dx_u w_u h_u \quad (\text{A.11})$$

From (A.10) and (A.11), we get

$$\frac{\rho_n A_n}{\rho_u A_u} = \frac{1}{1 + \varepsilon_n} \quad (\text{A.12})$$

Ignoring the effect of the strain in width and thickness directions and substituting into (A.12) into (A.9), we obtain

$$\frac{d}{dt} \left[\int_0^{L_n} \frac{\rho_u(x, t) A_u(x, t)}{1 + \varepsilon_x(x, t)} dx \right] = \frac{\rho_{u-1} A_{u-1} v_{n-1}}{1 + \varepsilon_{n-1}} - \frac{\rho_u A_u v_n}{1 + \varepsilon_n} \quad (\text{A.13})$$

Assuming the density (ρ_u), cross sectional area (A_u) and the modulus of elasticity (E_n) of the web in the unstretched state are constant along the length of the web, equation (A.13) can be written as

$$\frac{d}{dt} \left[\int_0^{L_n} \frac{1}{1 + \varepsilon_x(x, t)} dx \right] = \frac{v_{n-1}}{1 + \varepsilon_{n-1}} - \frac{v_n}{1 + \varepsilon_n} \quad (\text{A.14})$$

Assuming that the strain is very small, $\varepsilon_x \ll 1$, we can say $1/(1 + \varepsilon_x) \approx (1 - \varepsilon_x)$. Then, (A.14) can be written as

$$\frac{d}{dt} \left[\int_0^{L_n} (1 - \varepsilon_x(x, t)) dx \right] = v_{n-1}[1 - \varepsilon_{n-1}] - v_n[1 - \varepsilon_n] \quad (\text{A.15})$$

Under the assumption that strain along the web is uniform, we obtain

$$\left[\int_0^{L_n} (1 - \varepsilon_x(x, t)) dx \right] = L_n(1 - \varepsilon_n) \quad (\text{A.16})$$

From equations (A.15) and (A.16), we obtain

$$-L_n \frac{d}{dt}(\varepsilon_n) = v_{n-1} - v_{n-1}\varepsilon_{n-1} - v_n + v_n\varepsilon_n \quad (\text{A.17})$$

Assuming the web is perfectly elastic, and applying Hooke's law to the web

$$t_n = E_n A_n \epsilon_n \quad (\text{A.18})$$

Substituting this result into (A.17) and rearranging, the dynamics of free span can be written as

$$L_n \dot{t}_n = v_{n-1} t_{n-1} - v_n t_n + E_n A_n (v_n - v_{n-1}) \quad (\text{A.19})$$

A.8 Downstream Span of the Dancer

This section considers the mathematical model of a web span downstream to the dancer. There are two factors that affect the tension in the web span next to the dancer. The first is the velocity of the web and the second is the translational velocity of the dancer roller. The net tension is due to the combined effect of both these factors, that is,

$$t_n = [t_n]_v + [t_n]_d \quad (\text{A.20})$$

Differentiating equation (A.20) and multiplying by L_n , we obtain

$$L_n \dot{t}_n = L_n [\dot{t}_n]_d + L_n [\dot{t}_n]_v \quad (\text{A.21})$$

Each of the terms on the right hand side of equation (A.21) is evaluated to get the dynamics of the downstream web span next to a dancer.

Consider the web span equation given by (A.19)

$$L_n [\dot{t}_n]_v = v_{n-1} [t_{n-1}]_v - v_n [t_n]_v + E_n A_n (v_n - v_{n-1}) \quad (\text{A.22})$$

To evaluate the effect of the dancer velocity on tension, invoke Hooke's law for the web span

$$[t_n]_d = E_n A_n [\epsilon_n]_d \quad (\text{A.23})$$

Strain due to dancer movement is

$$[\epsilon_n]_d = \frac{x_n \sin\left(\frac{\theta_n}{2}\right)}{L_n} \quad (\text{A.24})$$

Substituting equation (A.24) into equation (A.23), we get

$$L_n[t_n]_d = E_n A_n x_n \sin\left(\frac{\theta_n}{2}\right) \quad (\text{A.25})$$

Differentiating (A.25),

$$L_n[\dot{t}_n]_d = E_n A_n \dot{x}_n \sin\left(\frac{\theta_n}{2}\right) \quad (\text{A.26})$$

The above equation gives the effect of dancer displacement on the tension in the web span and corresponds to the first term in equation (A.21). The other term in equation (A.21) is the effect of web velocity on the tension.

From the equations (A.25) and (A.20), we obtain

$$[t_n]_v = t_n - \frac{E_n A_n}{L_n} x_n \sin\left(\frac{\theta_n}{2}\right) \quad (\text{A.27})$$

Equation (A.27) for (n-1)-th span will be,

$$[t_{n-1}]_v = t_{n-1} - \frac{E_n A_n}{L_{n-1}} x_n \sin\left(\frac{\theta_n}{2}\right) \quad (\text{A.28})$$

Substituting equations (A.26) and (A.22) into equation (A.21), result in

$$L_n \dot{t}_n = v_{n-1} [t_{n-1}]_v - v_n [t_n]_v + E_n A_n (v_n - v_{n-1}) + E_n A_n \dot{x}_n \sin\left(\frac{\theta_n}{2}\right) \quad (\text{A.29})$$

Now use the values of $[t_n]_v$ and $[t_{n-1}]_v$ as given by (A.27) and (A.28) in the above equation and simplify to get,

$$\begin{aligned} L_n \dot{t}_n = & E_n A_n v_n \left(1 - \frac{t_n}{E_n A_n} + \frac{x_n}{L_n} \sin\left(\frac{\theta_n}{2}\right) \right) - \\ & E_n A_n v_{n-1} \left(1 - \frac{t_{n-1}}{E_n A_n} + \frac{x_n}{L_{n-1}} \sin\left(\frac{\theta_n}{2}\right) \right) + E_n A_n \dot{x}_n \sin\left(\frac{\theta_n}{2}\right) \end{aligned} \quad (\text{A.30})$$

Assuming the wrap angle $\theta_n = 180^\circ$, the above equation simplifies to,

$$L_n \dot{t}_n = E_n A_n (v_n - v_{n-1}) + v_{n-1} t_{n-1} - v_n t_n + E_n A_n x_n \left(\frac{v_n}{L_n} - \frac{v_{n-1}}{L_{n-1}} \right) + E_n A_n \dot{x}_n \quad (\text{A.31})$$

A.9 Upstream Span of the Dancer

We begin by noting that the net tension is the combined effect of dancer movement and velocity of the web, that is,

$$t_{n-1} = [t_{n-1}]_d + [t_{n-1}]_v \quad (\text{A.32})$$

The terms on the right hand side of the above equation are evaluated to find the tension in the upstream web span. Strain due to the dancer movement is

$$[\epsilon_{n-1}]_d = \frac{x_{n-1}}{L_{n-1}} \sin\left(\frac{\theta_n}{2}\right) \quad (\text{A.33})$$

Using Hooke's law $[t_{n-1}]_d = E_n A_n [\epsilon_{n-1}]_d$, we get,

$$L_{n-1} [t_{n-1}]_d = E_n A_n x_{n-1} \sin\left(\frac{\theta_n}{2}\right) \quad (\text{A.34})$$

Differentiating the above equation,

$$L_{n-1} [\dot{t}_{n-1}]_d = E_n A_n \dot{x}_{n-1} \sin\left(\frac{\theta_n}{2}\right) \quad (\text{A.35})$$

Substituting equation (A.34) in equation (A.32) and rearranging,

$$[t_{n-1}]_v = t_{n-1} - \frac{E_n A_n}{L_{n-1}} x_{n-1} \sin\left(\frac{\theta_n}{2}\right) \quad (\text{A.36})$$

Differentiating (A.32) and multiplying by L_n

$$L_{n-1} \dot{t}_{n-1} = L_{n-1} [\dot{t}_{n-1}]_v + L_{n-1} [\dot{t}_{n-1}]_d \quad (\text{A.37})$$

Substituting the equations (A.35) and (A.36) into above equation, we get

$$L_{n-1} \dot{t}_{n-1} = v_{n-2} [t_{n-2}]_v - v_{n-1} [t_{n-1}]_v + E_n A_n (v_{n-1} - v_{n-2}) + E_n A_n \dot{x}_{n-1} \sin\left(\frac{\theta_n}{2}\right) \quad (\text{A.38})$$

Substituting equation (A.36) into above equation and noting that $[t_{n-2}]_v = t_{n-2}$, we get

$$\begin{aligned} L_{n-1} \dot{t}_{n-1} &= v_{n-2} t_{n-2} - v_{n-1} \left(t_{n-1} - \frac{E_n A_n}{L_{n-1}} x_{n-1} \sin\left(\frac{\theta_n}{2}\right) \right) \\ &+ E_n A_n (v_{n-1} - v_{n-2}) + E_n A_n \dot{x}_{n-1} \sin\left(\frac{\theta_n}{2}\right) \end{aligned} \quad (\text{A.39})$$

Simplifying

$$L_{n-1}\dot{t}_{n-1} = E_n A_n v_{n-1} \left(1 - \frac{t_{n-1}}{E_n A_n} + \frac{x_{n-1}}{L_{n-1}} \sin\left(\frac{\theta_n}{2}\right) \right) - E_n A_n v_{n-2} \left(1 - \frac{t_{n-2}}{E_n A_n} \right) + E_n A_n \dot{x}_{n-1} \sin\left(\frac{\theta_n}{2}\right) \quad (\text{A.40})$$

Assuming the wrap angle $\theta_n = 180^\circ$, equation (A.40) can be written as,

$$L_{n-1}\dot{t}_{n-1} = E_n A_n (v_{n-1} - v_{n-2}) + v_{n-2} t_{n-2} - v_{n-1} t_{n-1} + \frac{E_n A_n}{L_{n-1}} v_{n-1} x_{n-1} + E_n A_n \dot{x}_{n-1} \quad (\text{A.41})$$

A.10 Web Span next to the Unwind Roller

Considering equation A.1 for the unwind roller

$$J_n(\tau)\dot{v}_n = -B_{fn}v_n - R_n(\tau)u_n + R_n^2(\tau)t_{n+1} \quad (\text{A.42})$$

Assuming steady-state conditions where $\dot{v}_n = 0$, $B_{fn} = 0$ and $t_{n+1} = t_n$. Applying into the equation A.1, we obtain

$$R_n(\tau)u_n - R_n^2(\tau)t_n = 0 \quad (\text{A.43})$$

Using (A.43), t_n can be written as

$$t_n = \frac{u_n}{R_n(\tau)} \quad (\text{A.44})$$

Consider the equation for the free web span derived in the previous section

$$L_n \dot{t}_n = v_{n-1} t_{n-1} - v_n t_n + E_n A_n (v_n - v_{n-1}) \quad (\text{A.45})$$

The web span next to the unwind roller does not have any upstream spans. So tension derived in (A.44) can be considered as the downstream tension to the web span. So assuming $t_{n-1} = \frac{u_{n-1}}{R_{n-1}(\tau)}$, the dynamics of the web span next to unwind roller can be written as

$$L_n \dot{t}_n = \frac{1}{R_{n-1}(\tau)} v_{n-1} u_{n-1} - v_n t_n + E_n A_n (v_n - v_{n-1}) \quad (\text{A.46})$$

A.11 Linearized Dynamics

This section focuses on linearization of those equations around given reference values of velocity v_r , tension t_r and dancer position x_r . The deviations of web velocity, tension and dancer displacement given by

$$\begin{aligned} v_n &= V_n + v_r \\ t_n &= T_n + t_r \\ x_n &= X_n + x_r \end{aligned} \tag{A.47}$$

where V_n, T_n and X_n are deviations of velocity, tension and dancer displacement from the reference point given by v_r, t_r and x_r respectively. Substituting equation (A.47) into equations (A.19), (A.31) and (A.41) following linearized dynamic equations can be obtained.

- General free span

$$L_n \dot{T}_n = EA(V_n - V_{n-1}) + v_r T_{n-1} + t_r V_{n-1} - v_r T_n - t_r V_n \tag{A.48}$$

- Web span upstream to the dancer roller

$$\begin{aligned} L_n \dot{T}_n &= EA(V_n - V_{n-1}) + v_r T_{n-1} + t_r V_{n-1} - v_r T_n - t_r V_n \\ &\quad + \frac{EA}{L_n} v_r X_n \sin\left(\frac{\theta_n}{2}\right) + EA \dot{X}_n \sin\left(\frac{\theta_n}{2}\right) \end{aligned} \tag{A.49}$$

- Web span downstream to the dancer roller

$$\begin{aligned} L_n \dot{T}_n &= EA(V_n - V_{n-1}) + v_r T_{n-1} + t_r V_{n-1} - v_r T_n - t_r V_n \\ &\quad + EAX_n v_r \left(\frac{L_{n-1} - L_n}{L_n L_{n-1}}\right) \sin\left(\frac{\theta_n}{2}\right) + EA \dot{X}_n \sin\left(\frac{\theta_n}{2}\right) \end{aligned} \tag{A.50}$$

A.12 Transfer Functions

The linearized dancer system equations in Laplace domain are presented in this section. The following constants are defined to simplify the system equations: $\tau_n = \frac{L_n}{v_r}$, $\alpha =$

$\frac{EA - t_0}{v_\tau}$, $\beta_n = \frac{J_n}{R_n^2}$ and $\gamma_n = \frac{B_f}{R_n^2}$. Also in the following it is assumed that $t_0 \ll EA$ which results in $\frac{\alpha}{\tau_n} \approx \frac{EA}{L_n}$.

- **General free span**

$$T_n(s) = \frac{1}{(\tau_n s + 1)} T_{n-1}(s) + \frac{\alpha}{(\tau_n s + 1)} (V_n(s) - V_{n-1}(s)) \quad (\text{A.51})$$

- **Web span upstream to the dancer roller**

$$T_n(s) = \frac{1}{(\tau_n s + 1)} T_{n-1}(s) + \frac{\alpha}{(\tau_n s + 1)} (V_n(s) - V_{n-1}(s)) + \frac{\alpha (\tau_n s + 1)}{\tau_n (\tau_n s + 1)} X_n(s) \quad (\text{A.52})$$

- **Web span downstream to the dancer roller**

$$T_n(s) = \frac{1}{(\tau_n s + 1)} T_{n-1}(s) + \frac{\alpha}{(\tau_n s + 1)} (V_n(s) - V_{n-1}(s)) + \frac{\alpha}{(\tau_n s + 1)} \left(s + \frac{1}{\tau_n} - \frac{1}{\tau_{n-1}} \right) X_n(s) \quad (\text{A.53})$$

- **Free roller**

$$V_n(s) = \frac{1}{\beta_n s + \gamma_n} (T_{n+1} - T_n) \quad (\text{A.54})$$

- **Dancer roller**

$$X_n(s) = -\frac{1}{(Ms^2 + bs + k)} T_n(s) - \frac{1}{(Ms^2 + bs + k)} T_{n+1}(s) \quad (\text{A.55})$$

APPENDIX B

INPUT/OUTPUT MODEL FOR ACTIVE AND PASSIVE DANCER SYSTEMS

B.1 Active Dancer System

This chapter presents the analysis of active dancer system. The linearized equations are written for the each web handling element in the system shown in the Fig. B.1. The equations are given below

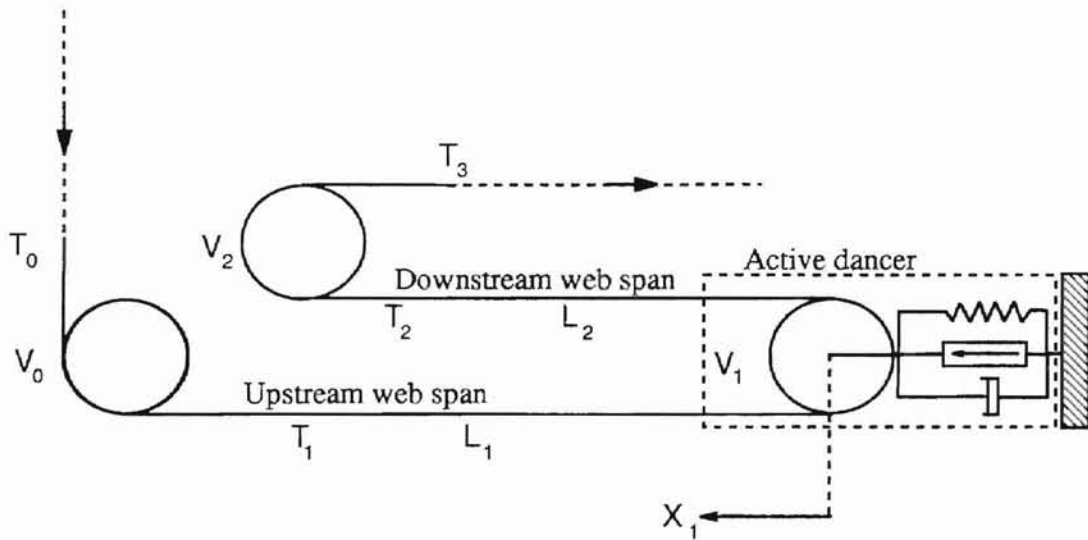


Figure B.1: Active dancer system

B.1.1 System Equations

- Roller V_0

$$V_0(s) = \frac{1}{\beta_0 s + \gamma_0} (T_1(s) - T_0(s)) \quad (\text{B.1})$$

- Web span T_1

$$T_1(s) = \frac{1}{(\tau_1 s + 1)} T_0(s) + \frac{\alpha}{(\tau_1 s + 1)} (V_1(s) - V_0(s)) + \frac{\alpha}{\tau_1} X_1(s) \quad (\text{B.2})$$

- Roller V_1

$$V_1(s) = \frac{1}{\beta_1 s + \gamma_1} (T_2(s) - T_1(s)) \quad (\text{B.3})$$

- Dancer Roller X_1

$$X_1(s) = -\frac{1}{(Ms^2 + bs + k)} T_1(s) - \frac{1}{(Ms^2 + bs + k)} T_2(s) \quad (\text{B.4})$$

- Web Span T_2

$$T_2(s) = \frac{1}{(\tau_2 s + 1)} T_1(s) + \frac{\alpha}{(\tau_2 s + 1)} (V_2(s) - V_1(s)) + \frac{\alpha}{(\tau_2 s + 1)} \left(s + \frac{1}{\tau_2} - \frac{1}{\tau_1} \right) X_1(s) \quad (\text{B.5})$$

- Roller V_2

$$V_2(s) = \frac{1}{\beta_2 s + \gamma_2} (T_3(s) - T_2(s)) \quad (\text{B.6})$$

B.1.2 Simplified Dancer Subsystem Model and Analysis

Following assumptions are used to simplify the equations derived in the previous section.

- All roller has the same dimension so $\beta_0 = \beta_1 = \beta_2 = \beta$
- Similarly the friction constant for all rollers $\gamma_0 = \gamma_1 = \gamma_2 = \gamma$

Using equations (B.1) and (B.3) we can rewrite the systems equations

$$V_1 - V_0 = \frac{1}{\beta s + \gamma} (T_2 - 2T_1 + T_0) \quad (\text{B.7})$$

Using equations (B.3) and (B.6) we can rewrite the systems equations

$$V_2 - V_1 = \frac{1}{\beta s + \gamma} (T_3 - 2T_2 + T_1) \quad (\text{B.8})$$

Applying into equation (B.2) and (B.4)

$$T_1(s) = \frac{(\beta s + \gamma + \alpha)}{((\beta s + \gamma)(\tau_1 s + 1) + 2\alpha)} T_0(s) + \frac{\alpha}{((\beta s + \gamma)(\tau_1 s + 1) + 2\alpha)} T_2(s) + \frac{\alpha(\beta s + \gamma) \left(s + \frac{1}{\tau_1} \right)}{((\beta s + \gamma)(\tau_1 s + 1) + 2\alpha)} X_1(s) \quad (\text{B.9})$$

$$T_2(s) = \frac{(\beta s + \gamma + \alpha)}{((\beta s + \gamma)(\tau_2 s + 1) + 2\alpha)} T_1(s) + \frac{\alpha}{((\beta s + \gamma)(\tau_2 s + 1) + 2\alpha)} T_3(s) + \frac{\alpha(\beta s + \gamma) \left(s + \frac{1}{\tau_2} - \frac{1}{\tau_1} \right)}{((\beta s + \gamma)(\tau_2 s + 1) + 2\alpha)} X_1(s) \quad (\text{B.10})$$

Applying the equation (B.4) into equations (B.9) and (B.10)

$$T_1(s) = \frac{(\beta s + \gamma + \alpha)(Ms^2 + bs + k)}{\left(((\beta s + \gamma)(\tau_1 s + 1) + 2\alpha)(Ms^2 + bs + k) + \alpha(\beta s + \gamma) \left(s + \frac{1}{\tau_1} \right) \right)} T_0(s) + \frac{\alpha \left((Ms^2 + bs + k) - (\beta s + \gamma) \left(s + \frac{1}{\tau_1} \right) \right)}{\left(((\beta s + \gamma)(\tau_1 s + 1) + 2\alpha)(Ms^2 + bs + k) + \alpha(\beta s + \gamma) \left(s + \frac{1}{\tau_1} \right) \right)} T_2(s) \quad (\text{B.11})$$

So using the equations (B.9) and (B.10) the system equations can be written as

$$T_2 = \frac{(\beta s + \gamma + \alpha)^2}{\left(((\beta s + \gamma)(\tau_1 s + 1) + 2\alpha)((\beta s + \gamma)(\tau_2 s + 1) + 2\alpha) - \alpha(\beta s + \gamma + \alpha) \right)} T_0(s) + \frac{\alpha((\beta s + \gamma)(\tau_1 s + 1) + 2\alpha)}{\left(((\beta s + \gamma)(\tau_1 s + 1) + 2\alpha)((\beta s + \gamma)(\tau_2 s + 1) + 2\alpha) - \alpha(\beta s + \gamma + \alpha) \right)} T_3(s) + \frac{\alpha(\beta s + \gamma) \left((\beta s + \gamma + \alpha) \left(s + \frac{1}{\tau_1} \right) + ((\beta s + \gamma)(\tau_1 s + 1) + 2\alpha) \left(s + \frac{1}{\tau_1} - \frac{1}{\tau_2} \right) \right)}{\left(((\beta s + \gamma)(\tau_1 s + 1) + 2\alpha)((\beta s + \gamma)(\tau_2 s + 1) + 2\alpha) - \alpha(\beta s + \gamma + \alpha) \right)} X_1(s) \quad (\text{B.12})$$

So final system equations can be written as

$$T_2(s) = A_1(s)T_0(s) + B_1(s)T_3 + C_1(s)X_1(s) \quad (\text{B.13})$$

Where $A_1(s)$, $B_1(s)$ and $C_1(s)$ defined as

$$A_1(s) = \frac{(\beta s + \gamma + \alpha)^2}{\left(((\beta s + \gamma)(\tau_1 s + 1) + 2\alpha)((\beta s + \gamma)(\tau_2 s + 1) + 2\alpha) - \alpha(\beta s + \gamma + \alpha) \right)} \quad (\text{B.14})$$

$$B_1(s) = \frac{\alpha((\beta s + \gamma)(\tau_1 s + 1) + 2\alpha)}{(((\beta s + \gamma)(\tau_1 s + 1) + 2\alpha)((\beta s + \gamma)(\tau_2 s + 1) + 2\alpha) - \alpha(\beta s + \gamma + \alpha))} \quad (\text{B.15})$$

$$C_1(s) = \frac{\alpha(\beta s + \gamma) \left((\beta s + \gamma + \alpha) \left(s + \frac{1}{\tau_1} \right) + ((\beta s + \gamma)(\tau_1 s + 1) + 2\alpha) \left(s + \frac{1}{\tau_1} - \frac{1}{\tau_2} \right) \right)}{(((\beta s + \gamma)(\tau_1 s + 1) + 2\alpha)((\beta s + \gamma)(\tau_2 s + 1) + 2\alpha) - \alpha(\beta s + \gamma + \alpha))} \quad (\text{B.16})$$

Where the plant transfer function can be written as

$$G_p(s) = \frac{\alpha(\beta s + \gamma) \left((\beta s + \gamma + \alpha) \left(s + \frac{1}{\tau_1} \right) + ((\beta s + \gamma)(\tau_1 s + 1) + 2\alpha) \left(s + \frac{1}{\tau_1} - \frac{1}{\tau_2} \right) \right)}{(((\beta s + \gamma)(\tau_1 s + 1) + 2\alpha)((\beta s + \gamma)(\tau_2 s + 1) + 2\alpha) - \alpha(\beta s + \gamma + \alpha))} \quad (\text{B.17})$$

Following assumptions are considered to simplify the plant model

- $\gamma \approx 0$, where the bearing friction of the rollers are negligible
- $\frac{\beta}{\alpha} = \eta$ where $\eta = \frac{Jv_r}{R^2 EA}$

$$\begin{aligned} T_2 = & \frac{(\beta s + \alpha)^2}{((\beta s(\tau_1 s + 1) + 2\alpha)(\beta s(\tau_2 s + 1) + 2\alpha) - \alpha(\beta s + \alpha))} T_0(s) \\ & + \frac{\alpha(\beta s(\tau_1 s + 1) + 2\alpha)}{((\beta s(\tau_1 s + 1) + 2\alpha)(\beta s(\tau_2 s + 1) + 2\alpha) - \alpha(\beta s + \alpha))} T_3(s) + \\ & \frac{\alpha\beta s \left((\beta s + \alpha) \left(s + \frac{1}{\tau_1} \right) + (\beta s(\tau_1 s + 1) + 2\alpha) \left(s + \frac{1}{\tau_1} - \frac{1}{\tau_2} \right) \right)}{((\beta s(\tau_1 s + 1) + 2\alpha)(\beta s(\tau_2 s + 1) + 2\alpha) - \alpha(\beta s + \alpha))} X_1(s) \end{aligned} \quad (\text{B.18})$$

So final dancer system transfer function can be written as

$$\begin{aligned} T_2 = & \frac{(\eta s + 1)^2}{((\eta s(\tau_1 s + 1) + 2)(\eta s(\tau_2 s + 1) + 2) - (\eta s + 1))} T_0(s) \\ & + \frac{(\eta s(\tau_1 s + 1) + 2)}{((\eta s(\tau_1 s + 1) + 2)(\eta s(\tau_2 s + 1) + 2) - (\eta s + 1))} T_3(s) + \\ & \frac{\beta s \left((\eta s + 1) \left(s + \frac{1}{\tau_1} \right) + (\eta s(\tau_1 s + 1) + 2) \left(s + \frac{1}{\tau_2} - \frac{1}{\tau_1} \right) \right)}{((\eta s(\tau_1 s + 1) + 2)(\eta s(\tau_2 s + 1) + 2) - (\eta s + 1))} X_1(s) \end{aligned} \quad (\text{B.19})$$

Equation B.19 represents the dancer system. Modified version of equation B.19 can be written as active or passive dancer system. Active and passive dancer models are derived in following sections.

B.2 Active Dancer System

Using equation (B.19) and noting that $\dot{X}_1(s) = sX_1(s)$. Active dancer equations can be written as

$$T_2(s) = \frac{A_{ad}(s)}{C_{ad}(s)}T_0(s) + \frac{B_{ad}(s)}{C_{ad}(s)}T_3(s) + \frac{D_{ad}(s)}{C_{ad}(s)}\dot{X}_1(s) \quad (\text{B.20})$$

$$A_{ad}(s) = (\eta s + 1)^2 \quad (\text{B.21})$$

$$B_{ad}(s) = (\eta s(\tau_1 s + 1) + 2) \quad (\text{B.22})$$

$$D_{ad}(s) = \beta \left((\eta s + 1) \left(s + \frac{1}{\tau_1} \right) + (\eta s(\tau_1 s + 1) + 2) \left(s + \frac{1}{\tau_2} - \frac{1}{\tau_1} \right) \right) \quad (\text{B.23})$$

$$C_{ad}(s) = ((\eta s(\tau_1 s + 1) + 2)(\eta s(\tau_2 s + 1) + 2) - (\eta s + 1)) \quad (\text{B.24})$$

B.3 Passive Dancer System

Working on the same lines as given in the section C.3, the linearized transfer functions for the web spans upstream and downstream to dancer roller can be written as

$$T_1(s) = \frac{(\eta s + 1)}{(\eta s(\tau_1 s + 1) + 2)}T_0(s) + \frac{1}{(\eta s(\tau_1 s + 1) + 2)}T_2(s) + \frac{\beta s \left(s + \frac{1}{\tau_1} \right)}{(\eta s(\tau_1 s + 1) + 2)}X_1(s) \quad (\text{B.25})$$

$$T_2(s) = \frac{(\eta s + 1)}{(\eta s(\tau_2 s + 1) + 2)}T_1(s) + \frac{1}{(\eta s(\tau_2 s + 1) + 2)}T_3(s) + \frac{\beta s \left(s + \frac{1}{\tau_2} - \frac{1}{\tau_1} \right)}{(\eta s(\tau_2 s + 1) + 2)}X_1(s) \quad (\text{B.26})$$

Considering the dancer equation derived from the previous section

$$X_1(s) = -\frac{1}{(Ms^2 + bs + k)}(T_1(s) + T_2(s)) \quad (\text{B.27})$$

Following constants are defined to simplify the system model: $\bar{b} = \frac{b}{M}$, $\bar{k} = \frac{k}{M}$ and $\bar{\beta} = \frac{\beta}{M}$. So equations (B.25) and (B.26) can be written as

$$(\eta s(\tau_1 s + 1) + 2)T_1(s) = (\eta s + 1)T_0(s) + T_2(s) - \frac{\bar{\beta}s \left(s + \frac{1}{\tau_1} \right)}{s^2 + \bar{b}s + \bar{k}}(T_1(s) + T_2(s)) \quad (\text{B.28})$$

$$(\eta s(\tau_2 s + 1) + 2)T_2(s) = (\eta s + 1)T_1(s) + T_3(s) - \frac{\bar{\beta}s \left(s + \frac{1}{\tau_2} + \frac{1}{\tau_1} \right)}{(s^2 + \bar{b}s + \bar{k})}(T_1(s) + T_2(s)) \quad (\text{B.29})$$

Simplified equations can be written as

$$T_1(s) = \frac{(\eta s + 1)(s^2 + \bar{b}s + \bar{k})}{\left((\eta s(\tau_1 s + 1) + 2)(s^2 + \bar{b}s + \bar{k}) + \bar{\beta}s \left(s + \frac{1}{\tau_1} \right) \right)} T_0(s) + \frac{(s^2 + \bar{b}s + \bar{k}) - \bar{\beta}s \left(s + \frac{1}{\tau_1} \right)}{\left((\eta s(\tau_1 s + 1) + 2)(s^2 + \bar{b}s + \bar{k}) + \bar{\beta}s \left(s + \frac{1}{\tau_1} \right) \right)} T_2(s) \quad (\text{B.30})$$

$$T_2(s) = \frac{(\eta s + 1)(s^2 + \bar{b}s + \bar{k}) - \bar{\beta}s \left(s + \frac{1}{\tau_2} - \frac{1}{\tau_1} \right)}{\left((\eta s(\tau_2 s + 1) + 2)(s^2 + \bar{b}s + \bar{k}) + \bar{\beta}s \left(s + \frac{1}{\tau_2} - \frac{1}{\tau_1} \right) \right)} T_1(s) + \frac{(s^2 + \bar{b}s + \bar{k})}{\left((\eta s(\tau_2 s + 1) + 2)(s^2 + \bar{b}s + \bar{k}) + \bar{\beta}s \left(s + \frac{1}{\tau_2} - \frac{1}{\tau_1} \right) \right)} T_3 \quad (\text{B.31})$$

Using the equation (B.30) into (B.31)

$$T_2(s) = \frac{A_{pd}(s)}{C_{pd}(s)} T_0(s) + \frac{B_{pd}(s)}{C_{pd}(s)} T_3(s) \quad (\text{B.32})$$

Where the transfer functions can be defined as

$$A_{pd} = \left((\eta s + 1)(s^2 + \bar{b}s + \bar{k}) - \bar{\beta}s \left(s + \frac{1}{\tau_2} - \frac{1}{\tau_1} \right) \right) (\eta s + 1)(s^2 + \bar{b}s + \bar{k}) \quad (\text{B.33})$$

$$B_{pd} = (s^2 + \bar{b}s + \bar{k}) \left((\eta s(\tau_1 s + 1) + 2)(s^2 + \bar{b}s + \bar{k}) - \bar{\beta}s \left(s + \frac{1}{\tau_1} \right) \right) \quad (\text{B.34})$$

$$\begin{aligned}
C_{pd}(s) = & \left((\eta s(\tau_1 s + 1) + 2)(s^2 + \bar{b}s + \bar{k}) + \bar{\beta}s \left(s + \frac{1}{\tau_1} \right) \right) \\
& \left((\eta s(\tau_2 s + 1) + 2)(s^2 + \bar{b}s + \bar{k}) + \bar{\beta}s \left(s + \frac{1}{\tau_2} - \frac{1}{\tau_1} \right) \right) \\
& - \left((s^2 + \bar{b}s + \bar{k}) - \bar{\beta}s \left(s + \frac{1}{\tau_1} \right) \right) \\
& \left((\eta s + 1)(s^2 + \bar{b}s + \bar{k}) - \bar{\beta}s \left(s + \frac{1}{\tau_2} - \frac{1}{\tau_1} \right) \right)
\end{aligned} \tag{B.35}$$

APPENDIX C

MATLAB PROGRAM FOR LQR CONTROLLER AND LUENBERGER OBSERVER

```
close all;
clear;
delete diary.dat;
vr=1.1684; % m/s
MofE=4.136854*10^9; % Pa
Ar=3.2258*10^(-6); % m^2
Jr=0.014078; % kg/m^2
R=0.0635; % m
L1=0.9144; L2=0.2286; % m
gamma=0.001;
tau1=L1/vr; tau2=L2/vr;
tau3=L3/vr;
alpha=MofE*Ar/vr;
beta=Jr/(R*R);
A=[
    0          1/beta  0          0          0
   -alpha/tau1 -1/tau1 alpha/tau1  0          0
    0          -1/beta -gamma/beta 1/beta  0
    0          1/tau2 -alpha/tau2 -1/tau2 alpha/tau2
    0          0      0          -1/beta  0
];
Bu=[
    -1/tau1
    alpha/tau1
    0
    alpha/tau2
    (1/tau2-1/tau1)
];
Bw=[
    -1/beta  0
    1/tau1  0
    0       0
    0       0
    0       1/beta
];
```

```

];
C=[ 0, 0, 0, 1, 0; 0, 0, 1, 0, 0 ];
Cc=[ 0, 0, 0, 1, 0];
Du=[0;0];
Dw=[0 0; 0,0];

sysc = ss(A,Bu,C,Du);
sysc1 = ss(A,Bw,C,Dw);

Ts = 0.005;
sysd1 = c2d(sysc1,Ts);
[G,Hw,C,Dw,Ts]=ssdata(sysd1);

sysd = c2d(sysc,Ts);
[G,Hu,C,Du,Ts]=ssdata(sysd);

Q = Cc'*Cc;
R=0.1;
[K,S,E]=dlqr(G,Hu,Q,R);

P=0.05*E;
L = place(G',C',P);

GK = G-Hu*K;
GL = G-L'*C;
[MK,NK]=size(GK);
[ML,NL]=size(GL);

Ge = [GK, Hu*K; zeros(ML,NK), GL];
He = [Hw; Hw];

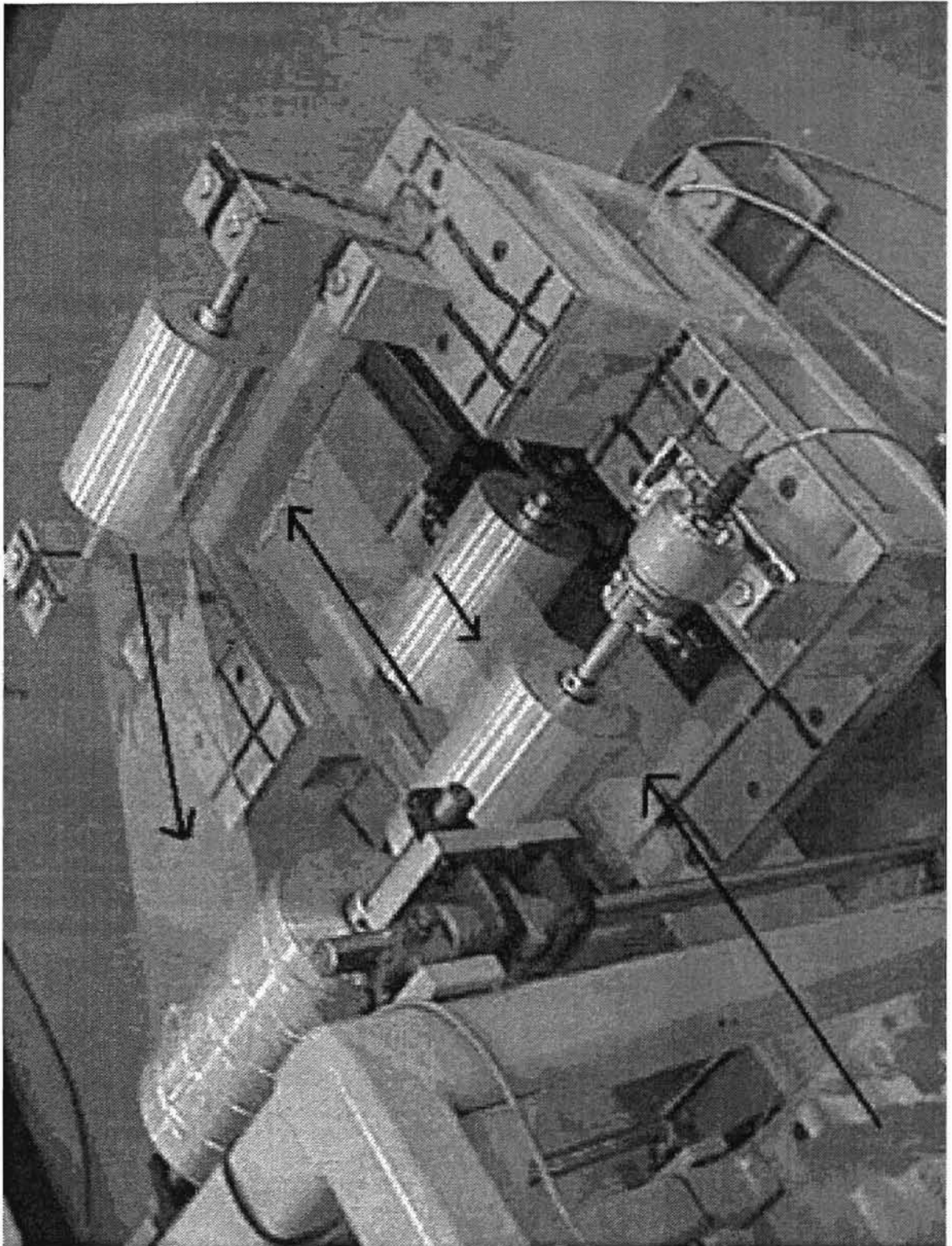
Ce = [0,0,0,1,0,0,0,0,0,0];
De = [0,0];

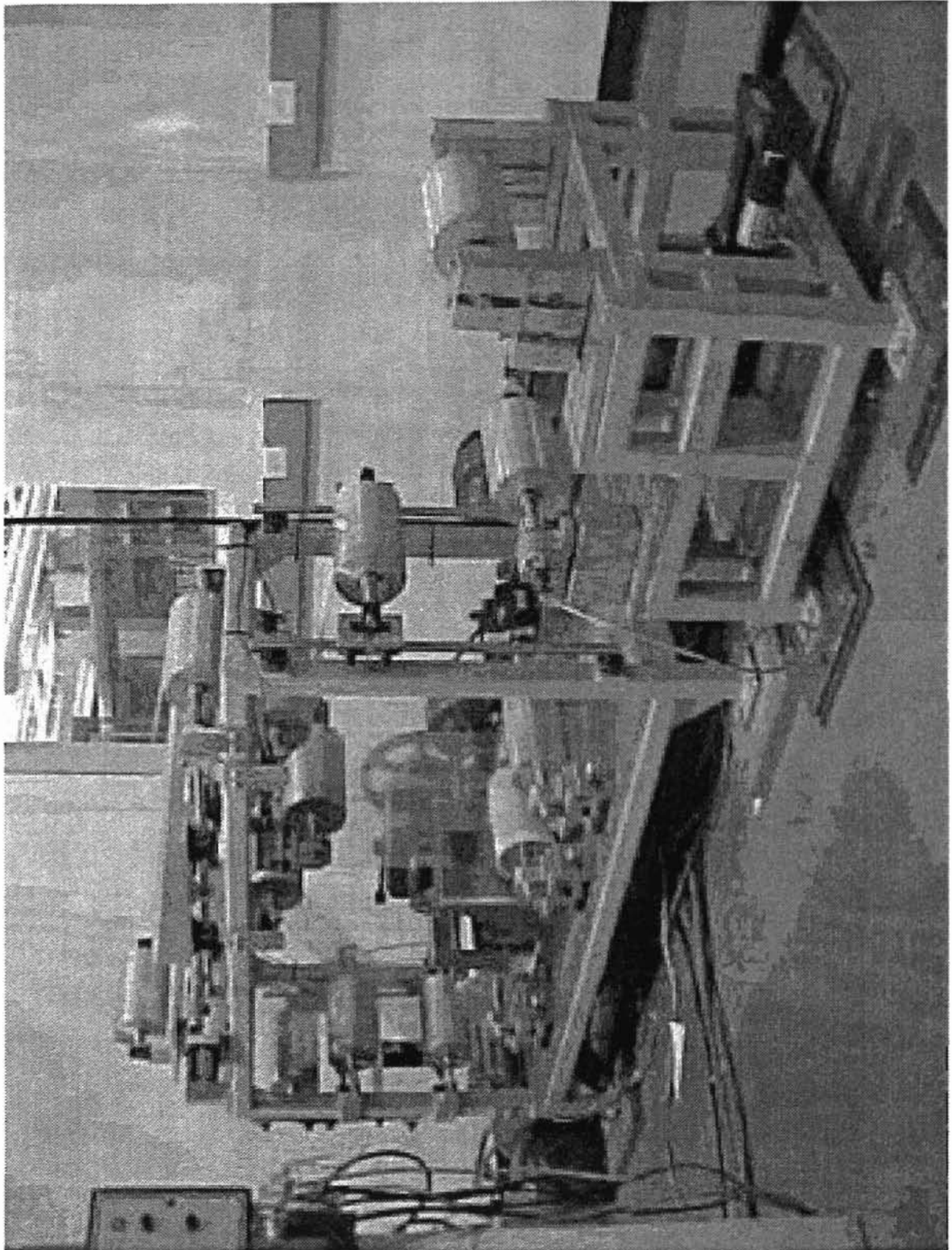
diary('diary.dat')
Ts
G
Hu
Hw
K
L
diary off

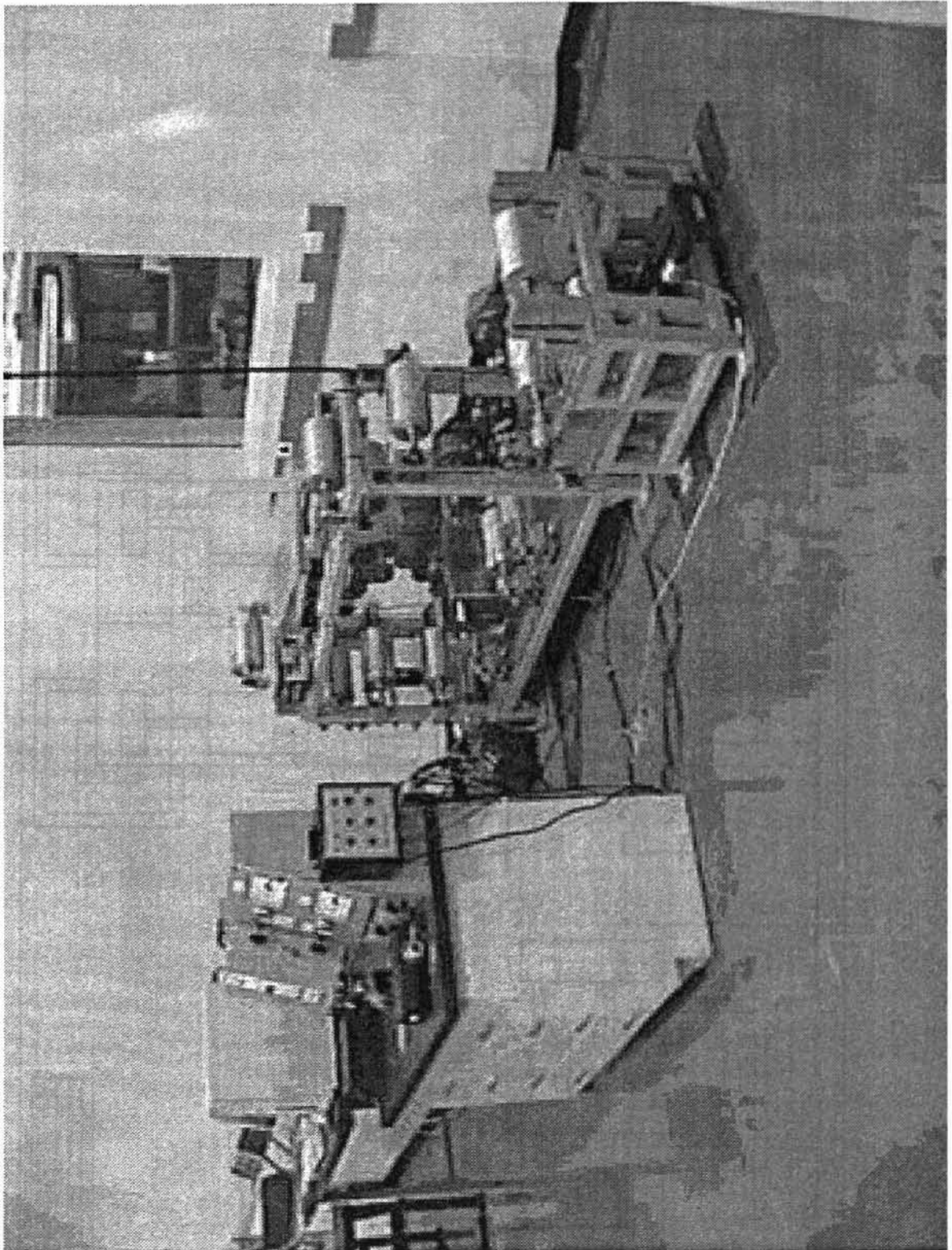
```

APPENDIX D

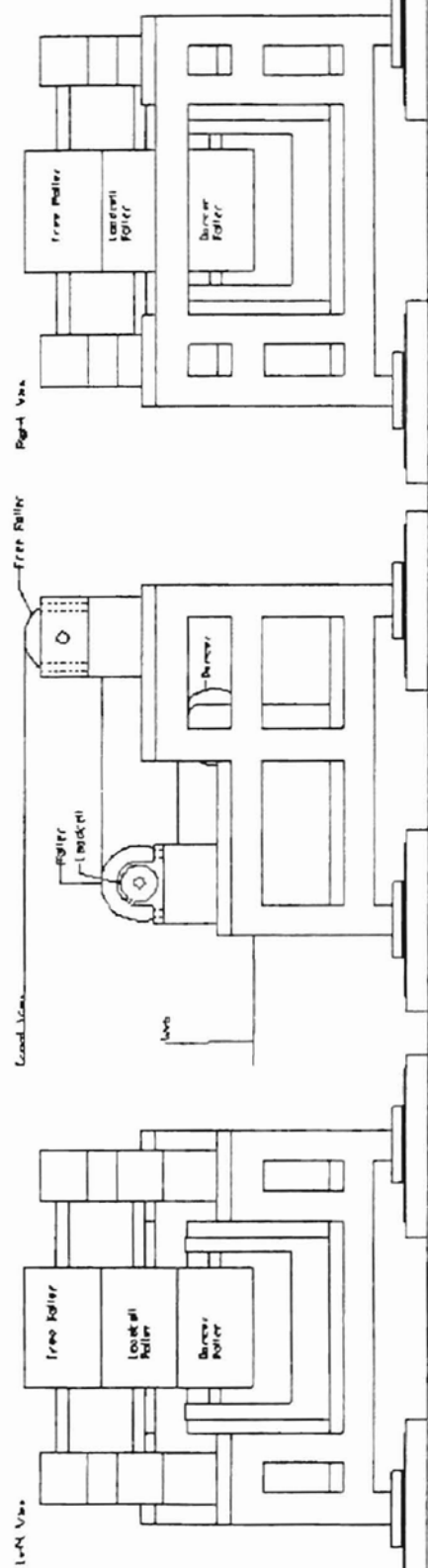
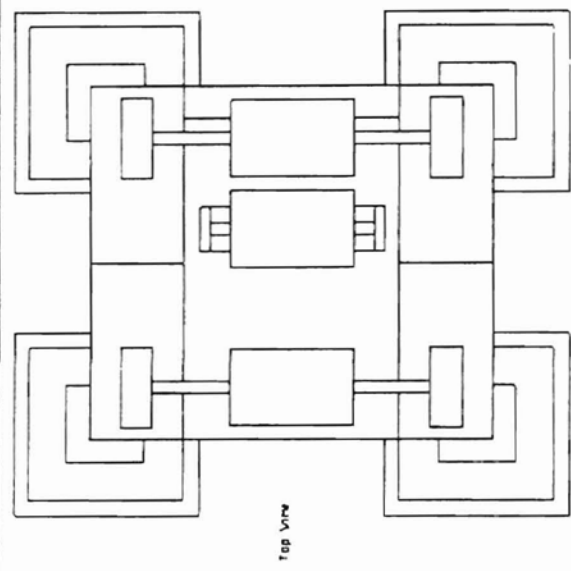
**AUTOCAD DRAWINGS AND PHOTOGRAPHS OF EXPERIMENTAL
PLATFORM**



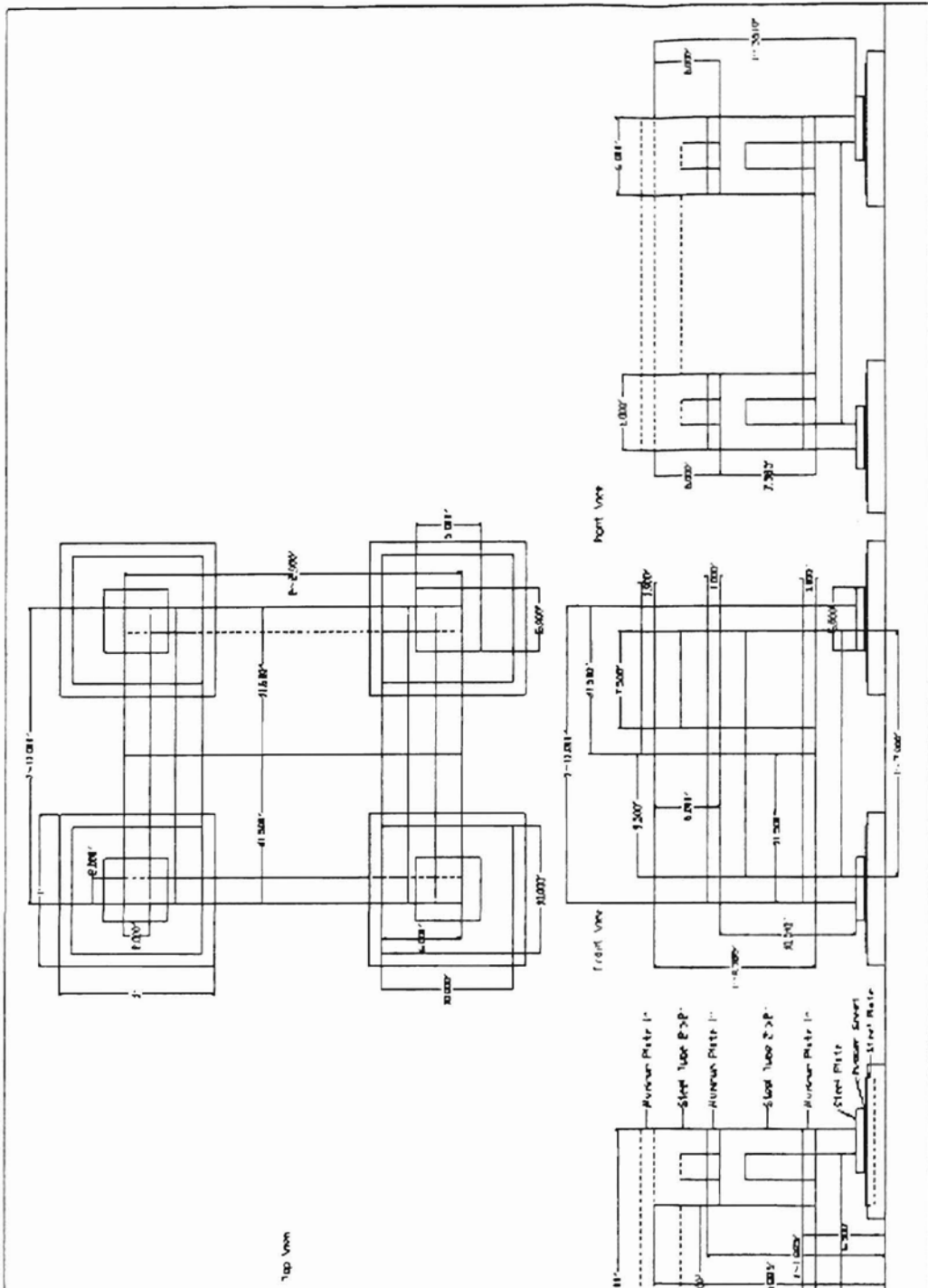




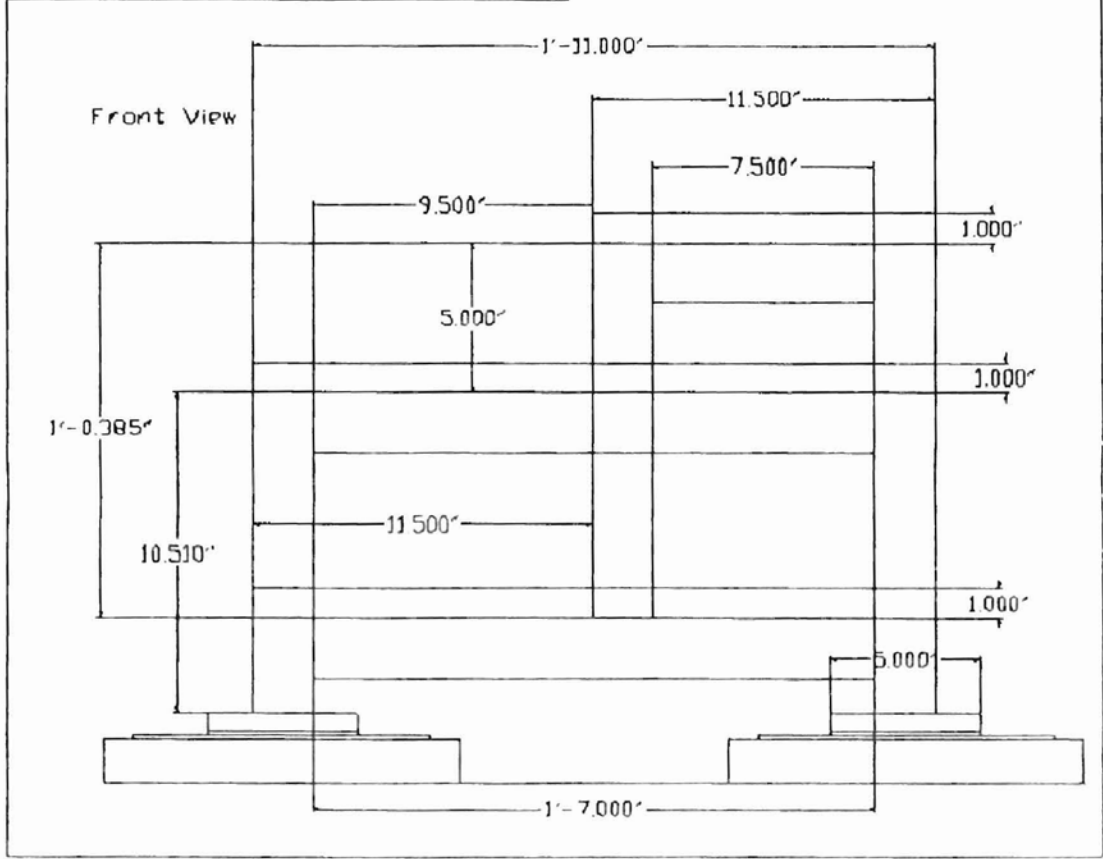
Project: Active Burner Design
 Title: Liquid Burner Structure 1-6
 Date: 12/27/1988
 Author: [Name]
 Design By: Fredrick [Name]
 Reviewed By: Dr. [Name]



Project: Clinton County, New York
 Date: 11/14/2018
 Reference: 10-370-1-170-1-18
 Drawn by: Michael Brown
 Reviewed by: D. Prosser/AR/12/1/19

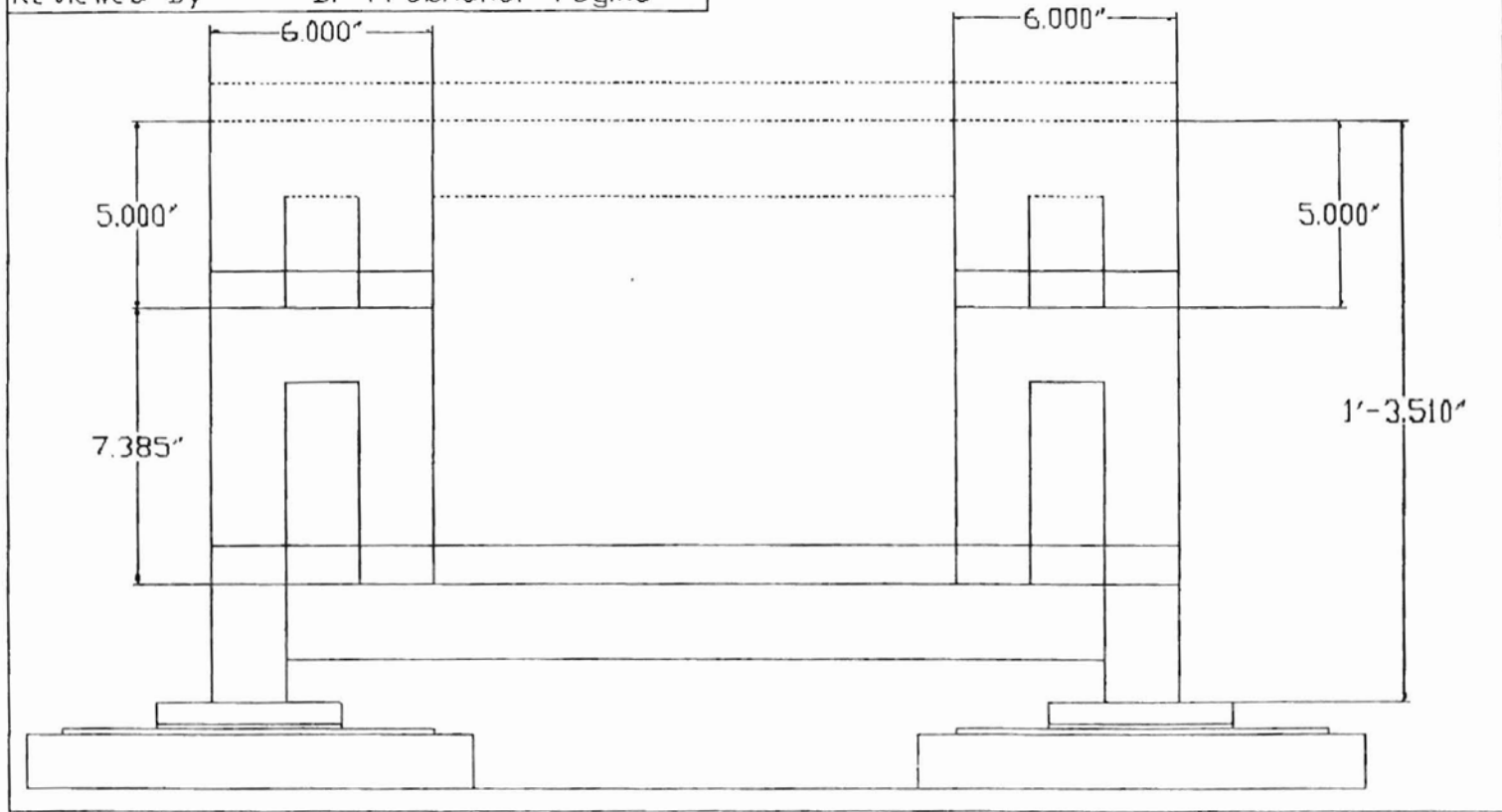


Project	: Active Dancer Design
Title & Figure No	Front View, Fig S-6
Date	: 12/27/1998
Reference	: Fig S-3
Drawn By	: Prasad Perera
Reviewed By	: Dr Prabhakar Pagillo

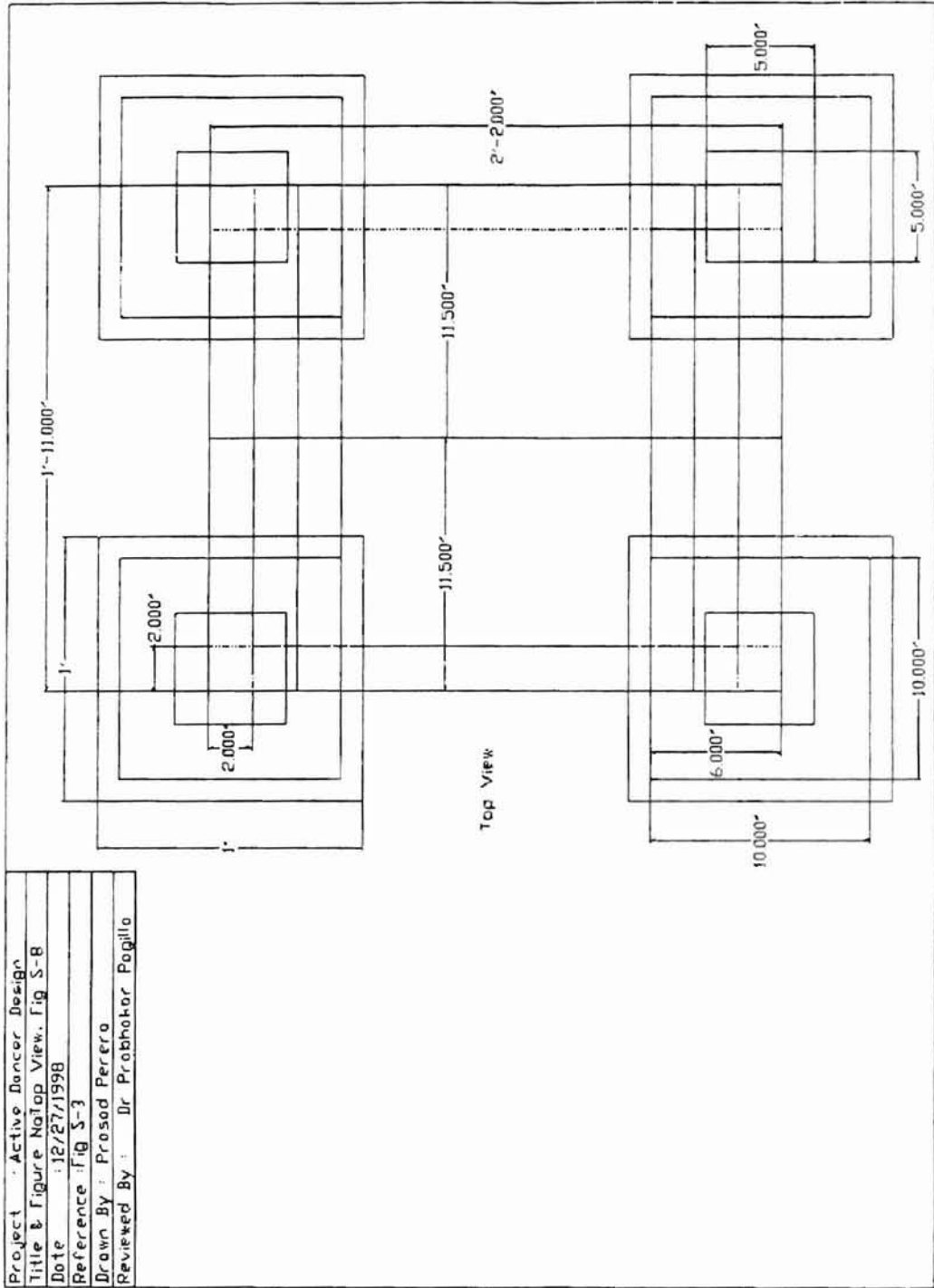


Project	: Active Dancer Design
Title & Figure No	: Right View ,Fig S-7
Date	: 12/27/1998
Reference	: Fig S-3
Drawn By	: Prosad Perera
Reviewed By	: Dr Prabhakar Pagilla

Right View

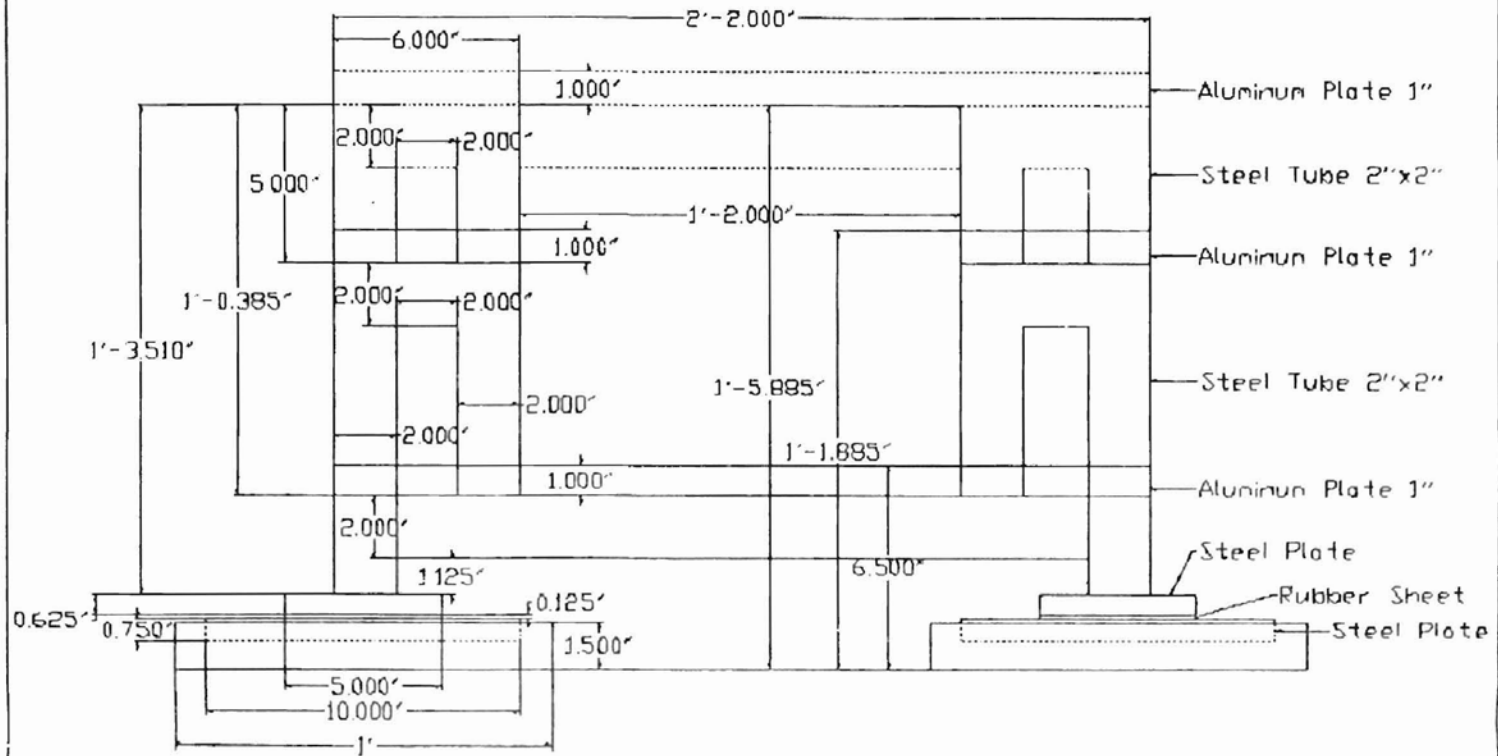


Project	: Active Dancer Design
Title & Figure No/Top View	: Fig S-B
Date	: 12/27/1998
Reference	: Fig S-3
Drawn By	: Prasad Perera
Reviewed By	: Dr. Prabhakar Pagilla



Project	: Active Dancer Design
Title & Figure No	: Left View, Fig S-5
Date	: 12/27/1998
Reference	: Fig S-3
Drawn By	: Prasad Perera
Reviewed By	: Dr Prabhakar Pagilla

Left View



VITA²

Lokukaluge Prasad Perera

Candidate for the Degree of

Master of Science

Thesis: THE ROLE OF ACTIVE DANCERS IN TENSION CONTROL OF WEBS.

Major Field: Mechanical Engineering

Biographical:

Personal Data: Born in Colombo, Sri Lanka, on March 29, 1974, the son of L.G.W. Perera and H. M Perera.

Education: Received Bachelor degree in Mechanical Engineering from Oklahoma

State University, May 1999. Completed the requirements for the Master of Science degree with a major in Mechanical Engineering at Oklahoma State University in August, 2001.

Experience: Research Assistant at Oklahoma State University from 1998 to present.

Professional Memberships: American Society of Mechanical Engineers, Institute of Electrical and Electronics Engineers, Honorary Mechanical Engineering Society (Pi Tau Sigma), Golden Key National Honor Society, and Technical Association of the Pulp and Paper Industry.